THE UNIVERSITY
of EDINBURGH

Towards a correlation of specific post-translational modifications of tau protein with characteristics of amyloid deposition

Christiana Kontaxi

Master of Science by Research in Neurobiology

The University of Edinburgh

August 2017

Declaration

I declare that this thesis has been composed completely by myself. The experiments were designed by my supervisors and myself. All experiments and analysis of data were performed by myself unless stated otherwise in the text. References have been provided on all supporting literature. This work has not been submitted for any other degree or professional qualification.

Christiana Kontaxi

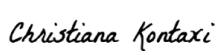

31st August 2017

Abstract

Tau is a microtubule-associated protein mainly responsible for stabilizing the neuronal microtubule network in the brain. Under normal conditions, tau is a highly soluble protein adopting an 'unfolded' monomeric conformation. However, it undergoes conformational changes resulting in a less soluble form with weakened stabilizing properties. Altered tau forms pathogenic inclusions characteristically seen in Alzheimer's disease and related tauopathies. Tau aggregates have been observed to be deposited surrounding prion protein amyloid plaques in mouse brains infected with the 87V murine adapted scrapie (87V-VM). Although tau hyperphosphorylation is widely considered as the major trigger of tau malfunction, tau is subject to a variety of other post-translational modifications, the site-specific impact of which on tau physiology and pathology remains unclear. Therefore, we used mass spectrometry to map post-translationally modified sites on tau purified from normal and 87V-VM mouse brains. We identified five types of site-dependent modifications in normal soluble tau, seven types in soluble tau extracted form 87V-VM brains and six types in insoluble aggregated tau. In preliminary, we showed that we can use LC-MS with a multiple reaction monitoring approach to determine relative levels of specific post-translational modifications of tau after only crude extractions. Once optimized, this workflow could be used to correlate the abundance of a wide variety of different modifications with specific properties of tau, such as solubility or morphologies of deposits.

Lay summary

Tauopathies are common diseases of the central nervous system that lead to cognitive decline and eventually death, including Alzheimer's disease, which is the most common form of dementia worldwide. A typical feature of these diseases is the alteration of the structure of tau protein that results in tau abnormal accumulation into fibrils. Whereas this process disables tau from serving its normal roles in the neurons, it allows to acquire novel neurotoxic roles. One of the most studied features of tau is its phosphorylation. Phosphorylation is one of the biochemical modifications that occur in cellular proteins after being translated from mRNA (post-translational modifications). The phosphorylation of tau protein controls its ability to bind and stabilize neuronal microtubules. However, under pathological conditions, tau phosphorylation is abnormally increased leading to impaired tau functions. Apart from phosphorylation, several other post-translational modifications that occur on tau have been discovered. The role of each post-translational modification either in normal or abnormal tau, especially concerning at which specific position on tau protein occurs, has not been completely investigated. Neither it is completely clarified what post-translational modifications are involved in turning tau from normal to abnormal. In this study, we used mass spectrometry in order to find post-translational modifications of tau protein that was isolated from normal and pathological brains. In these pathological brains, abnormal tau co-exists with another abnormal protein, called prion, which is the main feature of another group of central nervous system disorders, the prion diseases. This allows to compare the post-translational modifications between normal and abnormal tau and understand which of them are responsible for tau pathology. In addition, we developed a method in a preliminary stage to quantify tau post-translational modifications. This could be potentially used to elucidate different properties of tau and as a diagnostic tool for tau pathologies, but further optimization is needed.

Acknowledgements

First and foremost, I would like to thank my primary supervisor, Dr Andrew Gill, for accepting me into his group and giving me the opportunity to work on this project. His guidance and continuous encouragement while researching, writing and publishing could not have been more valuable. I am truly grateful for all his understanding and support throughout this project.

Moreover, I would like to thank my second supervisor, Prof. Pedro Piccardo, for his help during this project.

Also, I must thank Dr Dominic Kurian for generously providing his mass spectrometric expertise for this project, Dr Greg Papadakos for his help in the lab as well as the staff and students of the Neurobiology Division at the Roslin Institute, who were willing to help me whenever was needed.

Last but not least, I would like to express my gratitude to my family and my boyfriend. Their continuous support and patience made my journey into science possible so far.

Contents

1. Introduction

1.1 Neurodegenerative tauopathies

Neurodegenerative diseases represent a group of nervous system disorders, which are characterized by selective loss of neurons and synapses, glial activation, progressive irreversible dysfunction resulting in motor and cognitive impairment and eventually death[1, 2]. The main processes that lead to neurodegeneration are caused by genetic and/or environmental factors; however, advancing aging is widely considered the major factor responsible for the development and progression of neurodegenerative diseases. Common pathogenic processes underpinning neurodegenerative diseases include abnormal protein misfolding and aggregation, impaired protein degradation, proteasomal dysfunction and autophagy dysregulation, deficiency of molecular chaperones, oxidative stress and formation of free radicals, metabolic dysregulation, mitochondrial dysfunction, damage of neuronal Golgi apparatus, disruption of cellular and axonal transport, dysregulation of neurotrophins and neuroinflammation[3, 4].

Some neurodegenerative diseases are also known as proteinopathies due to the presence of pathological forms of proteins that accumulate and deposit in the brain. For this reason, it has been assumed that the aggregation of misfolded proteins is the molecular cause of neurodegeneration. In general, a particular protein switches to an unfolded state, which is thermodynamically unstable and, as a result, unfolded molecules have the tendency to interact with each other seeking more stability[5]. The formed aggregates come from endogenous proteins with different initial conformational state ranging from native to fully unfolded, but degraded proteins can be subject to self-association reactions as well[6]. In any case, proteins participating in aggregates lack their normal conformational arrangement and, hence, they are incapable of serving their typical functions in living cells, whilst they possibly acquire a novel neurotoxic role.

A common class of neurodegenerative diseases includes the disorders associated with the filamentous inclusions of tau protein, which are known collectively as tauopathies[7, 8]. Tauopathies include progressive supranuclear palsy, frontotemporal dementia with parkinsonism-17, corticobasal degeneration, argyrophilic grain disease, Pick's disease, Huntington's disease and several other cases[9, 10] (**Table 1.1**). The basic features that portray tauopathies are the transition of tau into a hyperphosphorylated state, the

Table 1.1 Neurodegenerative diseases with tau pathology (modified after Spillantini and Goedert, 2013; Arendt *et al*., 2016)[10-12].

Tauopathies	
Predominant tau pathology	**Associated with other types of pathology**
• Progressive supranuclear palsy • Argyrophilic grain disease • Corticobasal degeneration • Pick's disease • Frontotemporal dementia with parkinsonism-17 • Postencephalitic parkinsonism • Parkinson's dementia complex of Guam • Guadeloupean parkinsonism • Globular glial tauopathies • Aging-related tau astrogliopathy • Tangle-only dementia	• Alzheimer's disease • Down's syndrome • Lewy body disorder • Prion disease • Familial British dementia • Familial Danish dementia • Chronic traumatic encephalopathy • Myotonic dystrophy • Niemann-Pick disease type C • Subacute sclerosing panencephalitis • Frontotemporal lobar degeneration (some cases caused by C9orf72 mutations) • Diffuse neurofibrillary tangles with calcification • Neurodegeneration with brain iron accumulation • SLC9A6-related mental retardation • Cerebrotendinous xanthomatosis with the c.379C>T (p.R127W) mutation in the CYP27A1 gene • TARDBP mutation p.Ile383Val associated with semantic dementia • Huntington's disease

missorting of tau from the axonal cytoplasm into the somatodendritic compartment and the formation of characteristic fibrous bundles that accumulate in neurons and glia cells[12]. On the other hand, tauopathies can have different neuropathological phenotypes due to various aspects, such as the tau isoforms that are aggregated, the phosphorylation pattern, the conformation of the filaments, the cellular and subcellular distribution of tau species in neurons and glia cells, the anatomical distribution in brain tissues and, lastly, the co-existence with other types of pathology[1, 12].

One of the main pathological hallmarks of Alzheimer's disease (AD) is the intraneuronal accumulation of neurofibrillary tangles (NFTs) consisting of "misfolded" tau protein and, therefore, AD is considered to be partly a tauopathy and is, in fact, one of the most well studied. In AD, tau protein is abnormally hyperphosphorylated and aggregated into insoluble paired helical filaments (PHFs), which deposit in neuronal cell bodies as NFTs, in neuronal processes (neurites) as neuropil threads and in dystrophic neurites surrounding amyloid plaques that consist of aggregated Aβ peptides, the second main neuropathological hallmark of AD[13, 14] (**Figure 1.1A, 1.1B**). Each of the two filaments, winding helically around each other so that PHF structures are formed, consists of four protofilaments[15]. At the ultrastructural level, PHFs have a diameter of approximately 8-20 nm and a periodicity of 80 nm[16] (**Figure 1C**). Except for PHFs that represent the most abundant form of tau filaments, straight filaments about 15 nm wide are also found in NFTs[17]. It is well known that the severity of cognitive decline observed in AD correlates positively with the presence of NFTs in AD brains. This is due to the number of brain regions that are affected rather than the density of NFTs within a certain brain region[18].

In contrast to AD, for which tau aggregates deposit only in neurons, tau-positive glial inclusions are detected in various tauopathies, such as progressive supranuclear palsy, corticobasal degeneration and Pick's disease[19]. Neuropathological glial lesions seen in tauopathies include ramified astrocytes, coiled bodies, threads, tufted astrocytes, astrocytic plaques and bushy astrocytes[20]. Another aspect that differentiates AD from other tauopathies is the pattern of tau isoforms (see below) that generate pathological species, so that all tau isoforms are seen in tau deposits in AD, whilst preferential accumulation of some tau isoforms can be found in various tauopathies, such as Pick's disease. Moreover, except for PHFs and straight

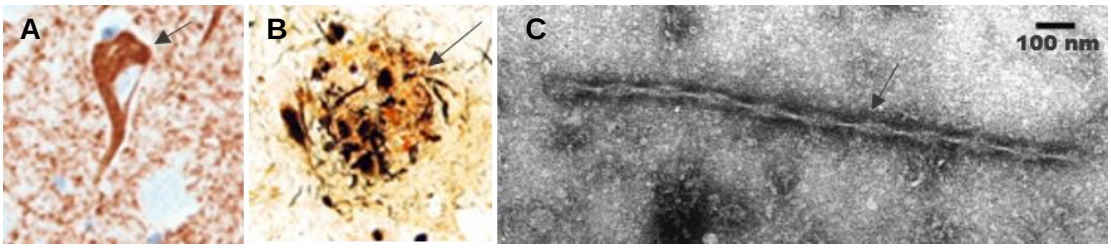

Figure 1.1 A. In AD, tau deposits as NFTs in the neuronal soma surrounding nucleus at the medial temporal cortex, as detected by using PHF-phosphorylated tau antibody (modified after Murray *et al*., 2014)[21]. B. In AD, tau deposits in dystrophic neurites surrounding Aβ amyloid plaques forming a neuritic plaque at the medial temporal cortex, as observed with Bielschowsky silver stain (modified after Murray *et al*., 2014)[21]. C. Electron micrograph of tau PHF from AD (modified after Spillantini and Goedert, 1998)[22].

filaments typical for AD, variable filamentous profiles are observed in other tauopathies, including tubules, PHF-like and twisted ribbon-like filaments[22].

Despite their differences, tauopathies share abundant aggregates consisting predominantly of tau and, consequently, numerous studies are focused on investigating tau dysfunction in the brain. Several aspects have been implicated in underpinning tau neuropathogenesis including the loss of normal tau function in the cell, the toxic gain of function of aggregated tau and/or oligomeric forms of tau, the toxicity caused by tau missorting within the neuron and the transmission of toxic tau species among neurons[23, 24]. Notably, it has been proposed that the polymerization of toxic tau products into tau aggregates might represent a neuroprotective response against oxidative stress[25]. Since tau is involved in various normal functions in the brain and tau pathology results in many neurodegenerative diseases, it is worth discussing in more detail the cell biology of tau protein itself.

1.2 The cell biology of tau protein

In 1975, a specific microtubule-associated protein (MAP) was isolated from porcine brain by Weingarten *et al*., which was named tau (τ) due to its ability to induce tubulin polymerization[26]. Tau is found in vertebrates, especially in mammals, and belongs to the highly conserved MAP2/Tau family of MAPs, which also includes the vertebrate proteins MAP2 and MAP4 and other

homologs[27-29]. In invertebrates, proteins showing homology to the MAP2/Tau family have been detected in *Escherichia coli*, *Caenorhabditis elegans* and *Drosophila melanogaster*, although this homology is rather limited[30-33]. In non-mammal vertebrates, MAP2/tau-related genes were identified in *Tetraodon* (pufferfish) and *Xenopus laevis* (frog) genome, whilst products of the MAP2/tau family were detected in *Coturnix coturnix* (quail) as well[27, 28, 34]. Consequently, tau is found throughout much of the animal kingdom and no homologs have been detected in other eukaryotic organisms so far. Phylogenetic analysis revealed that MAP4 derives from the earliest vertebrates, in contrast to tau and MAP2 that share a more recent common ancestor and have the same distribution in different species throughout vertebrates[35]. In mammals, tau is typically expressed in the central nervous system and predominantly in the brain, where it is located in neurons and, to a lesser extent, in glial cells[36-38]. Whilst tau can be detected in the spinal cord and peripheral nervous system, it is considerably less abundant[36]. Lastly, tau has been also found in some peripheral tissues, such as the heart, kidney, submandibular gland and liver, where it is present in remarkably lower levels than the brain[39, 40].

1.2.1 Tau expression

Human tau is encoded by a single gene, the microtubule-associated protein tau gene (*MAPT*), extending over an area of 100 kb on the chromosomal locus 17q21.31, which consists of 16 exons numbered as -1, 1, 2, 3, 4, 4A, 5, 6, 7, 8, 9, 10, 11, 12, 13, 14[41, 42] (**Figure 1.2**; see *MAPT* gene). Two extended haplotypes that cover entirely the *MAPT* gene, known as H1 and H2, have been characterized and result from an inversion polymorphism spanning over an area of 900 kb[43]. H1 haplotype has been associated with increased risk for developing many tauopathies, such as progressive supranuclear palsy and corticobasal degeneration[43, 44]. Numerous repeated sequences are spread throughout *MAPT* gene including *Alu* elements, DNA transposons, microsatellites and minisatellites, the effect of which on *MAPT* expression is not fully understood[45]. In addition, three CpG islands associated with *MAPT* are present, one related to the promoter region, the other to exon 4A, and the last one to exon 9[42, 46]. One *MAPT* promoter has been mapped so far, which is

located directly upstream of the exon -1 and is characterized by a high G + C content and the absence of TATA boxes indicating possibly the presence of multiple transcription initiation sites[47]. The transcription factors SP1 and AP2 bind to the *MAPT* promoter region and are essential for its activity; however, putative binding sites have been identified for various alternative transcription factors, such as Nrf1, MTF1 and MBF1[45, 48].

MAPT produces three primary transcripts (preRNAs) of 2, 6 and 9 kb that are differentially expressed depending on the neuronal maturation and neuronal type[49, 50]. The 6-kb transcript encodes the most abundant form of tau found in the adult brain and throughout development and is primarily targeted to the axons, whilst the 2-kb transcript that arises due to an alternative polyadenylation site is targeted to the nucleus, where tau might serve a special function during the early stages of development[51, 52]. Indeed, two polyadenylation sites have been identified, indicating the presence of two alternative transcription termination sites[46, 53]. On the other hand, the 9-kb transcript is targeted to the peripheral nervous system[54]. Tau preRNA (from now on referring to the 6-kb transcript) contains 16 exons, of which exons 1, 4, 5, 7, 9, 11, 12 and 13 are constitutive exons, whilst exons 4A, 6 and 8 are not found in any mRNA[55] (**Figure 1.2**; see Tau preRNA). Exon -1 and exon 14 are transcribed to mRNA, but they are not translated into protein as they are part of the 5′ and 3′ untranslated regions[55]. The translation initiation codon ATG is located in exon 1[56], while the AATAAA polyadenylation site is found within the exon 14[46].

The remaining exons 2, 3 and 10, are subject to alternative splicing generating six mRNA combinations and, as a result, tau can be found in six different isoforms in adult human brain varying from 352 to 441 residues[57] (**Figure 1.2;** see Tau isoforms). These isoforms differ depending on the number of 29-residue N′-inserts encoded by exon 2 and 3, so that an isoform can contain 0, 1 or 2 inserts, termed as 0N, 1N or 2N, respectively. Whilst exon 2 can appear alone, exon 3 never appears independently of exon 2, so that 1N isoforms contain one N′-insert that is coded by exon 2 instead of exon 3[58]. 0N, 1N and 2N constitute about 37 %, 54 % and 9 % of total tau, respectively[59]. In addition, an isoform can contain 3 or 4 C′-repeat regions, known as 3R or 4R, respectively, due to the presence of exon 10 that encodes for the additional second repeat domain; the other C′-repeat domains are encoded by exons 9,

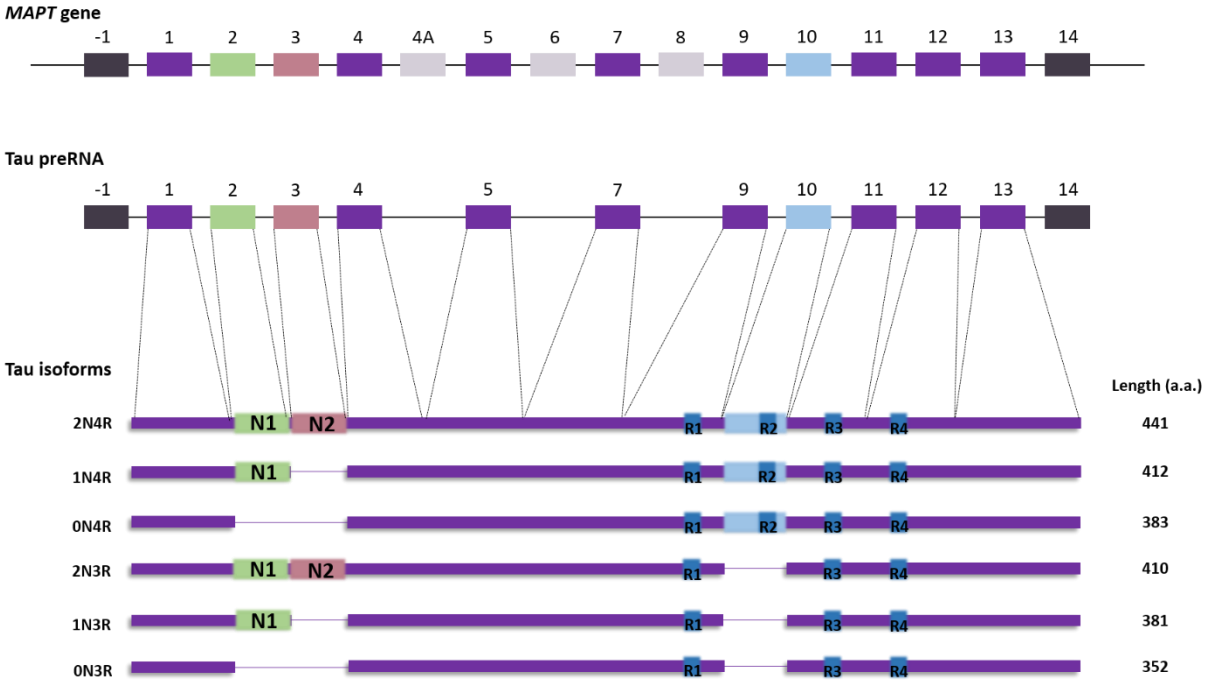

Figure 1.2 The human MAPT gene coding for tau protein consists of 16 exons, which are transcribed to a 6-kb primary transcript (tau preRNA). Exon 1, 4, 5, 7, 9, 11, 12, 13 (purple) are constitutive, whilst exons 4A, 6 and 8 (plum) are not found in any mRNA. Exon -1 and exon 14 (dark purple) are transcribed to mRNA, but they are not translated into protein as they are part of the 5′ and 3′ untranslated sequences of tau mRNA. The remaining exons 2 (green), 3 (coral) and 10 (sky blue), are subject to alternative splicing generating six mRNA combinations and, as a result, tau can be found in six different isoforms in adult human brain. These isoforms differ due to the presence of 0, 1, or 2 short N′-inserts (0N, 1N or 2N, respectively) and 3 or 4 C′-repeat domains (3R or 4R, respectively), so the length of the isoforms ranges from 352 to 441 residues.

11 and 12, respectively[60]. In the human cortex, the ratio of 4R tau to 3R tau isoforms is about 1:1[59]. The expression of tau isoforms differs among the species and is developmentally regulated. The adult rodent brain almost exclusively expresses the three isoforms of 4R tau (0N4R, 1N4R, 2N4R), whilst the adult human brain expresses all six tau isoforms[61]. Unlike the adult human brain, the dominant tau isoform in fetal human brain is the shortest one (0N3R) that contains neither N′-inserts nor the additional C′-repeat domain and, as a result, this 0N3R isoform is known as fetal tau[61].

The alternative splicing of exon 10 has received much attention as tauopathies are related preferentially to a certain isoform type found in tau

lesions, and the normal ratio 1:1 is shifted under pathological conditions. Based on the balance of the 3R and 4R isoforms, three groups of tauopathies are distinguished: 4R tauopathies, such as progressive supranuclear palsy, 3R tauopathies, such as Pick's disease and 3R+4R tauopathies, such AD[1]. The splicing of exon 10 is regulated by intronic and exonic *cis*-elements in combination with splicing regulatory proteins. Both exon and intron 10 contain many *cis*-elements including splicing enhancers, splicing silencers and an intronic splicing modulator[62, 63]. The interface between exon and intron 10 displays complementarity indicating the formation of a stem loop, the destabilization of which has been shown to lead to exon 10 inclusion[62, 64]. Also, distal sequences found in exon 9, 12 and 13 as well as the length of the flanking introns might affect exon 10 alternative splicing[50, 63]. Several splicing regulatory proteins are involved in exon 10 splicing regulation divided into two groups: the SR/SR-like factors, such as the SRp54 and SF2 that promote exon 10 exclusion and inclusion, respectively, and the hnRNPs factors, such as the hnRNPE2 factor that stimulates exon 10 inclusion[65-67]. Except for cis-elements and splicing factors, exon 10 splicing is controlled by the activity of several kinases since the phosphorylation of splicing factors seems to regulate their activity[68]. Also, miRNAs may affect tau splicing, such as miR-132 that was shown to correlate negatively with exon 10 inclusion in neuroblastoma cells[69]. Lastly, *MAPT* mutations associated with high affinity binding sites for splicing factors within or near exon 10 influence its splicing and alter the stoichiometry of 3R/4R tau isoforms[70].

The rather long 3' untranslated region is essential for the post-transcriptional stability as well as the axonal localization of tau mRNA. Binding sites for the miR-34a and miR-485-5p within the 3' untranslational region have been associated with downregulation of tau expression[71, 72]. On the other hand, apart from the poly(A) tail that protects mRNA, heterogeneous stabilization signals within the 3' untranslated region including an AU-rich and pyrimidine-rich region, in combination with possible secondary structures, increase tau mRNA half-life[73]. The initial event that determines the 6 kb-derived mRNA localization to neuronal axons is the interaction of *cis*-acting signals present in the 3' untranslated region with RNA-binding proteins forming ribonucleo-protein granules that transport along microtubules[74, 75]. Several RNA-binding proteins associated with tau mRNA axonal targeting have been identified including the interleukin enhancer binding factor 3, NF90

and HuD[76, 77]. Notably, the presence of ribosomal proteins, tau mRNA and its translated product in the axons of differentiated P19 neurons supports the notion that tau mRNA is initially targeted to axons, where it is subsequently translated[78].

The translation of tau mRNA depends on an internal ribosomal entry site situated in the leader sequence of the 5′ untranslated region (5′ leader) and required for recruiting the translational machinery[79]. Moreover, specific regulatory proteins bind to the mRNA molecule and contribute to its translation. The tau RNA-binding proteins G3BP1, IMP1, and HuD have been found to interact with translating polysomes and tau mRNA leading to inhibition of tau mRNA translation through association with the 3′ untranslated region[80, 81]. Except for the preferential targeting of tau mRNA in neuronal axons, as discussed above, the axonal distribution of tau is also assisted by preferential translation of tau mRNA in axons due to a 5′ terminal oligopyrimidine tract within the 5′ untranslated region, which facilitates the mammalian target of rapamycin kinase-mediated protein synthesis[82]. After translation, tau isoforms undergo a variety of post-translational modifications that determine their functional potential in the cell (see 1.3 Tau post-translational modifications).

1.2.2 Tau structure

The polypeptide chain of the longest tau isoform (2N4R) consists of 441 residues, and, within those residues, there is a low proportion of hydrophobic amino acids (about 24 %), which makes tau a highly soluble protein. Also, about 26 % of the residues are charged amino acids (D, E, L, R, H) with the positively charged residues slightly dominating and, thereby, tau is overall a basic protein; two small regions, which consist of a high proportion of acidic residues are found in tau sequence, one near the N-terminal end including the additional N′-inserts and the other near the C-terminal end of the molecule[83]. Circular dichroism, nuclear magnetic resonance, small angle X-ray scattering, and Fourier transform infrared spectroscopy showed that tau is natively unfolded with few β-sheet, α-helix and poly-proline helix secondary structures[84-86]. Since tau is a highly hydrophilic protein, it does not adopt the compact tertiary structure of cytosolic proteins and, as a result, it is considered

as an "intrinsically disordered" protein in solution[85]. However, the tau molecule was shown to have the propensity to adopt a hairpin-like folding, according to which the C-terminal end of tau folds approaching the microtubule-binding repeats and, thereby, the N-terminal end[87]. Consistent with its mainly unfolded character, tau displays flexibility and resistance to heating, denaturing or acidic treatment by keeping its biological function[88].

Based on its functional interaction with the microtubules, tau can be divided into two major domains: the N'-terminal projection domain that protrudes from the microtubule surface to which tau is bound and the microtubule-assembly domain, which is essential for interacting with microtubules[88, 89] (**Figure 1.3**). Alternatively, considering both the amino acid composition and functional interactions, tau can be divided into four main regions: (i) an N'-terminal projection region; (ii) a proline-rich region that contains seven PXXP motifs; (iii) a microtubule-binding domain (MBD) that contains three or four repeat regions, R1, (R2), R3 and R4, which are essential for binding to microtubules through their conserved KXGS motifs, and the flanking regions between them; (iv) a C-terminal region[89, 90].

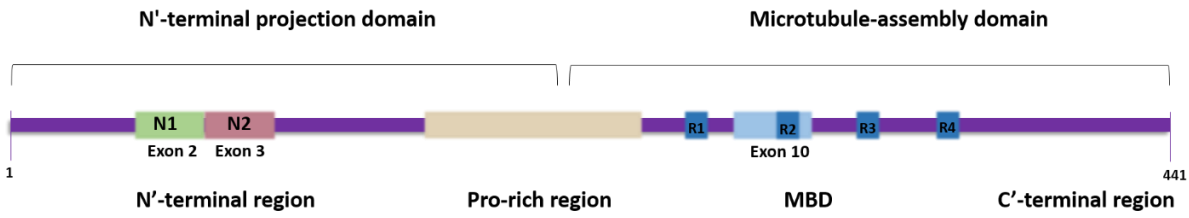

Figure 1.3 Diagram of the elongated longest tau isoform. Tau is divided structurally into the N'-terminal projection domain, which includes the N'-terminal region and part of the proline-rich region, and the microtubule-assembly domain, which consists of the rest of the proline-rich region, the microtubule-binding domain and the C'-terminal region. The N'-terminal region contains the two additional highly acidic N'-inserts encoded by the exon 2 and 3, respectively, whereas the microtubule-binding domain contains the three or four repeats essential for binding to microtubules.

1.2.3 Tau sorting

The subcellular localization of tau seems to be developmentally regulated and isoform-dependent. During neurogenesis, fetal tau is equally distributed

in the cell soma and developing neurites[91]. When neurons become polarized after the outgrowth of axons and dendrites, tau displays polarized distribution residing predominantly in axons, where it is found along microtubules and related to ribosomal polysomes[37, 92, 93]. For this reason, it has been implicated that the preferential distribution of tau is required for the development of neuronal polarity[94]. However, low amounts of tau can be detected in the somatodendritic compartment, in the nucleus and in association with the plasma membrane and several intracellular membranes, such as the Golgi or endoplasmic reticulum membranes[95-98]. Although tau is primarily a cytoplasmic protein, it can be detected outside cells and studies have shown that its release into the extracellular space is stimulated by neuronal activity *in vivo*[99, 100]. However, tau isoforms show different distribution in distinct subcellular compartments[101, 102]. Tau isoforms without the N'-inserts (0N3R, 0N4R) were highly enriched in axons in primary neurons, while the longest isoform (2N4R) was partly retained in cell bodies and dendrites, where it enhanced spine and dendrite growth[101].

Two possible mechanisms explaining the abundance of tau in axons have been already discussed above, according to which tau mRNA is preferentially sorted into the axonal compartment being locally translated there, or tau mRNA also transports into other compartments, but it is preferentially translated in the axon. Other factors underlying tau axonal distribution have been suggested including differential degradation of tau in the axons compared to the somatodendritic compartment and prevention of the retrograde (axon to soma) diffusion of axonal tau owning to the axon initial segment barrier thereby trapping tau in the axons[101, 103].

1.2.4 Tau functions

The cellular function of tau depends primarily on its subcellular localization, but, even within the same compartment, tau serves different roles based on different interacting partners. In addition, the phosphorylation state of tau, in combination with other post-translational modifications, are important in regulating the biochemical properties and activity of tau in the neurons. Tau is a microtubule-associated protein, but seems to serve several other functions within neurons not related to microtubules, such as iron export and cell

signaling[104]. Therefore, known roles of tau in different subcellular compartments are described next.

1.2.4.1 Axonal tau

The most well established biological function of tau is to promote microtubule assembly and stabilization in neuronal axons. Microtubules are long tubular structures of the cytoskeleton consisting of polymerized α- and β-tubulin heterodimers. Tau binds at the interface between tubulin heterodimers through the three or four repeat regions found within the MBD[105]. Due to the additional repeat region, 4R isoforms bind more effectively to microtubules than 3R isoforms[106]. Two distinct tau-binding sites were identified on both α- and β-tubulin units, one C-terminal, where the R1 repeat and/or the R1-R2 flanking region of tau binds to, and the other internal, where the binding of tau is mediated by one of its other repeats[107]. In neurons, the ratio of tau to tubulin is about 0.5, that is one tau molecule for two tubulin heterodimers[108]. By binding to tubulins, tau promotes microtubule nucleation, elongation and bundle formation[108]. In this case, tau is incorporated into the inner surface of the developing microtubules[109]. Also, tau can bind to the outer surface of previously assembled microtubule bundles maintaining their stability and more than 86 % of tau was found to be bound in the neurons[110]. The flanking regions remain flexible, while tau is bound, but they might also control tau affinity for microtubules[105]. The N'-terminal projection domain, which is negatively charged, protrudes from microtubules, when tau is bound, owning to electrostatic repulsion, and its length has been suggested to influence the spacing between microtubules[111].

Apart from its role in stabilizing microtubules, tau also modulates the microtubule dynamic instability by protecting the microtubule ends from growing and lessening randomly, while avoiding overstabilization that could damage the cell sustainability[112, 113]. The ability of tau to control microtubule dynamics is primarily regulated by its phosphorylation[113]. Given that microtubules are responsible for establishing the axonal architecture, tau seems to be essential for stabilizing the axonal shape as well. Moreover, overexpression of tau in ovarian cells was shown to induce the formation of neurites indicating that tau may be important for axonal outgrowth and maturation[114, 115]. Since microtubules facilitate the intracellular transport of

cargos and organelles with the aid of motor proteins, such as kinesin and dynein, tau may influence this process by competing with motor proteins for binding sites on microtubules[116].

1.2.4.2 Tau in dendrites

The function of tau in dendrites as well as dendritic spines remains elusive. By inducing a long-term synaptic activation in murine cultured cortical neurons, it was shown that tau translocates from the dendritic to the postsynaptic compartment and, thus, it has been suggested that dendritic tau may be involved in activity-dependent synaptic re-organization underpinning synaptic plasticity[117]. Furthermore, dendritic tau has been reported to be essential for the postsynaptic targeting of the kinase Fyn, a substrate of which is the NMDA receptor, and seems to affect the trafficking of the GluA2-containing AMPA-type glutamate receptor within neuronal dendrites[118, 119]. Lastly, a selective deficit in NMDAR-dependent long-term depression was observed in CA1 synapses *in vivo* in tau-knockout mice, suggesting that tau is required for long-term depression in the hippocampus[120].

1.2.4.3 Tau in nucleus

Apart from its localization in neuronal processes, tau has been detected in the nucleus, where it is specifically localized in the nucleolus in both neuronal and non-neuronal cells[121, 122]. The cytoplasmic translocation of tau into the nucleus depends on post-translational modifications, including phosphorylation and glycosylation[121, 123]. Nuclear tau can bind to both single- and double-stranded DNA through the second half of the proline-rich region and the R2 repeat within the MBD[124, 125]. Nuclear magnetic resonance revealed that an AT-rich or GC-rich 22 bp oligonucleotide is responsible for interacting with tau[125]. However, phosphorylation seems to decrease the interaction of tau with DNA and this agrees with data showing that tau is not phosphorylated in the nucleus[121, 125]. Similar to histone activity, tau is likely to serve several roles in the nucleus, including the protection of genomic DNA against stress-induced damage, chromosome stability, modulation of gene expression and RNA metabolism[124, 126, 127]. Moreover, owning to its specific localization in the nucleolus, it has been proposed that ribosomal biogenesis and/or rRNA

transcription are facilitated by tau activity, whereas it may be involved in the nucleolus organization itself[122, 128].

1.2.4.4 Tau associated with the plasma membrane

Tau has been reported to interact with the inner leaflet of the plasma membrane through its N'-terminal projection domain and possibly its MBD repeats in a process mediated by the plasma membrane-binding protein annexin A2[97, 129, 130]. However, it may be also present within cell-surface lipid-rich microdomains of the plasma membrane[131]. Similar to tau-DNA interaction, phosphorylation prevents tau association with the plasma membrane[132]. To date, the interaction of tau with the plasma membrane has not been studied extensively, but plasma membrane-associated tau might be involved in two possible process. Firstly, tau has been proposed to bring developing microtubules close to the plasma membrane of growth cones thereby facilitating neurite outgrowth[129]. Moreover, certain motifs (PXXP) within the proline-rich region of tau interact with signaling proteins, such the src tyrosine kinases, targeting tau into the plasma membrane, where it seems to facilitate intracellular signaling pathways[131, 133].

1.2.4.5 Extracellular tau

To date, the function of extracellular tau remains unclear. In cultured neuronal cells, extracellular full-length tau increased the concentration of intracellular calcium by activating the cholinergic muscarinic receptor M1 and/or M3 inducing neuronal death[134]. Notably, repeated stimulation of the muscarinic receptors with tau failed to induce their desensitization, in contrast to acetylcholine[135]. Tau released in the extracellular space, where was found to be very stable, has been associated with increasing neuronal activity, indicating that the synaptic activity serves the spread of tau pathology to neighboring neuronal cells causing tau-mediated neurotoxicity[100, 135].

1.2.5 Tau turnover

In neurons, tau can be proteolytically processed by the proteasome through a ubiquitin-dependent process[136] (see 1.3.4.3 Tau ubiquitylation). However, it

was shown that tau degradation might not require its preceding ubiquitylation at all, since tau was bi-directionally degraded *in vitro* by the 20s proteasome in a ubiquitin-independent manner that could be further supported by the "unfolded" character of tau protein[137, 138]. Impaired tau clearance has been widely considered a critical factor causing tau accumulation in the cell and, thus, contributing to tau pathology.

1.3 Tau post-translational modifications

Tau undergoes a variety of post-translational modifications, including phosphorylation, glycosylation, truncation, acetylation, methylation, ubiquitylation, SUMOylation, glycation, nitration, oxidation, prolyl-isomerization and deamidation[139]. Tau post-translational modifications are enzymatically regulated, with the exception of glycation and deamidation, and occur at different residues throughout the tau sequence. Each type influences the physical and chemical properties of tau in a site-specific manner thereby determining tau activity within different subcellular compartments. In addition, considerable evidence supports the notion that tau misfolding and dysfunction are favored by certain post-translational modifications that alter the biophysical properties of tau. Thereby, the post-translational modifications occurring on tau will be discussed immediately afterwards with regard to the biochemical reaction that takes place (for figures of the biochemical reactions see Appendix I) and their impact on both tau function and dysfunction.

1.3.1 Tau phosphorylation

One of the most well studied post-translational modifications of tau is phosphorylation, which refers to the addition of the terminal phosphate group from ATP to hydroxyl groups of serine, threonine or tyrosine side chains by esterification. Tau phosphorylation is regulated by the balance between protein kinases and phosphatases. Several protein kinases have been identified to phosphorylate tau protein in a site-dependent manner including the proline-directed S/T-protein kinases, such as GSK-3β, Cdk5 and MAPKs, the non-proline-directed S/T-protein kinases, such as CK1, DYRK1A and TTBK1/2, and the protein kinases specific for tyrosine residues, such as Src and

Fyn[139]. Conversely, tau dephosphorylation is controlled primarily by PP2A, but PP5 has also been shown to be able to dephosphorylate tau *in vitro*[140, 141]. The longest tau isoform (2N4R) contains 85 putative phosphorylation sites (45 serine, 35 threonine and 5 tyrosine residues), of which 28 have been detected to be possibly phosphorylated in AD brains, whereas 31 have been found exclusively in normal brains distributed along the tau sequence[17]. The remaining sites either have been detected in both brains or have not been fully characterized yet.

The phosphorylation of tau appears to be developmentally regulated, since fetal tau was shown to be more phosphorylated than adult tau in human and rat brains[142]. Under normal conditions, the phosphorylation of adult tau, controls its physiological activity as mentioned above, including tau affinity for microtubules, DNA and plasma membrane. However, PHF-tau is abnormally hyperphosphorylated[13, 143]. The abnormal increase in tau phosphorylation has been extensively studied and seems to result from the upregulation of tau kinases and/or downregulation of tau phosphatases. Also, it is considered the main cause for reducing tau affinity for microtubules given that phosphorylation of specific sites within the MBD has been related to weakened tau binding to microtubules[144]. Moreover, hyperphosphorylation possibly precedes and facilitates the self-assembly of tau isoforms into PHFs and straight filaments[145]. These data indicate that hyperphosphorylation is likely to be the main trigger of tau pathology by causing tau to unbind from microtubules, which are subsequently depolymerized, and facilitating its aggregation.

1.3.2 Tau glycosylation

Tau protein can be also modified by the addition of a sugar. This process, termed glycosylation, can occur on either the hydroxyl group of serine or threonine side chains (O-glycosylation) or the amino group of asparagine side chain (N-glycosylation). In human AD brains, tau was found to be N-glycosylated and it was suggested that this modification is responsible for maintaining and stabilizing the PHF structures[146]. Additionally, it was revealed that tau N-glycosylation may precede its hyperphosphorylation in AD brains by promoting phosphorylation and suppressing

dephosphorylation of tau by altering tau conformation[147]. Three potential N-glycosylation sites have been identified in human tau including N167, N359 and N410[148].

A special type of glycosylation found on tau is the addition of a single N-acetyl glucosamine (GlcNAc) group to serine or threonine residues, termed as tau O-GlcNAcylation. In contrast to tau N-glycosylation, O-Glc-NAcylation occurs at serine and threonine residues that can be also phosphorylated. Consequently, it has been suggested that this modification competes with phosphorylation for the same residues on tau both *in vivo* and *in vitro*, protecting tau against phosphorylation[149]. At the same time, O-Glc-NAcylation has been shown to inhibit tau aggregation by either enhancing the solubility of tau monomers or destabilizing tau aggregates[150]. In AD brains and other tauopathies, O-Glc-NAcylation appears reduced probably due to impaired brain glucose metabolism contributing to tau hyperphosphorylation and fibrillization[149]. Mass spectrometric analysis of O-Glc-NAcylated recombinant tau revealed three putative sites that are possibly modified at T123, S400 and either S409, S412 or S413, whereas only S400 has been identified in rat brain[151]. Tau O-Glc-NAcylation is catalyzed by the O-GlcNAc transferase; loss of the O-GlcNAc transferase led to increased production of hyperphosphorylated tau in forebrain excitatory neurons[152].

1.3.3 Tau truncation

Truncation is another post-translational modification of tau that occurs in AD and other tauopathies and seems to be an early pathological event[153]. In AD, four putative cleavage sites have been mapped on tau: D13 cleaved by caspase-6, R230 cleaved by calpains, E391 cleaved by caspases and D421 cleaved by the apoptotic protease caspase-3[154-157]. Two possible mechanisms have been proposed according to which truncation may facilitate tau-induced neurodegeneration[158]. Firstly, tau truncation may generate fragments with higher propensity for aggregation given that the hairpin-like folding is disturbed. Besides, it has been shown that tau structure after truncation is conformationally different compared to non-truncated tau[159]. Additionally, toxic fragments produced by tau cleavage may induce neurodegeneration

independently of tau aggregation. Lastly, tau truncation was demonstrated to follow tau hyperphosphorylation, but precede the formation of NFTs[160, 161].

1.3.4 Lysine-directed post-translational modifications

Tau post-translational modifications that extend to lysine residues have not been yet analysed as extensively as phosphorylation and glycosylation, but it is likely that they may be as important as phosphorylation in dictating the biophysical properties of tau. During this project I wrote and published a review article (see Appendix II) that provides a complete insight of the research up to date that focuses on lysine-directed post-translational modifications including tau acetylation, methylation, ubiquitylation, SUMOylation and glycation. Consequently, they will be discussed only briefly here.

1.3.4.1 Tau acetylation

Tau acetylation regards the addition of an acetyl group deriving from acetyl-CoA to the side chain of lysine residues of tau. It can be catalyzed by either the protein p300 or the CBP acetyltransferase, whereas tau can be deacetylated by the NAD^+-dependent sirtuin 1 deacetylase or the histone deacetylase 6[162-164]. Remarkably, tau has also intrinsic acetyltransferase activity and, hence, can catalyze its self-acetylation[165]. So far, 31 lysine residues have been identified as putative acetylation sites, most of which are distributed within or near the MBD. In general, acetylation that is elevated by cellular stress, such as Aβ accumulation, seems to be responsible for impairing both tau homeostasis and tau-microtubule interactions[162, 166]. However, acetylation at KXGS motifs has been reported to prevent tau phosphorylation and decrease its aggregation *in vitro*[164, 166].

1.3.4.2 Tau methylation

Tau methylation refers to the enzymatic addition of one or more methyl groups deriving from S-adenosyl methionine to the terminal amino group of lysine or arginine side chains of tau protein. To date, 26 lysine and three arginine residues have been detected to be possibly methylated in tau protein

isolated from both pathological and normal brains[167-169]. Given that the putative methylated sites are distributed throughout tau sequence, lysine methylation may suppress tau binding to microtubules and other partners. Moreover, lysine residues have been shown to participate in electrostatic interactions facilitating abnormal aggregation and, as a result, it has been suggested that lysine methylation may enable interactions between tau molecules enhancing tau self-assembly and NFT formation[170]. In contrast, the impact of lysine methylation on endogenous normal tau remains unclear.

1.3.4.3 Tau ubiquitylation

Ubiquitylation of tau involves the formation of an isopeptide bond between the C'-terminal carboxyl group of the small regulatory protein ubiquitin and the ε-amino group present in lysine side chains of tau by a multistep enzymatic process. Several enzymes have been reported to ubiquitylate tau, including the C-terminus of the Hsc70-interacting protein, TNF receptor-associated factor 6 and axotrophin/MARCH7[136, 171, 172]. The reverse process can be catalyzed by the cysteine protease deubiquitinating enzyme Otub1 that cleaves the isopeptide bond between tau and ubiquitin[173]. Apart from K44 that is located on the N'-terminal region, the remaining 16 lysine residues that can be potentially ubiquitylated are distributed within the MBD. The most well-known role of ubiquitylation in cells is the induction of the proteolytic degradation of targeted proteins by the proteasome, including tau[136]. Also, tau was identified as the ubiquitin-targeted protein in PHFs raising, thus, questions about the insufficient clearance of pathological fibrillary inclusions of tau[174].

1.3.4.4 Tau SUMOylation

SUMOylation is another post-translational modification of tau, in which the small ubiquitin-like modifier (SUMO) protein is enzymatically attached to the terminal amino group of lysine side chains forming an isopeptide bond in a way similar to ubiquitylation. Tau was shown to be preferentially monoSUMOylated by SUMO1 and, to a lesser extent, by SUMO2 and SUMO3[175]. So far, only K340 has been identified as a putative SUMOylation site, which is part of the consensus motif VKSE located within the MBD[175, 176]. Consistent with this, SUMOylation occurs only after tau is released from

microtubules[175]. Evidence shows that tau hyperphosphorylation facilitates its SUMOylation, whereas tau SUMOylation reciprocally enhances its hyperphosphorylation at several AD-related sites[176]. Moreover, it was revealed that SUMOylation of tau at K340 inhibits its ubiquitylation and subsequent degradation[175].

1.3.4.5 Tau glycation

The non-enzymatic attachment of a reducing sugar, especially glucose, to the terminal amino group of a lysine side chain of tau is called tau glycation or tau non-enzymatic glycosylation. Glycation is one of the modifications detected in PHF-tau purified from AD human brains, but not in soluble tau[177]. From the 32 putative glycation sites identified in tau both *in vitro* and *in vivo*, 21 are distributed within the MBD[178]. Tau glycation has been implicated in inhibiting microtubule-tau interactions *in vitro*, assisting tau hyperphosphorylation and facilitating tau aggregation[177, 178]. Lastly, the formation of advanced glycation end products by developing irreversible cross-links between tau glycation products and other proteins has been related to oxidative stress in neurons[179].

1.3.5 Other tau post-translational modifications

1.3.5.1 Tau nitration

The addition of nitrogen dioxide on the aromatic ring found in the side chain of a tyrosine residue of tau is termed as nitration. Tau can be nitrated at four possible sites including Y18, Y29 and, to a lesser extent, Y197 and Y394[180]. Nitration may facilitate tau aggregation into filamentous inclusions in AD and other tauopathies or, conversely, may inhibit tau polymerization depending on the modified sites[180, 181]. In the neuroblastoma N2a cell line, nitrated tau was shown to accumulate in the cells, whereas impaired binding to microtubules was observed *in vitro*[182]. Immunoblotting analysis using antibodies that react specifically with nitrated tau at Y18, Y29 and Y394 revealed that these sites are nitrated only in AD and other tauopathies, indicating that these modifications may be a disease-related event[183-185]. On the other hand, nitration at Y197 located within the proline-rich region has been detected in soluble tau from

normal brains and, as a result, it is likely to serve physiological functions in neurons[185]. However, the impact of the site-specific tyrosine nitration on tau biology seems to vary between different tauopathies and tau lesions[184].

1.3.5.2 Tau oxidation

Protein oxidation is a chemical reaction that involves loss of electrons leading to amino acid side chain modifications and is part of normal regulatory processes or appear when oxidative stress overcomes antioxidant defenses[186]. Tau protein can be oxidized at C322, located within the MBD, enabling the formation of intermolecular disulfide bridges between C322 residues and tau oxidation was shown to induce its self-association *in vitro*[187, 188]. Consistent with this, treatment with tau fibrillization inhibitors, such as the aminothienopyridazines, found to promote the oxidation of both cysteine residues within the MBD of tau molecule, C291 and C322, leading to a compact monomer that contains an intramolecular disulfide bond and is resistant to aggregation[189]. Moreover, cysteine oxidation of tau to disulfide formation was shown to weaken tau ability to promote microtubule assembly[190].

1.3.5.3 Tau prolyl-isomerization

Prolyl-isomerization refers to the interconversion between *cis* and *trans* conformation of the peptide bond of a targeted protein that is formed by the amino group of proline. In contrast to other amino acids, the amino group of proline is part of its cyclic side chain. Tau prolyl-isomerization can be catalyzed by the Pin1 prolyl isomerase and the FKBP52 protein[191, 192]. Pin1 has been shown specifically to isomerize the phosphorylated T231-P232 bond in tau affecting its *cis-trans* conformation[191]. Also, the activity of PIN1 seems to regulate the PP2A-dependent dephosphorylation, since PP2A phosphatase displays *trans*-specificity, and can restore the ability of hyperphosphorylated tau to bind to microtubules and promote microtubule assembly *in vitro*[191, 193].

1.3.5.4 Tau deamidation

Tau deamidation refers to the replacement of the amide group of the side chain of asparagine to a hydroxyl group resulting in the irreversible, non-enzymatic conversion of asparagine to aspartic acid or isoaspartic acid.

Aggregated tau extracted from AD brains was shown to include two isoaspartic acids at the position of tau asparagine residues N381 and N387[194]. The isoaspartate formation at these sites has been related to both oligomerization and PHF formation *in vivo*[194]. Another asparagine residue that was found to undergo deamidation in AD brains was N279, located within the MBD[195]. Deamidation of N279 to aspartic acid seems to reduce tau binding to microtubules similarly to tau hyperphosphorylation[195].

1.4 Tau aggregation

Even though tau protein adopts an "unfolded" conformation under normal conditions, its self-association results in the formation of well-ordered filamentous structures. Three factors are essential for facilitating tau aggregation. The first concerns the release of tau from microtubules, which contributes to increasing the pool of available-to-aggregate tau in the cytosol. Secondly, the charge neutralization of basic regions of the tau molecule caused by polyanions enables tau self-association[196]. The last factor that contributes to tau aggregation is the tendency of two hexapeptide motifs, VQIINK and VQIVYK within the R2 and R3 repeat region of the MBD, respectively, to form β-structures[196, 197]. When tau accumulates into highly ordered PHFs, the MBD has been shown to compose the fibril core of PHFs consisting of β-structures, whereas a highly flexible "fuzzy coat" that consists of the N'- and C'-terminal regions exists surrounding the fibril core[198].

Studies of the kinetics of PHF assembly revealed that tau fibrillization follows a nucleation-elongation process[197] (**Figure 1.4**). According to this mechanism, a thermodynamically unstable nucleus in equilibrium with the assembly-competent monomer population is formed randomly (nucleation)[199]. When this nucleus reaches a critical size, the subsequent addition of monomers is energetically favorable and the aggregation proceeds forming initially short oligomers and later long fibrils (elongation)[199]. Consequently, the rate of tau fibrillization depends on both the nucleation efficiency and the elongation rate. Different tau isoforms have been shown to display different propensity to aggregate *in vitro*. The first N'-insert encoded by exon 2 has been reported to promote tau fibrillization due to its contribution to the nucleation and elongation steps of the aggregation process, in contrast to the antagonist effect of exon 3-encoded N'-insert[200]. Also, 4R isoforms have been reported to

aggregate more efficiently than 3R isoforms *in vitro*, which require higher concentration and longer nucleation time to support the aggregation level of 4R isoforms[200]. Since tau aggregation is clearly a biophysical process, it is not surprising that several site-directed post-translational modifications, which may or may not compete each other, have a profound impact on it.

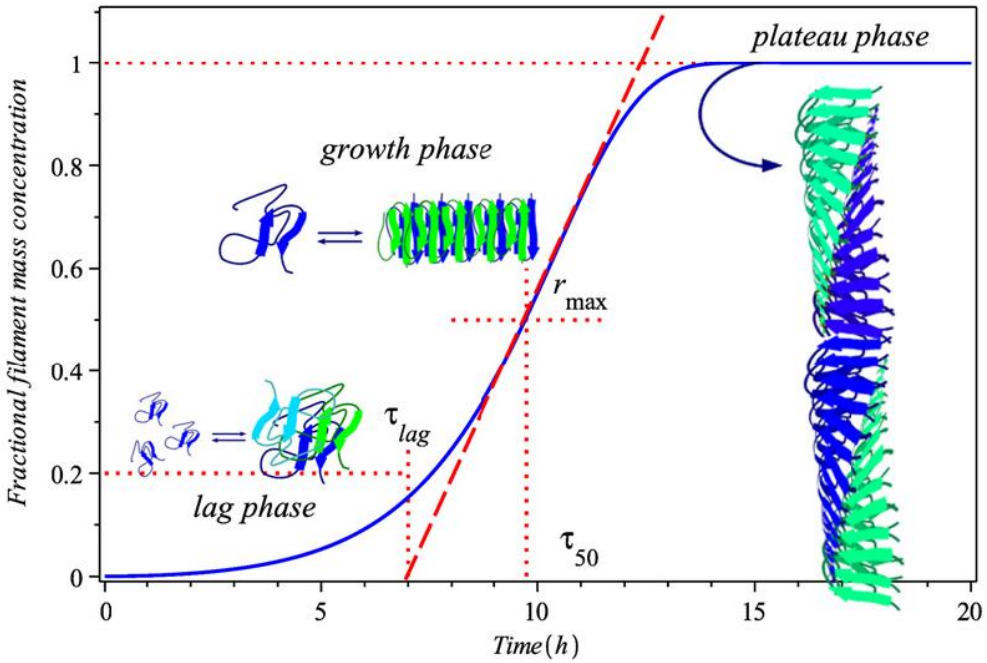

Figure 1.4 The sigmoidal graph represents a typical protein fibrillization process that is characterized by a nucleation (lag)-elongation (growth) phase followed by a plateau phase (adapted after Gillam and MacPhee, 2013)[199]. τ_{50} represents the time, when half of the protein molecules have formed filamentous aggregates and the elongation rate (r_{max}) is maximum.

2. Project objectives

Tau undergoes a variety of post-translational modifications as discussed above and, amongst them, phosphorylation has received most attention for two main reasons. Firstly, it is well established that phosphorylation influences the biological activity of tau under normal conditions (see 1.2.4 Tau functions). Secondly, pathological tau aggregates found in AD and related tauopathies are characterized by a hyperphosphorylated state of tau, which has been associated with the loss of tau major function to bind and stabilize microtubules and is widely considered one of the initial events resulting in tau misfolding (see 1.3.1 Tau phosphorylation). However, increasing evidence supports the notion that other post-translational modifications occurring on tau, such as acetylation and glycosylation, might be equally important for regulating tau normal function and misfolding in a site-specific manner. Despite the increasing focus on tau post-translational modifications, the identification of possible sites that are found to be modified is not complete yet. In addition, the biological role that each site-specific post-translational modification facilitates in normal tau as well as in different types of pathological tau, remains to be elucidated.

Immunohistochemical data available from previous work revealed that tau aggregates can deposit surrounding prion protein amyloid plaques in mouse brains infected with the 87V murine adapted scrapie (87V-VM; **Figure 2.1**). This observation raised the question whether tau post-translational modifications are altered by the pathology of prion protein *in vivo* compared to normal tau. Consistent with this, we hypothesized that the prion pathology in 87V-VM mouse brains causes the biochemical shift of normal endogenous tau into misfolded aggregated tau by inducing alterations of specific tau post-translational modifications. Therefore, the primary aim of the project was to identify site-specific post-translational modifications occurring on tau isoforms derived from normal and 87V-VM mouse brains, respectively. To do that, mass spectrometry was used given that it allows large-scale analysis of

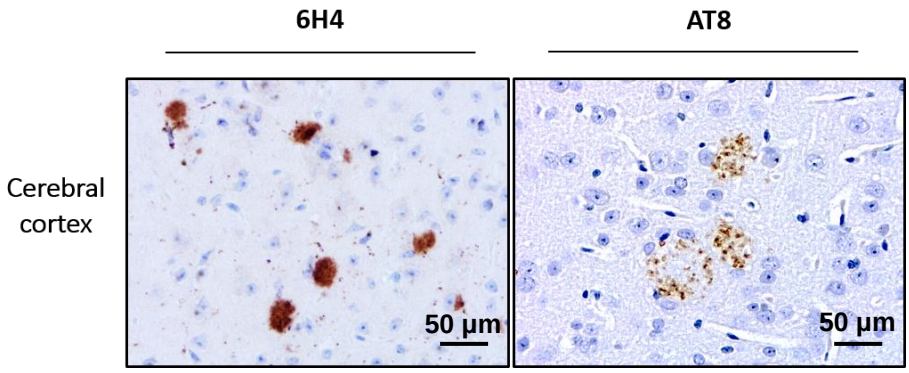

Figure 2.1 Immunohistochemistry using the anti-prion antibody 6H4 and the anti-tau antibody AT8 reveals the co-existence of prion protein amyloid plaques (left) and tau deposits (right) in the cerebral cortex of 87V-VM mouse brains (stained with hematoxylin; magnification 40x). The figure was kindly provided by Prof. P. Piccardo (Piccardo *et al.*, Variable tau-protein accumulation in animal models with prion protein deposits, in submission).

protein post-translational modifications. Furthermore, since certain site-specific post-translational modifications may be prevalent in one type of pathological tau, whereas they may be absent or less abundant in other types, the development of a method at a preliminary stage to quantify site-specific modifications from crudely isolated tau was another major objective. This study contributes to our understanding of the biochemical transition occurring on tau protein in neuropathology, which could be the ground for therapeutic approaches aiming at certain site-specific post-translational modifications of high risk. In addition, it would increase our knowledge of the impact of site-specific post-translational modifications on tau biology, since tau seems to be involved in many important cellular functions of neurons.

The specific technical objectives of the project were as follows:

- Extract biochemically soluble endogenous tau from normal mouse brain samples and identify tau isoforms by immunoblotting.
- Extract biochemically soluble endogenous tau from 87V-VM mouse brain samples and identify tau isoforms by immunoblotting.
- Optimize the biochemical extraction of insoluble aggregated tau from 87V-VM mouse brain samples and identify tau isoforms by immunoblotting.

- Detect both normal and pathological tau post-translational modifications by mass spectrometry and analyze the data.
- Investigate the phosphorylation state of soluble tau in the 87V-VM mouse brain underlying tau pathology.
- Investigate whether it is possible to develop a method of quantifying specific tau post-translational modifications of interest by mass spectrometry.

Last but not least, since the scientific field lacked an overview of the latest findings concerning tau post-translational modification occurring on lysine residues, a review of the literature on the subject was an additional aim during this project.

3. Materials and methods

3.1 Materials

The chemicals and reagents that were used during this project are listed below: perchloric acid 70 % (PCA; Aristar/Primar), tris base (Fisher BioReagents), sodium chloride (Fisher BioReagents), sarkosyl (N-Lauroylsarcosine sodium salt; Sigma-Aldrich), nonidet P-40 Alternative (NP-40; Calbiochem), sodium deoxycholate (BDH 430353P), ethylene diamine tetraacetic acid (EDTA; Sigma-Aldrich), ethylene glycol bis(β-aminoethyl ether) N,N,N′,N′-tetraacetic acid (EGTA; Sigma-Aldrich), phenylmethylsulfonyl fluoride (PMSF; Sigma), sucrose (Fisher BioReagents), β-mercaptoethanol (BDH 44143), trichloroacetic acid (TCA; Fisher BioReagents), methanol (Fisher Chemicals), magnesium sulfate (Scientific Laboratories Supplies), dithiothreitol (DTT; Fisher BioReagents), formic acid (Rathburn Chemicals), sodium phosphate (Sigma-Aldrich), potassium iodide (Sigma-Aldrich), sodium thiosulphate (VWR Chemicals BDH), urea (Sigma-Aldrich), glycerol (Fisher BioReagents), sodium dodecyl sulphate (SDS; BDH Prolabo Chemicals), 3′, 3′′, 5′, 5′′-tetrabromophenolsulfonephalein (bromophenol blue; Sigma-Aldrich), glycine (Fisher BioReagents), tween-20 (AMPRESCO), iodoacetamide (IAA; Sigma-Aldrich), ammonium bicarbonate eluent additive for LC-MS (Fluka), trypsin from porcine pancreas (Sigma-Aldrich), trypsin resuspension buffer (Promega), formic acid LC-MS Grade (Thermo Scientific), acetonitrile (VWR Chemicals BDH Prolabo). All homogenizations were carried out by using the Wheaton Dounce Tissue Grinders by Fisher Scientific. Insoluble pellets were sonicated by using the Sonicator Ultrasonic Processor XL, if needed.

3.2 Animals

Frozen mouse brain tissues were available from previous work to investigate the changes of tau post-translational modifications induced by the prion protein pathology, for which the entire brain was removed and snap frozen in liquid nitrogen before storage at -80°C. Two groups of mouse brains were used in this study: a group of normal brains, which did not display any clinical signs, and a group of brains collected from mice infected by intracranial inoculation with the 87V mouse adapted scrapie strain. These mice displayed clinical signs prior to cull, as defined by validated scoring criteria. Both normal and 87V-VM brains were derived from mice of approximately the same age, nearly one year old, and of both sexes.

3.3 Biochemical extraction of soluble tau from mouse brain

The biochemical extraction of soluble tau from mouse brain was performed according to Ivanovova *et al*. (2008)[201]. Mouse brain was homogenized in ice-cold 1 % (w/v) perchloric acid (1.5 g tissue per 5 mL PCA) with a glass homogenizer and kept on ice for 20 min to allow the depolymerization of microtubules. The homogenization was performed in low temperature to prevent protease activity. The homogenate was centrifuged at 15,000 x g for 20 min at 4°C and the clear supernatant was concentrated using Amicon Microcon Centrifugal Filter Devices with simultaneous buffer exchange to washing buffer by spinning at 14,000 x g for 6 h overall at room temperature on an Eppendorf Refrigerated Microcentrifuge, Model 5417R, using the rotor FA-45-30-11. The washing buffer contained 20 mM Tris pH 7.4 and 150 mM NaCl. The concentrated supernatant was stored at -20°C. Aliquots of the brain and the pellet were kept for analysis. This protocol was used for the extraction of soluble tau from both normal and 87V-VM mouse brains.

3.4 Biochemical extraction of aggregated tau from mouse brain

Different protocols were used for the biochemical extraction of insoluble aggregated tau from the 87V-VM brains, all of which were based on fractional centrifugation and incubation with the detergent sarkosyl. Insoluble tau refers

to tau insoluble by 1 % (w/v) sarkosyl. Aliquots of intermediate fractions were kept and analysed along with the fraction of interest. The slow centrifugation steps were carried out on an Eppendorf Refrigerated Microcentrifuge, Model 5417R, using the rotor FA-45-30-11, which spins up to 20,800 x g maximum. When the rotational speed given by the protocol exceeded this value, the time of centrifugation was calculated according to the equations below:

$$k\left(\frac{mm}{g}\right) = \frac{2{,}83696\ x\ 10^5\ x\ r_{max}\ x \ln\left(\frac{r_{max}}{r_{min}}\right)}{RCF};$$

$$\frac{t_1}{k_1} = \frac{t_2}{k_2},$$

where k (k factor) represents the relative pelleting efficiency of a given centrifuge rotor at maximum rotational speed, r_{min} and r_{max} represent the minimum and maximum distance from the rotational axis (mm), respectively, RCF represents the rotational speed of the centrifuge (x g), t_1 (unknown) represents the time to precipitate a certain particle at the rotational speed given by the protocol that exceeds the maximum rotational speed of the centrifuge (min), k_1 represents the k factor of the rotor at the speed given by the protocol (mm/g), k_2 represents the k factor of the rotor at the maximum rotational speed (mm/g) and, lastly, t_2 represents the time to precipitate a certain particle at the maximum rotational speed of the centrifuge (min)[202]. Consequently, the centrifugation was carried out at the maximum rotational speed of the centrifuge for t_2 min. The fast centrifugation steps were carried out on the Beckman Optima TL 100 Ultracentrifuge using the rotor TLA-100.3 and Beckman Coulter Polyallomer Centrifuge thick-wall tubes, which were strictly weighed and balanced before centrifugation.

3.4.1 Biochemical extraction according to Planel et al.

The first protocol used for the extraction of aggregated tau was described previously by Planel *et al*. (2009)[203]. Mouse brain was homogenized in 5 vol. (v/w) of cold RIPA buffer with a glass homogenizer. RIPA buffer contained 50 mM Tris pH 7.4, 1 % (v/v) Nonidet P-40, 0.25 % (w/v) sodium deoxycholate,

150 mM NaCl and 1 mM EDTA. The homogenate was centrifuged at 20,000 x g for 20 min at 4°C and the supernatant representing total tau fraction was adjusted to 1 % (w/v) sarkosyl for 1h at room temperature with constant shaking. The supernatant was then centrifuged at 100,000 x g for 60 min at room temperature. Given that the Beckman Coulter Polyallomer Centrifuge thick-wall tubes were used for this centrifugation step with maximum fill volume 3 mL, the concentration of sarkosyl $c_{sarkosyl}$ (% w/v) that was used to reach a final concentration of 1 % (w/v) was calculated as below:

$$C_{sarkosyl}(\%\ w/v) = \frac{V_{sample}}{V_{sarkosyl\ with\ concentration\ c}} + 1;$$

$$V_{sample} + V_{sarkosyl\ with\ concentration\ c} = 3\ mL$$

where V_{sample} refers to the supernatant volume representing total tau fraction (mL), which emerged from the first centrifugation, and $V_{sarkosyl\ with\ concentration\ c}$ refers to the volume of sarkosyl that was added to reach final volume 3 mL (mL). The pellet containing sarkosyl-insoluble, aggregated tau was resuspended in distilled water and stored at -20°C. Aliquots of the homogenate, the initial pellet and the sarkosyl-soluble supernatant were kept for analysis.

3.4.2 Biochemical extraction according to Greenberg and Davies

The protocol that was published by Greenberg and Davies (1990) for the preparation of insoluble tau fractions was used after some modifications[204]. Mouse brain was homogenized in 10 vol (v/w) of cold H buffer with a glass homogenizer. The homogenization was performed in low temperature to prevent protease activity. H buffer contained 10 mM Tris, 1 mM EGTA, 1mM PMSF, 0.8 M NaCl and 10 % (w/v) sucrose, pH 7.4. The homogenate was kept on ice for 20 min to allow the depolymerization of microtubules and then centrifuged at 20,800 x g for 26 min at 4°C. The pellet was re-homogenized and spun similarly to the brain. The supernatants from both centrifugations representing total tau fraction were combined and adjusted to 1 % (w/v) sarkosyl and 1 % (v/v) β-mercaptoethanol by adding 11.11 μl of 10 % (w/v) sarkosyl and 1.11 μl of β-mercaptoethanol per 100 μl of supernatants. After

incubation for 2h at 37°C with constant shaking, the supernatants were centrifuged at 30,000 rpm for 30 min at room temperature. The pellet containing sarkosyl-insoluble, aggregated tau was resuspended in H buffer. The re-suspended pellet was adjusted to 0.1 % (v/v) β-mercaptoethanol as before (up to final volume 200 μl) and placed onto a discontinuous sucrose gradient that consisted of 1,3 mL of 35 % (w/v) sucrose and 1,5 mL of 50 % (w/v) sucrose in 10 mM Tris, 1 mM EGTA, 0.8 M NaCl and 0.1 % (v/v) β-mercaptoethanol, pH 7.4. After centrifugation at 35,000 rpm for 82 min at room temperature, the 35 % layer and 35-50 % interface that contain aggregated tau were collected with a 2.5-mL syringe. The proteins of the samples were precipitated with 10 % (w/v) TCA with ice-cold methanol and stored in -20°C. Aliquots of the homogenate, one of the initial pellets and the sarkosyl-soluble supernatant were kept for analysis.

3.4.3 Biochemical extraction according to Cohen et al.

The next protocol that was used for the biochemical extraction of aggregated tau was based on a previous protocol published by Cohen *et al*. (2011)[166]. Mouse brain was homogenized in 3 vol (v/w) of cold High Salt RAB buffer, which contained 0.75 M NaCl, 100 mM Tris, 1 mM EGTA, 0.5 mM $MgSO_4$, 2 mM DTT, pH 7.4. The homogenate was kept on ice for 20 min to allow the microtubule depolymerization and the homogenization was performed in low temperature to prevent protease activity. After centrifugation at 100,000 x g for 30 min at 4°C, the pellet was re-homogenized and centrifuged similarly to the brain. The resultant pellets were re-homogenized again in 5 vol (v/w) of cold PHF extraction buffer, which contained 10 mM Tris pH 7.4, 10 % (w/v) sucrose, 0.85 M NaCl, 1 mM EGTA, pH 7.4, and centrifuged at 15,000 x g for 20 min at 4°C. The supernatant was adjusted to 1 % (w/v) sarkosyl as previously and incubated at 4°C overnight. After centrifugation at 100,000 x g for 30 min at room temperature, the sarkosyl-insoluble pellet was solubilized by formic acid. The proteins of the sarkosyl-insoluble fraction were precipitated with 10 % (w/v) TCA with ice-cold methanol and the sample was stored in -20°C. Aliquots of the homogenate, the initial supernatant and one of the pellets as well as the sarkosyl-soluble supernatant were kept for analysis.

3.4.4 Biochemical extraction according to Hope et al.

A protocol for the extraction of pathological prion protein (PrP^{Sc}) was used, since aggregated tau is associated with PrP^{Sc} plaques in the same brain tissues, described previously by Hope *et al*. (1988)[205]. According to this protocol, mouse brains were homogenized in brain lysis buffer (20 mL of buffer per 2 g of tissue) and incubated for 30 min at room temperature. The brain lysis buffer consisted of 0.01 M sodium phosphate pH 7.4 and 10 % (w/v) sarkosyl. The homogenate was centrifuged in the Thermo Scientific Sorvall LYNX using the SS34 rotor and Nalgene Oakridge tubes at 13,500 rpm for 30 min at 10°C. The supernatant was collected and centrifuged in the Beckman L8-60M Ultracentrifuge using the Ti70 rotor and Beckman red topped polycarbonate tubes at 46,000 rpm for 2 h 30 min at 10°C. The resultant pellet was re-suspended in 3 ml/g of distilled water and 6 ml/g of iodide solution were added. The iodide solution contained 0.9 M potassium iodide, 9 mM sodium thiosulphate pH 8.5 and 1.5 % (w/v) sarkosyl. After incubation for 1 h at room temperature, the re-suspended pellet was placed onto a sucrose cushion, which consisted of 20 % (w/v) sucrose in iodide solution, and centrifuged in the Beckman L8-60M Ultracentrifuge using the SW41 rotor and Beckman Ultraclear tubes at 40,000 rpm for 1h 30 min at 10°C. The resultant pellet was stored at 4°C overnight and the next day was re-suspended in distilled water to approximately 1 μg/μl by sonicating in 10 sec pulses. The resuspended pellet that contains the pathological prion aggregates was stored at -20°C. Aliquots of the homogenate and the supernatants and pellets that emerged during the homogenization were kept for analysis.

3.5 Gel electrophoresis

The samples collected during the homogenization procedure were separated by sodium dodecyl sulfate polyacrylamide gel electrophoresis (SDS-PAGE), which was performed using the Novex NuPAGE gel system (Thermo Scientific). The identification of the total protein concentration of the samples was omitted since a Coomassie staining was done in almost all cases enabling to visualize the total protein content per sample (see 3.7.1 Coomassie staining) and the SDS-PAGE was to be used for exclusively qualitative Western blotting analysis. Protein samples were diluted in washing buffer or distilled water

depending on the homogenization procedure that was followed, and sample loading buffer was added in equal volumes with the samples. The sample loading buffer contained 125 mM Tris, 4.5 M urea, 20 % (v/v) glycerol, 4 % (w/v) SDS, 0.02 % (w/v) bromophenol blue and 5 % (v/v) β-mercaptoethanol. Proteins were denatured by heating at 100°C for 10 min (see Appendix III). Samples were loaded into NuPAGE 4-12 % Bis-Tris gels (15-well or 10-well) in the XCell SureLock Mini-Cell electrophoresis system, where NuPAGE MES SDS Running Buffer that is recommended for separating small- or medium-sized proteins and NuPAGE antioxidant that improves band sharpness were added. Except for protein samples, appropriate protein standards were loaded into the gels, including SeeBlue Plus2 Pre-Stained Standard or Precision Plus Protein Kaleidoscope Prestained Protein for observing the protein migration on the gel and MagicMark XP Western Protein Standard for matching the molecular weight size of the protein bands during imaging. Gel electrophoresis was performed at 180 V constant for 45 min.

3.6 Immunoblotting (Western blot)

3.6.1 Semi-dry transfer

Immobilon-FL PVDF transfer membrane cut into the appropriate size for the gel (usually 8.5 cm x 7.5 cm) was wet for 1 min in methanol and soaked for 5 min in transfer buffer, which consisted of 100 mM Tris, 192 mM glycine and 5 % (v/v) methanol. Several pieces of thin filter paper (Munktell, Grade 1 F), cut into the same size as the PVDF membrane, were briefly soaked in transfer buffer and stalked together to produce a 2.5-mm-thick layer. After SDS-PAGE, the gel was rinsed with transfer buffer. Transfer stacks were prepared in a Novex Semi-Dry Blotter consisting of a bottom layer of filter paper, the PVDF membrane, the gel and a top layer of filter paper. Transfer was carried out at 200 mA for 50 min.

3.6.2 Immunostaining

Following transfer, membranes were blocked in LI-COR Odyssey Blocking Buffer (PBS) overnight. After removing the blocking buffer, membranes were

incubated for 1 h at 4°C with primary antibody diluted in Odyssey Blocking Buffer (PBS) containing 0.1 % (v/v) Tween-20. The primary antibodies that were used include Tau46 mouse anti-tau antibody (dilution 1:1000, Cell Signaling Technology), BC6 mouse anti-prion antibody (dilution 1.5:2000) and AT8 human anti-tau IgG1 (dilution 1:500, Thermo Fisher Scientific). The dilutions of the primary antibodies were re-used up to 5 times. Membranes were washed four times with PBS containing 0.1 % (v/v) Tween-20 and then incubated in dark with secondary antibody for 50 min at room temperature under constant shaking. The IRDye 680RD goat anti-mouse IgG diluted 1:10000 in 1 part Odyssey Blocking Buffer: 3 parts PBS containing 0.1 % (v/v) Tween-20 was used as secondary antibody. Four washes with PBS containing 0.1 % (v/v) Tween-20 were then carried out, which were followed by two additional washes with PBS to remove residual detergent. Immunoblotting imaging was performed by using the LI-COR Biosciences Odyssey Infrared Imaging System as well as the ImageStudio Lite Ver 5.0 and 5.2 software.

3.7 Protein staining

After gel electrophoresis, a protein-specific chemical reaction must be performed to make the proteins within the gel visible. Two different methods for protein staining were used including Coomassie and, occasionally, silver staining. Protein staining allowed a relative estimation of the total protein concentration per sample as well as on-gel detection of bands including tau isoforms.

3.7.1 Coomassie staining

Following SDS-PAGE, the gel to be used for Coomassie staining was incubated in appropriate amount of Expedeon InstantBlue protein stain solution for 1 h. InstantBlue is a Coomassie protein dye, which binds to basic and hydrophobic residues of proteins, changing in color from brown to blue. After two washes in distilled water to reduce background, the stained proteins on the gel were visualized by the Biorad Molecular Imager Gel Doc XR+ imaging system and the QuantityOne Ver 4.6.9 software. In general, Coomassie staining can detect 25 ng per band for most proteins. Proteins

stained by using InstantBlue are also compatible with mass spectrometric analysis.

3.7.2 Silver staining

Proteins separated on a gel were stained with the Invitrogen SilverXpress Kit by a multi-step process that includes fixation of the proteins in the gel matrix and facilitation of the necessary chemical reaction. The staining reagent contains silver ions that interact and bind to certain functional groups of the proteins. The sensitizer reagent controls the specificity and efficiency of silver ion binding to proteins, whilst the enhancer reagent is essential for the development of the bound silver to metallic silver resulting in a brown-black color. The stained proteins on the gel were visualized by the Biorad Molecular Imager Gel Doc XR+ imaging system and the QuantityOne Ver 4.6.9 software. Silver staining can normally detect less than 0.5 ng of protein in gels.

3.8 Protein quantification by BCA assay

For quantifying the total protein content of samples, the Pierce Microplate BCA Protein Assay Kit-Reducing Agent Compatible (Thermo Scientific) was used. The Albumin Standard (BSA) provided by the kit (2 mg/mL) was diluted accordingly in washing buffer (for washing buffer composition see 3.3 Biochemical extraction of soluble tau from mouse brain) to give the concentrations 125, 250, 500, 750, 1,000, 1,500, 2,000 μg/mL of Protein Standards. The same washing buffer was used as Standard Control (control that does not contain protein), which served as blank. Samples were used without being diluted and in triplicates similarly to the Standard Control and Protein Standards. The absorbance of the standards and the unknown samples were measured at 562 nm on a Synergy HT plate reader. The average values of the standards and samples were calculated, and the blank average absorbance was subtracted accordingly. A standard curve was produced in Microsoft Excel by plotting the average values of each Protein Standard relative to its concentrations (μg/mL), which was used to determine the total protein concentration of each unknown sample.

3.9 Protein digestion

For in-solution digestion[168], proteins in tau-purified samples were incubated with urea (5 M final) and reduced with 10 mM DTT for 10 min at 56 °C. The samples were alkylated with 20 mM IAA for 30 min at 18-23°C in the dark and, after another reduction with 10 mM DTT, 100 mM ammonium bicarbonate buffer was added. Trypsin digestion was carried out overnight at 37 °C with a 1:50 ratio of enzyme to total protein. Trypsin (10 mg/mL) was diluted in 100 mM ammonium bicarbonate to final concentration 0.1 mg/mL. Digested samples were acidified with 10 % (v/v) formic acid to pH 2-3 before analysis.

In-gel digestion was performed according to the protocol provided by the Proteomics and Metabolomics Facility of the Roslin Institute. After Coomassie staining, bands including tau isoforms according to the Western blot analysis were cut out and diced into 1 mm cubes. The bands were washed with 25 mM ammonium bicarbonate for 30 min and then in 25 mM ammonium bicarbonate and acetonitrile at a ratio of 1:1. After another wash in acetonitrile, the bands were dried in the Savant SpeedVac for 10 min. The proteins were reduced with 10 mM DTT for 1 h at 56^{o}C and alkylated with 55 mM IAA for 30 min in dark. After being washed and dried as before, trypsin solution was added to cover completely the gel pieces and trypsin digestion was carried out at 37^{o}C overnight. Trypsin (10 mg/mL) was diluted in 100 mM ammonium bicarbonate to final concentration 0.005 mg/mL. Samples were acidified with 100 % (v/v) formic acid to stop digestion and digested peptides were collected by incubating with extraction buffer that contains distilled water and 100 % (v/v) acetonitrile at a ratio of 1:1 as well as formic acid and dried in the Savant SpeedVac before analysis.

3.10 Mass spectrometry

For the identification of digested peptides and the detection of post-translational modifications on modified peptides that were derived from tau isoforms, liquid chromatography-mass spectrometry (LC-MS) was used, which was performed by Dr D. Kurian. The digested peptides were cleaned up using Pierce C18 SPE cartridges by following standard protocol described by Rappsilber *et al*. (2007)[206]. NanoflowLC-MS/MS was performed on a micrOTOF-II mass spectrometer (Bruker) coupled to an RSLCnano LC system

(Thermo). Tryptic digest was delivered to a trap column (Acclaim PepMap100, 5 μm, 100 Å, 100 μm i.d. × 2 cm) at a flow rate of 20 μL/min in 100 % solvent A (0.1 % formic acid in LC-MS grade water). After initial loading and washing, peptides were transferred to an analytical column (Acclaim PepMap100, 3 μm, 100 Å, 75 μm i.d. × 25 cm) and separated at a flow rate of 300 nl/min using a 60-min gradient from 7 % to 35 % solvent B (solvent B, 0.1 % formic acid in acetonitrile). The eluted peptides from LC were electrosprayed directly on to the mass spectrometer for MS and MS/MS analysis in a data-dependent mode of acquisition. The m/z values of tryptic peptides were measured using a MS scan (300-2000 m/z), followed by MS/MS scans of the three most intense ions. Rolling collision energy for fragmentation was selected based on the precursor ion mass and a dynamic exclusion was applied for 30 sec.

Dr D. Kurian also processed the raw spectral data using DataAnalysis software (Bruker) and the resulting peak lists were searched using Mascot 2.4 server (Matrix Science) against a custom database containing mouse tau protein. Mass tolerance on peptide precursor ions was set at a maximum of 25 ppm and on fragment ions at 0.1 Da. The peptide charge was set to 2+ and 3+. Carbamidomethylation of cysteine was selected as a fixed modification and oxidation of methionine, acetylation, methylation, dimethylation and trimethylation of lysine, phosphorylation of serine, threonine and tyrosine and methylation of arginine residues were chosen as variable modifications.

The development of a quantitative LC-MS/MS methodology was performed with the help of Dr A. Gill. All mass spectrometry was performed by use of an EasyNano-LC (Bruker Daltonics) capillary HPLC system interfaced to an Amazon ETD ion trap mass spectrometer (Bruker Daltonics) that was equipped with an electrospray ion source. Protein samples were digested with trypsin, as detailed in section 3.9 Protein digestion, and 8 μl samples were injected onto a microtrapping device packed with Bioshell A400 Protein C4 beads of 3.4 μm diameter. The trap was washed with a further 30 μl of HPLC buffer A (0.1 % (v/v) formic acid in 96:4 water:acetonitrile) to remove non-retained components, such as salts. The peptide separation was developed by use of a capillary column of dimensions 200 μm i.d., 100 mm length packed with Halo Peptide ES-C18 beads of 2.7 μm diameter. Peptides were eluted by a gradient from HPLC buffer A to buffer B (0.1 % (v/v) formic acid in 4:96 water:acetonitrile) of 0-40% B over 45 minutes. The flow rate was 1.5 μl/min.

For initial full scan experiments, the mass spectrometer was set to scan between m/z 250-1500 in enhanced resolution mode, with a scan speed of 8,100 m/z /sec. For multiple reaction monitoring (MRM) experiments, the potential signals from the ions of interest were identified from shotgun proteomics data; the mass spectrometer was then operated in MS/MS mode and set to fragment each of the 3 parent ions. The following conditions were used: ion trap filling was set for 200000 ions or no more than 200 ms; amplitude 0.6, cutoff m/z 200, enhanced resolution scan mode. Full scan mass spectra of product ions were acquired between m/z 200 –1500. The data were processed to produce extracted ion chromatograms associated with the transitions 697.3→416.3; 737.3→416.3; 777.3→416.3. These chromatograms were smoothed and integrated according to standard algorithms and the area under each peak was calculated.

4. Results

4.1 Biochemical extraction of soluble endogenous tau from mouse brain and mass spectrometric identification of tau post-translational modifications

4.1.1 Extraction of soluble tau from normal mouse brain

The investigation of tau post-translational modifications by mass spectrometry enables large-scale identification and analysis of possible modified sites throughout the tau molecule. However, it requires the preparation of a sample that is enriched with tau extracted from brain tissues of interest, whereas it contains as little as possible of other proteins. Also, the sample preparation is necessary to be as simple as possible, because the more steps that are involved the more chance there is of quantitation being lost regarding that the same sample can be used for both identification and quantification of post-translational modifications. As a result, the first aim of this work was to extract soluble endogenous tau from normal mouse brains by using a protocol that achieves the highest possible enrichment and purity of tau in a single step. Thereby, the protocol based on tau solubility in 1 % (v/v) PCA was used for the extraction of soluble tau according to Ivanovova *et al*. (2008), which additionally allows tau to maintain its phosphorylation state[201]. Nevertheless, this agrees with the fact that tau displays resistance to acidic treatment, due to its unfolded character, maintaining thus its biological function that depends primarily on its phosphorylation[88]. However, there is no evidence on how other post-translational modifications might be affected by treatment with PCA.

One brain was homogenized manually each time and the homogenate was kept on ice to allow the depolymerization of microtubules and the highest possible harvest of tau. Next, the centrifugation of the homogenate at low

rotational speed produced a supernatant representing the soluble tau fraction and a pellet consisting of unbroken tissue, whole cells, nuclei, mitochondria, lysosomes and peroxisomes. The supernatant was concentrated with simultaneous buffer exchange (concentrated s/n) and along with the aliquots of the brain and the pellet was analyzed by immunoblotting incubating with the Tau46 primary antibody. Tau46 detects all isoforms of murine tau recognizing the amino acid sequence of an epitope within the C-terminal end of tau. In contrast to human brain, the adult mouse brain almost exclusively expresses the three 4R tau isoforms (0N4R, 1N4R, 2N4R) with apparent molecular weights on SDS-PAGE electrophoresis at 52, 59 and 67 kDa, respectively[61, 90].

As shown in **Figure 4.1A**, the western blot analysis of the samples using the Tau46 primary antibody reveals the presence of all three expected tau isoforms

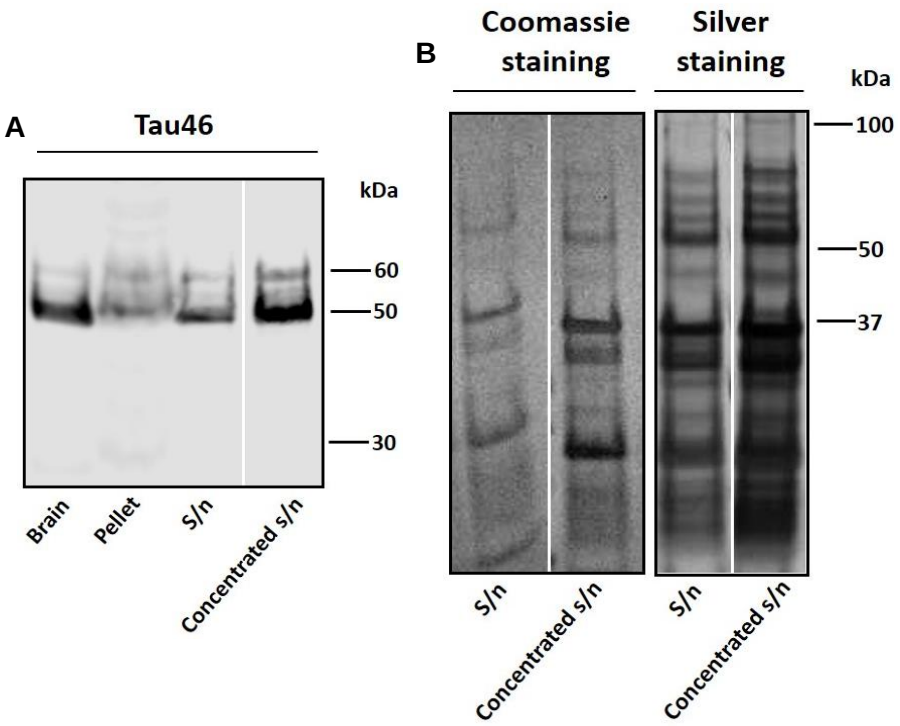

Figure 4.1 Normal mouse brain was homogenized in 1 % (w/v) PCA for the biochemical extraction of soluble endogenous tau. A. Western blot analysis using Tau46 shows that three tau isoforms are detected at about 50 - 70 kDa. B. Gels were stained with Coomassie and silver, showing that the amount of protein in the soluble-tau fraction is relatively low enabling to be further analysed by MS.

in all samples at about 50 – 70 kDa. Furthermore, low-signal bands that are present in lower molecular weights (see pellet lane) might represent truncated forms of tau isoforms. The pellet seems to include some soluble tau, presumably since it contains unbroken tissues and whole cells. In addition, the concentrated supernatant is the only case that it could be safely suggested that contains larger amount of tau compared to the supernatant, since it derives from the last. In all other cases, conclusions about the relative amounts of tau in each sample could not be extracted, because sample protein quantification did not precede the western blotting.

Moreover, a Coomassie and silver staining were carried out allowing to appreciate the purity level of tau in the soluble-tau fraction (**Figure 4.1B**). Both staining procedures suggest that the total amount of other non-tau proteins in the soluble-tau fraction is relatively low so as to allow further analysis and that there are protein bands that are quite distinguishable at about 50 – 70 kDa that contain tau, potentially amongst other proteins of the same molecular weight.

To confirm that the extraction procedure was suitable for purifying soluble tau and was repeatable, another brain was homogenized and analysed as above (**Figure 4.2A, B**). Both the immunoblot and protein staining analysis suggest that the extraction with 1 % (v/v) PCA achieved relatively high enrichment of tau and, hence, it was a suitable purification protocol of tau to be further analysed, whereas an additional purification step was not necessary. As a result, the total protein concentration of the soluble-tau fraction derived from this normal brain was identified by the BCA assay to be about 808 μg/ml (**Figure 4.2C**). The identification of the protein concentration was necessary in order to calculate the amount of trypsin required for protein digestion.

Having shown that the amount of other proteins in the soluble-tau fraction is relatively low, an in-solution preparation and trypsin digestion was performed (for the whole list of proteins detected by MS in the soluble-tau fraction see Appendix IV; **Supplementary Table 1**). Proteins in solution were denatured and their disulphide bonds were reduced by treatment with DTT. Next, cysteine residues were alkylated by treatment with IAA, in order to prevent the formation of inter- and intra-molecular disulphide bonds. In mouse tau, two cysteine residues, C291 and C322 found in the R2 and R3 repeat, respectively, are available to form disulphide bonds, given that the mouse brain expresses only 4R isoforms that include the additional R2 repeat.

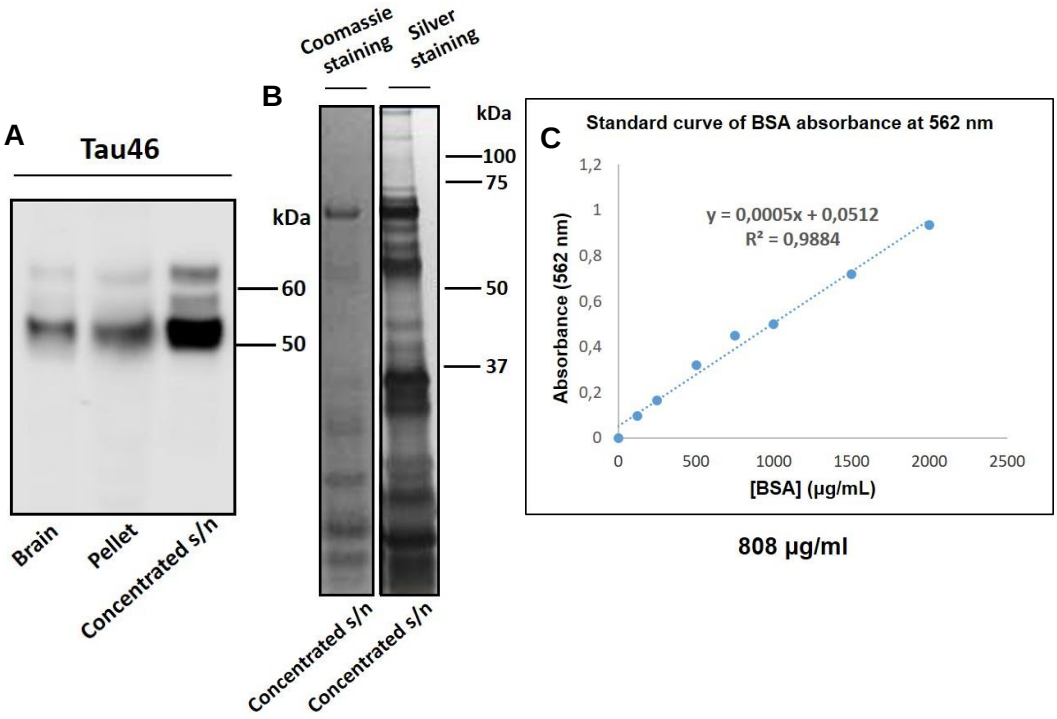

Figure 4.2 Normal mouse brain was homogenized in 1 % (w/v) PCA for the biochemical extraction of soluble endogenous tau. A. Western blot analysis using Tau46 shows that three tau isoforms are detected at about 50 - 70 kDa. B. Gels were stained with Coomassie and silver, showing that the amount of protein in the soluble-tau fraction is relatively low enabling to be further analysed by MS. C. The BCA assay was carried out for quantifying the total protein content of the soluble-tau fraction (concentrated s/n). Based on the BSA absorption of light at 562 nm, a standard curve was produced, and the protein concentration was identified to be about 808 µg/mL.

The sample was incubated with trypsin overnight and the resulting peptides were analysed by LC-MS. However, in a separate experiment an in-gel digestion was also carried out in order to further purify tau before mass spectrometric analysis by collecting the SDS-PAGE gel region from 50 to 70 kDa and, consequently, to enhance the specificity of the analysis.

Five types of post-translational modifications occurring on soluble endogenous tau under normal conditions were identified including serine phosphorylation, threonine phosphorylation, tyrosine phosphorylation, lysine acetylation and lysine trimethylation (**Table 4.1**). The specific modified sites were assigned according to the longest isoform of mouse tau (430 amino acids mouse isoform) as well as the homologous longest human isoform (441

amino acids human isoform). However, since tau peptides identified by MS were matched with the tau isoform found in the peripheral nervous system, which consists of 733 amino acids, some modified sites could not be found in either the homologous mouse or human isoform due to absence of these sequences. Since the literature typically follows the human numbering, the mass spectrometric data were analysed according to the human tau isoform, with the exception of S167 (serine phosphorylation) and K179 (lysine methylation) that are not found on the homologous human tau sequence. Two peptides were modified by methionine oxidation at M250 and M419, respectively. However, whether they truly represent biologically-significant post-translational modifications of tau or result from the preparation procedure was not able to be tested as part of this work and, consequently, they will not be considered as tau putative post-translational modifications. The following data include analysis of the modifications of tau peptides derived by both in-solution and in-gel digestion and were matched with Uniprot database against both overall protein entries and tau entries exclusively. Although the matching of the tryptic peptides with known entries indicates specific sites where post-translational modifications may occur, further analysis is needed in order to confirm these modifications.

Table 4.1 Endogenous post-translational modifications that have been detected on soluble tau under normal conditions. The tryptic peptides that were detected by mass spectrometry are listed, including both the modified and unmodified ones, along with the specific type and sites of post-translational modifications. The sites are numbered according to the mouse 430 isoform as well as the homologous human 441 isoform.

Peptides detected by MS	Post-translational modification	Modified residue (Mouse 430 isoform)	Modified residue (Human 441 isoform)
K.QMKLK.G	Lysine trimethylation Lysine acetylation	- -	- -
R.GAASPAQKGTSN ATRIPAK.T	-	-	-
R.GAASPAQKGTSN ATRIPAKTTPSPK.T	-	-	-
R.GAASPAQKGTSN ATRIPAKTTPSPK.T	Lysine acetylation	K152	K163
R.GAASPAQKGTSN ATRIPAKTTPSPK.T	Lysine trimethylation	K152	K163
K.TTPSPKTPPGSGEP PKSGER.S	Lysine acetylation	K169	K180

K.TTPSPKTPPGSGEPPKSGER.S	Serine phosphorylation Lysine acetylation	S167 K169	- K180
K.TTPSPKTPPGSGEPPKSGER.S	Threonine phosphorylation	T170	T181
K.TTPSPKTPPGSGEPPK.S	Serine phosphorylation Lysine methylation	S174 K179	S185 -
K.TPPGSGEPPKSGER.S	-	-	-
R.SGYSSPGSPGTPGSR.S	-	-	-
R.SGYSSPGSPGTPGSR.S	Serine phosphorylation	S187	S198
R.SGYSSPGSPGTPGSR.S	Serine phosphorylation	S188	S199
R.SGYSSPGSPGTPGSR.S	Serine phosphorylation	S191	S202
R.SGYSSPGSPGTPGSR.S	Serine phosphorylation Serine phosphorylation	S188 S191	S199 S202
R.SGYSSPGSPGTPGSR.S	Serine phosphorylation Serine phosphorylation	S187 S191	S198 S202
R.SRTPSLPTPPTREPK.K	-	-	-
R.SRTPSLPTPPTREPK.K	Serine phosphorylation	S203	S214
R.SRTPSLPTPPTREPK.K	Threonine phosphorylation	T206	T217
R.TPSLPTPPTREPK.K	-	-	-
K.KVAVVRTPPKSPSASK.S	Threonine phosphorylation	T220	T231
R.TPPKSPSASK.S	Lysine acetylation	K223	K234
R.LQTAPVPMPDLK.N	-	-	-
R.LQTAPVPMPDLK.N	Methionine oxidation	M239	M250
R.LQTAPVPMPDLKNVR.S	Methionine oxidation	M239	M250
K.LDLSNVQSK.C	-	-	-
K.KLDLSNVQSK.C	Lysine acetylation	K270	K281
K.HVPGGGSVQIVYKPVDLSKVTSK.C	Tyrosine phosphorylation Lysine trimethylation Lysine trimethylation Threonine phosphorylation Serine phosphorylation Lysine trimethylation	Y299 K300 K306 T308 S309 K310	Y310 K311 K317 T319 S320 K321
K.SEKLDFKDRVQSK.I	-	-	-
K.IGSLDNITHVPGGGNK.K	-	-	-

K.KIETHKLTFRENAK.A	-	-	-
R.HLSNVSSTGSIDMVDSPQLATLADEVSASLAK.Q	Serine phosphorylation	S405	S416
R.HLSNVSSTGSIDMVDSPQLATLADEVSASLAK.Q	Serine phosphorylation Methionine oxidation	S401 M408	S412 M419

The majority of the modified sites detected in soluble tau under normal conditions are located within the proline-rich region, whereas a few have been found in the MBD and C'-terminal region (**Figure 4.3**). Four lysine residues were detected to be acetylated during this project, including K163, K180, K234 and K281. Apart from K234, the remaining acetylated sites were identified previously by *in vivo* studies[162, 166, 168]. Furthermore, four lysine residues were detected to be trimethylated under normal conditions, at K163, K311, K317 and K321. In addition, lysine K163 seems to be target of both acetylation and trimethylation suggesting that tau post-translational modifications might compete for the same residues and, hence, it is likely they serve different physiological activities of tau in the brain. Most putative phosphorylation sites detected on soluble endogenous tau were also found in earlier studies in wild-type mouse brains. However, one phosphorylation site, at S185, was found in

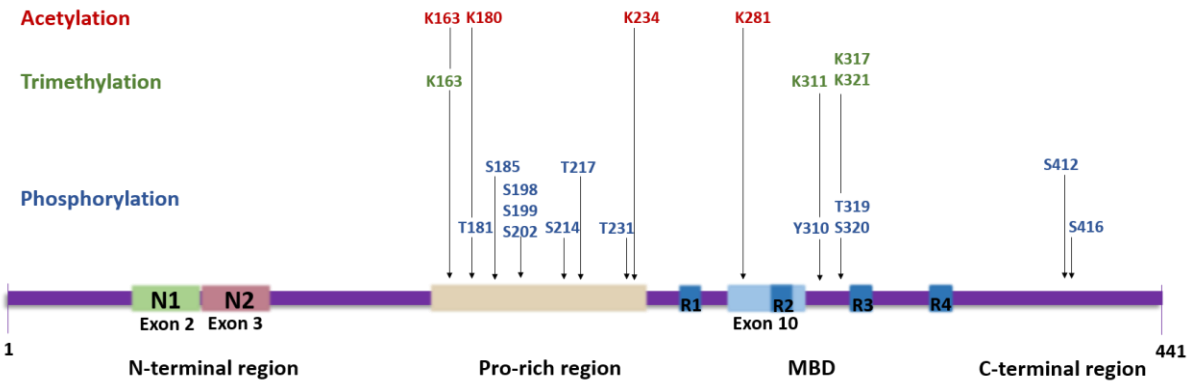

Figure 4.3 Putative post-translationally modified sites identified in soluble endogenous tau extracted from normal mouse brain by MS. Modifications are shown on the longest human tau isoform.

AD brain tissues exclusively, whereas this project shows that it is likely to be phosphorylated under normal conditions as well[139]. Y310 and T319, which were not fully characterized earlier, are shown here to be phosphorylated *in vivo* under normal conditions. Lastly, S320 is confirmed as a putative phosphorylation site seen under physiological conditions in endogenous mouse tau.

4.1.2 Extraction of soluble tau from 87V-VM mouse brain

To investigate the post-translational modifications that may be involved in differentiating pathological from normal tau, tau protein was extracted from 87V-VM mouse brain. Similar to the extraction of soluble tau from normal mouse brain, the isolation of soluble endogenous tau from 87V-VM mouse brain was carried out based on tau solubility in 1 % (v/v) PCA according to Ivanovova *et al*. (2008)[201]. The pool of the soluble-tau fraction collected from the 87V-VM brain consists possibly of various soluble tau molecules. Firstly, normally "folded" tau proteins are present most likely serving their normal biological functions in the brain. As characteristically seen in conformational diseases, some of the proteins responsible for the observed neuropathology are present in their proper folding[207]. In addition, the spreading of tau pathology in 87V-VM brains is restricted to limited brain tissues. Also, soluble tau molecules prior to aggregation may be included in the soluble-tau fraction, characterized by a differentiated biochemically state compared to normal tau. Another tau species possibly found in the soluble-tau fraction is abnormal tau derived from filamentous tau aggregates that deposit in 87V-VM brain tissues that are soluble in PCA[208].

One 87V-VM brain was homogenized manually similarly to the normal brain (See 4.1.1 Extraction of soluble tau from normal mouse brain). The samples were analysed by immunoblotting incubating with two different primary antibodies, Tau46 and AT8. As shown in **Figure 4.4A**, the western blot analysis of the samples using both primary antibodies demonstrates the presence of all three expected tau isoforms at about 50 – 70 kDa. In contrast to Tau46 that recognizes the amino acid sequence of an epitope within the C-

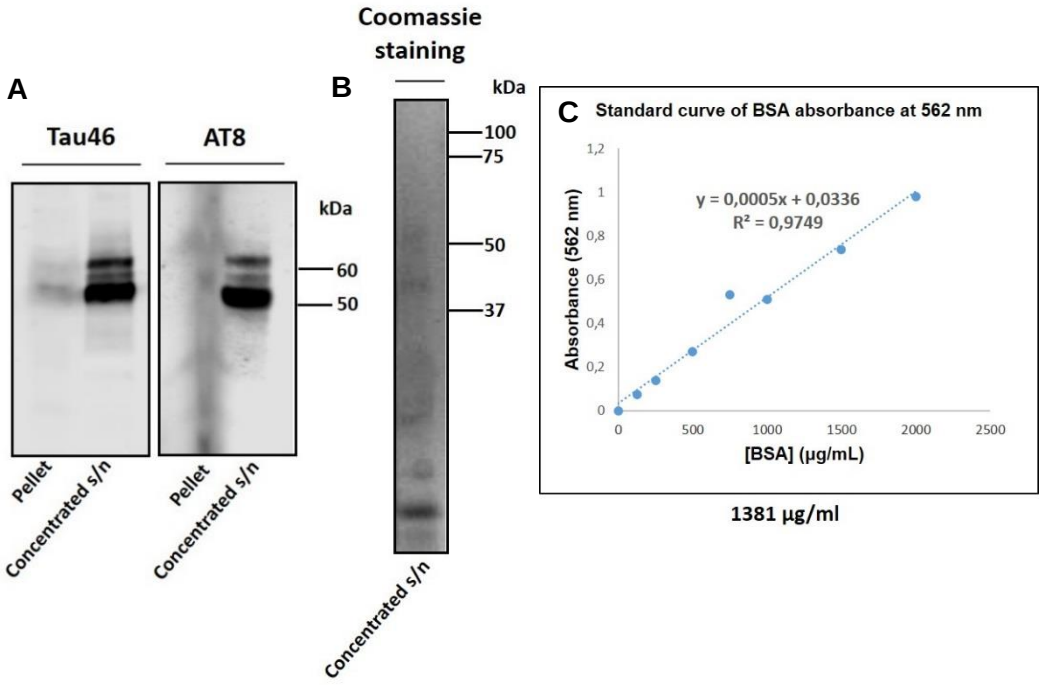

Figure 4.4 87V-VM mouse brain was homogenized in 1 % (w/v) PCA for the biochemical extraction of soluble endogenous tau. A. Western blot analysis using both Tau46 and AT8 shows that three tau isoforms are detected at about 50 - 70 kDa. By using the AT8 antibody is shown that soluble tau in the 87V-VM brain is phosphorylated at S202, T205 and S208. B. Gels were stained with Coomassie and silver, showing that the amount of protein in the soluble-tau fraction is relatively low enabling to be further analysed by MS. C. The BCA assay was carried out for quantifying the total protein content of the soluble-tau fraction (concentrated s/n). Based on the BSA absorption of light at 562 nm, a standard curve was produced, and the protein concentration was identified to be about 1381 µg/mL.

terminal end of tau, AT8 recognizes an epitope within the proline-rich region that is characterized by phosphorylation at S202, T205 and S208 exhibiting a hyperphosphorylated state associated with tau neuropathology[209, 210]. This shows that the soluble-tau fraction collected from the 87V-VM brain contains tau molecules that are phosphorylated at S202, T205 and S208. The phosphorylation of these sites on tau can be detected primarily in AD and, to a lesser extent, in normal brains, but S208 has been found to be possibly phosphorylated only in AD brains, indicating that the soluble-tau fraction includes abnormal soluble tau either prior to aggregation or derived from the filamentous aggregates directly after treatment with PCA. Moreover, a Coomassie staining was carried out allowing to appreciate the purity level of

tau in the soluble-tau fraction (**Figure 4.4B**) demonstrating that the total protein amount in the soluble-tau fraction is relatively low for further analysis. As a result, the overall protein concentration of the soluble-tau fraction derived from this 87V-VM brain was identified by the BCA assay to be about 1381 μg/ml (**Figure 4.4C**). The identification of the protein concentration was necessary in order to calculate the amount of trypsin required for protein digestion.

Having shown that the amount of total protein in the soluble-tau fraction is relatively low in the case of 87V-VM brain (for the whole list of proteins detected by MS in the soluble-tau fraction see Appendix IV; **Supplementary table 2**), an in-solution preparation and trypsin digestion were performed similarly to the sample derived from the normal mouse brain. Seven types of post-translational modifications occurring on soluble endogenous tau under pathological conditions were identified including serine phosphorylation, threonine phosphorylation, lysine acetylation, arginine methylation, lysine methylation, lysine dimethylation and lysine trimethylation (**Table 4.2**). The specific modified sites were assigned according to the longest isoform of mouse tau (430 amino acids mouse isoform) as well as the homologous longest human isoform (441 amino acids human isoform). Since tau peptides identified by MS were matched with the tau isoform found in the peripheral nervous system, which consists of 733 amino acids, some modified sites could not be matched with either the homologous mouse or human isoform due to absence of these sequences. In addition, the modified sites K139, S148, T165 and S167 are absent from the homologous human 441 isoform. Two peptides were detected to include methionine oxidation at M250 and M419, respectively, being the same sites that were found to be oxidized in the case of normal tau. Again, whether they represent truly post-translational modifications of tau or result from the preparation procedure was not able to be tested during this work, so they will not be considered as tau putative post-translational modifications. The following data include analysis of tau peptides derived by in-solution digestion after being matched with the Uniprot database against tau entries exclusively. Although the matching of the tryptic peptides with known entries indicates specific sites where post-translational modifications may occur, further analysis is needed to confirm these modifications.

Table 4.2 Endogenous post-translational modifications that have been detected on soluble tau under pathological conditions. The tryptic peptides that were detected by mass spectrometry are listed, including both the modified and unmodified ones, along with the specific type and sites of post-translational modifications. The sites are numbered according to the mouse 430 isoform as well as the homologous human 441 isoform.

Peptides detected by MS	Post-translational modification	Modified residue (Mouse 430 isoform)	Modified residue (Human 441 isoform)
R.QEFDTMEDHAGDYTLLQDQEGDMDHGLK.E	-	-	-
K.STPTAEDVTAPLVDER.A	-	-	-
R.APDKQAAAQPHTEIPEGITAEEAGIGDTPNQEDQAAGHVTQGR.R	Arginine methylation	R115	R126
K.QAAAQPHTEIPEGITAEEAGIGDTPNQEDQAAGHVTQGR.R	Arginine methylation	R115	R126
R.TGNDEKKAK.T	Lysine acetylation Lysine trimethylation	K127 K128	K140 K141
R.TGNDEKKAK.T	Lysine acetylation Lysine trimethylation	K128 K130	K141 K143
R.TGNDEKKAKTSTPSCAK.A	Lysine acetylation Lysine acetylation Lysine acetylation Threonine phosphorylation Lysine dimethylation	K127 K128 K130 - -	K140 K141 K143 - -
R.TGNDEKKAKTSTPSCAK.A	Lysine trimethylation Lysine acetylation Lysine acetylation Serine phosphorylation Lysine dimethylation	K127 K128 K130 - -	K140 K141 K143 - -
R.NGSPGTKQMK.L	Lysine trimethylation Methionine oxidation Lysine dimethylation	- - -	- - -
R.NGSPGTKQMKLKGADGKTGAK.I	Lysine dimethylation	-	-
R.NGSPGTKQMKLKGADGKTGAK.I	Serine phosphorylation Lysine dimethylation	- -	- -
R.NGSPGTKQMKLKGADGKTGAK.I	Lysine dimethylation Methionine oxidation Lysine trimethylation	- - -	- - -

	Lysine trimethylation	-	-
R.NGSPGTKQMKL KGADGKTGAK.I	Lysine dimethylation	-	-
	Methionine oxidation	-	-
	Lysine acetylation	-	-
	Lysine trimethylation	K135	K148
	Lysine dimethylation	K139	-
R.NGSPGTKQMKL KGADGKTGAK.I	Lysine dimethylation	-	-
	Methionine oxidation	-	-
	Lysine methylation	-	-
	Lysine trimethylation	-	-
	Lysine dimethylation	K135	K148
	Lysine dimethylation	K139	-
R.NGSPGTKQMKL KGADGKTGAK.I	Serine phosphorylation	-	-
	Lysine dimethylation	-	-
	Methionine oxidation	-	-
	Lysine dimethylation	-	-
	Lysine dimethylation	-	-
	Lysine trimethylation	K135	K148
	Lysine methylation	K139	-
K.QMKLK.G	Lysine acetylation	-	-
	Lysine trimethylation	-	-
K.LKGADGKTGAK IATPR.G	Lysine acetylation	K135	K148
	Threonine phosphorylation	T136	T149
K.TGAKIATPRGA ASPAQKGTSNATR IPAK.T	Lysine trimethylation	K139	K150
	Threonine phosphorylation	T142	T153
	Arginine methylation	R144	R155
	Serine phosphorylation	S148	-
	Lysine methylation	K152	K163
	Arginine methylation	R159	R170
R.GAASPAQKGTS NATRIPAK.T	Serine phosphorylation	S148	-
R.IPAKTTPSPK.T	Threonine phosphorylation	T165	-
	Serine phosphorylation	S167	-
	Lysine methylation	K169	K180
K.TTPSPKTPPGSG EPPKSGER.S	Threonine phosphorylation	T170	T181
K.TTPSPKTPPGSG EPPKSGER.S	Lysine methylation	K169	K180
	Lysine trimethylation	K179	K190
K.TTPSPKTPPGSG EPPK.S	Serine phosphorylation	S174	S185
	Lysine methylation	K179	K190
R.SGYSSPGSPGTP GSR.S	-	-	-
R.SGYSSPGSPGTP GSR.S	Serine phosphorylation	S188	S199
R.SRTPSLPTPPTRE PK.K	-	-	-

R.SRTPSLPTPPTREPK.K	Serine phosphorylation	S203	S214
R.SRTPSLPTPPTREPKK.V	Arginine methylation Threonine phosphorylation Threonine phosphorylation Arginine methylation Lysine trimethylation Lysine trimethylation	R200 T206 T209 R210 K213 K214	R211 T217 T220 R221 K224 K225
R.TPSLPTPPTR.E	-	-	-
R.TPSLPTPPTREPK.K	-	-	-
K.KVAVVRTPPKSPSASK.S	Threonine phosphorylation	T220	T231
K.KVAVVRTPPKSPSASK.S	Threonine phosphorylation Serine phosphorylation	T220 S224	T231 S235
R.LQTAPVPMPDLK.N	-	-	-
R.LQTAPVPMPDLK.N	Methionine oxidation	M239	M250
R.LQTAPVPMPDLKNVR.S	-	-	-
R.SKIGSTENLKHQPGGGKVQIINK.K	-	-	-
K.IGSTENLKHQPGGGKVQIINK.K	-	-	-
K.KLDLSNVQSK.C	Lysine acetylation	K270	K281
K.LDLSNVQSK.C	-	-	-
K.CGSKDNIKHVPGGGSVQIVYKPVDLSK.V	-	-	-
K.DNIKHVPGGGSVQIVYKPVDLSK.V	-	-	-
K.HVPGGGSVQIVYKPVDLSK.V	-	-	-
K.CGSLGNIHHKPGGGQVEVK.S	-	-	-
K.CGSLGNIHHKPGGGQVEVKSEK.L	-	-	-
K.SEKLDFKDR.V	Lysine acetylation Lysine methylation	K332 K336	K343 K347
K.SEKLDFKDR.V	Lysine acetylation Arginine methylation	K332 R338	K343 R349
K.SEKLDFKDRVQSK.I	Lysine methylation Serine phosphorylation Lysine trimethylation	K336 S341 K342	K347 S352 K353

K.IGSLDNITHVPG GGNK.K	-	-	-
K.IGSLDNITHVPG GGNK.K	Serine phosphorylation	S345	S356
K.IGSLDNITHVPG GGNKK.I	-	-	-
K.IGSLDNITHVPG GGNKK.I	Serine phosphorylation	S345	S356
K.IGSLDNITHVPG GGNKKIETHK.L	-	-	-
K.IGSLDNITHVPG GGNKKIETHK.L	Threonine phosphorylation Lysine acetylation Lysine dimethylation Lysine acetylation	T350 K358 K359 K364	T361 K369 K370 K375
K.AKTDHGAEIVY KSPVVSGDTSPR.H	-	-	-
K.AKTDHGAEIVY KSPVVSGDTSPR.H	Serine phosphorylation Serine phosphorylation	S385 S389	S396 S400
K.AKTDHGAEIVY KSPVVSGDTSPR.H	Serine phosphorylation	S393	S404
K.AKTDHGAEIVY KSPVVSGDTSPR.H	Serine phosphorylation Serine phosphorylation	S389 S393	S400 S404
K.AKTDHGAEIVY KSPVVSGDTSPR.H	Serine phosphorylation Serine phosphorylation Serine phosphorylation	S385 S389 S393	S396 S400 S404
K.TDHGAEIVYKSP VVSGDTSPR.H	-	-	-
K.TDHGAEIVYKSP VVSGDTSPR.H	Serine phosphorylation Serine phosphorylation Serine phosphorylation	S385 S389 S393	S396 S400 S404
K.TDHGAEIVYKSP VVSGDTSPR.H	Serine phosphorylation	S393	S404
K.TDHGAEIVYKSP VVSGDTSPRHLSN VSSTGSIDMVDSP QLATLADEVSASL AK.Q	Serine phosphorylation Serine phosphorylation Threonine phosphorylation	S385 S389 T392	S396 S400 T403
R.HLSNVSSTGSID MVDSPQLATLAD EVSASLAK.Q	-	-	-
R.HLSNVSSTGSID MVDSPQLATLAD EVSASLAK.Q	Serine phosphorylation Serine phosphorylation Serine phosphorylation	S398 S401 S402	S409 S412 S413
R.HLSNVSSTGSID MVDSPQLATLAD EVSASLAK.Q	Threonine phosphorylation Serine phosphorylation	T403 S405	T414 S416

R.HLSNVSSTGSID MVDSPQLATLAD EVSASLAK.Q	Serine phosphorylation	S405	S416
R.HLSNVSSTGSID MVDSPQLATLAD EVSASLAK.Q	Serine phosphorylation Methionine oxidation	S405 M408	S416 M419
K.SPVVSGDTSPRH LSNVSSTGSIDMV DSPQLATLADEVS ASLAK.Q	Serine phosphorylation Serine phosphorylation	S405 S411	S416 S422

The majority of the modified sites detected in soluble tau isolated from 87V-VM brain are located within the proline-rich and C'-terminal region, whereas a few have been found in other regions (**Figure 4.5**). Eight putative acetylation sites have been detected to occur on soluble tau under pathological conditions. Acetylation at K148 was found only by *in vitro* studies before, while three acetylation sites detected during this project were shown previously to be acetylated *in vivo* in wild-type mouse tau (K281, K343 and K369)[162, 168]. Several trimethylation sites were identified throughout tau sequence, four of which seem to can be possibly acetylated as well (K140, K141, K143 and K148). Two possible dimethylated sites were identified including K148, which is also target of acetylation and trimethylation, and K370, both of which agree with previous data collected by *in vitro* studies[169]. Five arginine residues were found to be probably methylated during this project. The remaining putative methylated sites include K163 that has been discovered previously in both normal and AD brains, K180 and K190 detected both *in vitro* and *in vivo* and, lastly, K347[167, 169]. Most putative phosphorylation sites detected on soluble endogenous tau from 87V-VM were found in earlier studies in both normal and AD brains[17, 139]. Three phosphorylation sites, at T153, S185 and S422, were found exclusively in AD brains in previous studies. On the other hand, T149, T220, S352, T361 and T414 that were assigned during this project as putative phosphorylation sites were demonstrated to be phosphorylated under normal conditions previously, indicating either that the soluble tau in 87V-VM brains is likely to include normal tau molecules or these sites are not responsible for differentiating normal tau to pathogenic, since they are commonly found under both normal and pathological conditions.

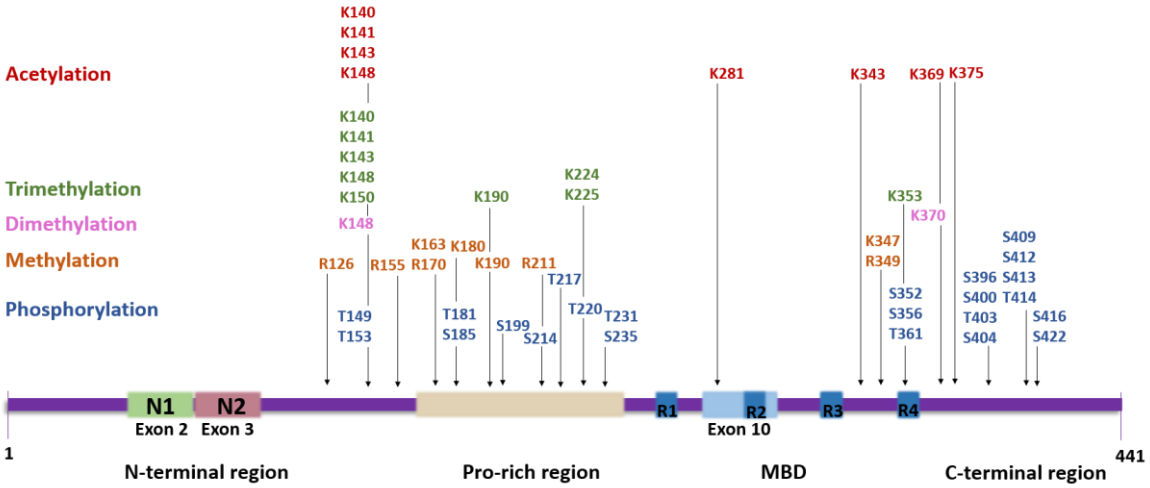

Figure 4.5 Putative post-translationally modified sites identified in soluble endogenous tau extracted from 87V-VM mouse brain by MS. Modifications are shown on the longest human tau isoform.

4.2 Biochemical extraction of insoluble aggregated tau from 87V-VM mouse brain and mass spectrometric analysis of tau post-translational modifications

The study of post-translational modifications that may govern the pathological shift of normal tau to insoluble aggregated that deposits in brain tissues, as observed characteristically in 87V-VM mouse brain, requires the collection and analysis of samples enriched with purified insoluble aggregated tau. Several methods are available in the literature for the isolation of aggregated tau species and, during this project, three of them were used with some modifications for the biochemical extraction of insoluble tau, including the protocols published by Planel *et al*. (2009), Greenberg and Davies (1990) and Cohen *et al*. (2011)[166, 203, 204]. Given that tau aggregates deposit surrounding prion amyloid plaques in the same tissues, a protocol for the extraction of pathological prion protein was used additionally according to Hope *et al*. (1988), in order to test if the immunohistochemical association of these two proteins allows their common biochemical extraction[205]. All methods were based on fractional centrifugation and incubation with the detergent sarkosyl. Significantly, tau in the sarkosyl-insoluble pellet has been characterized by immuno-electron microscopy to be filamentous in agreement with that identified by immunohistochemistry in NFTs[211].

The first protocol for the isolation of enriched insoluble tau (Greenberg and Davies) was used for homogenizing only one 87V-VM brain initially. In **Figure 4.6A1**, the sarkosyl-insoluble pellet that represents the insoluble aggregated tau fraction along with aliquots of other fractions were analysed by immunoblotting using the Tau46 primary antibody. Three tau isoforms are detected in both supernatants (s/n) at about 50 – 70 kDa that agrees with the fact that mouse brain expresses 4R tau isoforms almost exclusively. However, the insoluble-tau fraction seems to contain a low amount of tau implying that either the homogenization procedure was not successful or little aggregated tau was present in the 87V-VM brain. Apart from the inadequate enrichment of insoluble tau, the method did not also allow a sufficient purification, since the insoluble-tau fraction seems to contain many proteins stained with Coomassie making it necessary to further purify tau (**Figure 4.6C1**).

To try to increase the amount of insoluble tau isolated from 87V-VM brains, two and a half 87V-VM brains were homogenized according to Greenberg and Davies (**Figure 4.6A2**, **4.6C2**). Whereas the amount of insoluble tau was increased slightly compared to the sample derived from one brain and the total amount of proteins stained with Coomassie was not increased, this was probably not enough for insoluble tau to be detected by MS. For the same reason, two other protocols by Planel *et al*. (RIPA buffer) and Cohen *et al*. (Formic acid) were used and analyzed by immunoblotting showing that the amount of aggregated tau in 87V-VM brains is relatively low to be analysed by MS (**Figure 4.6A3**, **4.6A4**). Furthermore, four 87V-VM brains were used in the case of the protocol for extracting pathological prion protein. This protocol was performed successfully since the western blot analysis by incubating with the anti-prion BC6 primary antibody revealed that the pathological prion protein is enriched in the sarkosyl-insoluble pellet (**Figure 4.6B1**). On the contrary, the protocol failed to harvest appreciable levels of insoluble aggregated tau, as the western blot analysis by incubating with both Tau46 and AT8 primary antibodies suggests (**Figure 4.6B2**, **4.6B3**). Bands that are found out of the 50 – 70 kDa region may represent truncated forms of tau or result from various post-translational modifications that influence the migration of tau isoforms to larger molecular weights. Since all methods systematically led to an insoluble-sarkosyl pellet that contains low amount of aggregated tau, it is likely that the amount of aggregated tau in 87V-VM brains is relatively low.

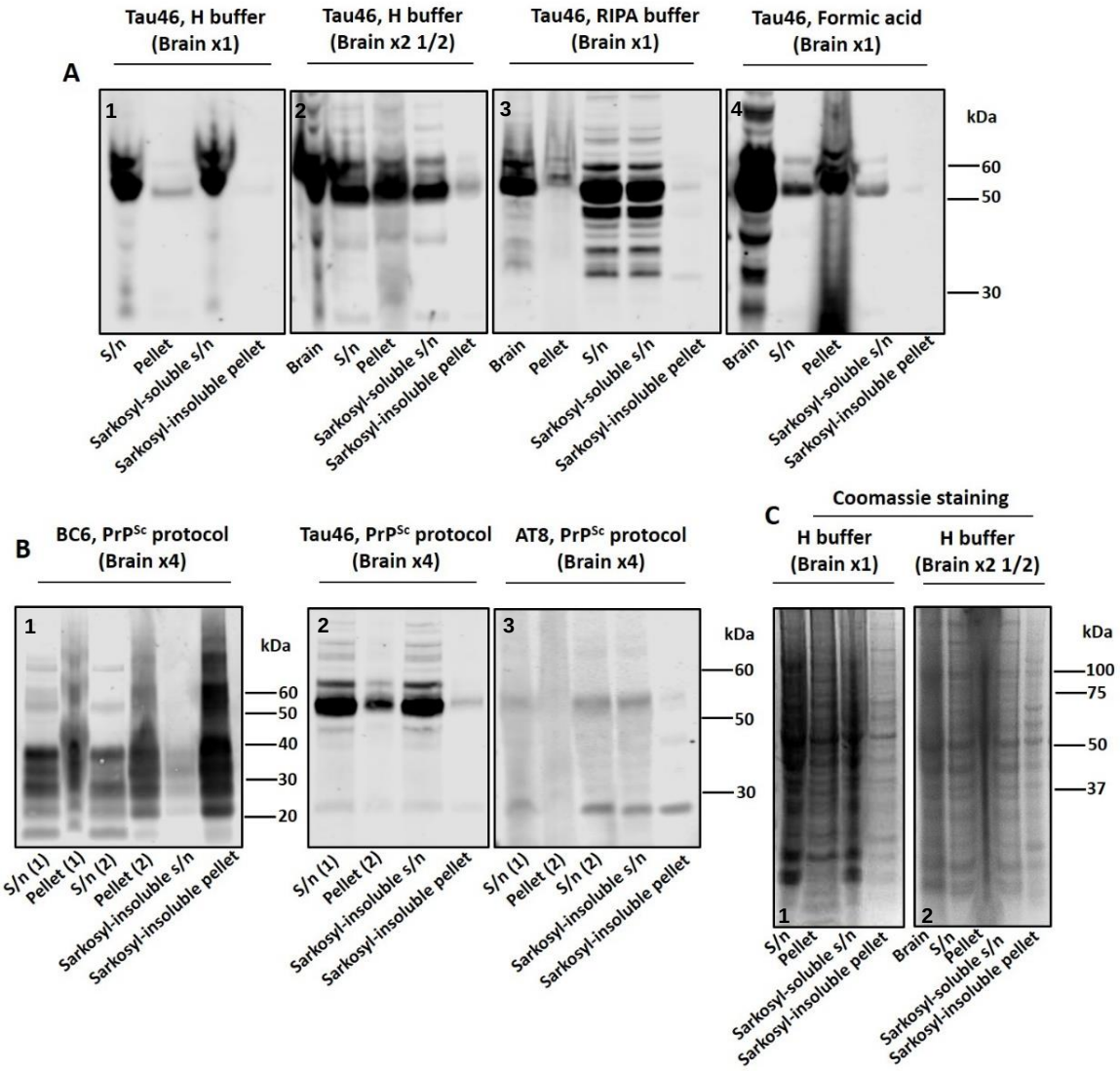

Figure 4.6 A. Different protocols were used for the extraction of insoluble aggregated tau from 87V-VM brains including those published by Greenberg and Davies using H buffer for the homogenization step (blot 1 and 2), Planet *et al*. using RIPA buffer for the homogenization step (blot 3) and Cohen *et al*. using formic acid for the extraction of insoluble tau (blot 4). The insoluble-tau fraction seems to contain low amount of aggregated tau in order to be further analysed by mass spectrometry in all cases. B. A protocol for the extraction of pathological prion protein was carried out enabling to identify the characteristic bands of PrP^{Sc} (blot 1). However, incubation with both Tau46 and BC6 reveals that the content of insoluble-tau fraction in aggregated tau is low, in agreement with previous protocols (blot 2 and 3). C. SDS-PAGE gels stained with Coomassie for the protocol by Greenberg and Davies are shown indicating that this protocol allows to reach a satisfactory purity level in the case of the sarkosyl-insoluble pellet, but an additional step is needed for enhancing the purification of tau (staining 1 and 2).

Owing to the fact that the protocol by Greenberg and Davies achieves a relatively adequate purification of the insoluble-tau fraction and, therefore, could be a suitable protocol for extracting purified insoluble tau, another 87V-VM brain was homogenised aiming to enhance the yield of insoluble tau. In this case, the insoluble-tau fraction was collected as previously and concentrated by using the Amicon Microcon Centrifugal Filter Devices until reaching a quarter of the initial volume used to resuspend the sarkosyl-insoluble pellet. The samples were analyzed by western blotting using Tau46. As shown in **Figure 4.7A**, the concentrated insoluble-tau fraction included increased amounts of aggregated-derived tau compared to the initial fraction allowing to proceed in analysis of the sample by mass spectrometry. Despite that, the purification level of the protocol was not sufficient, the protein bands were quite distinguishable, as revealed by Coomassie staining (**Figure 4.7B**), pointing out that an additional purification step was necessary.

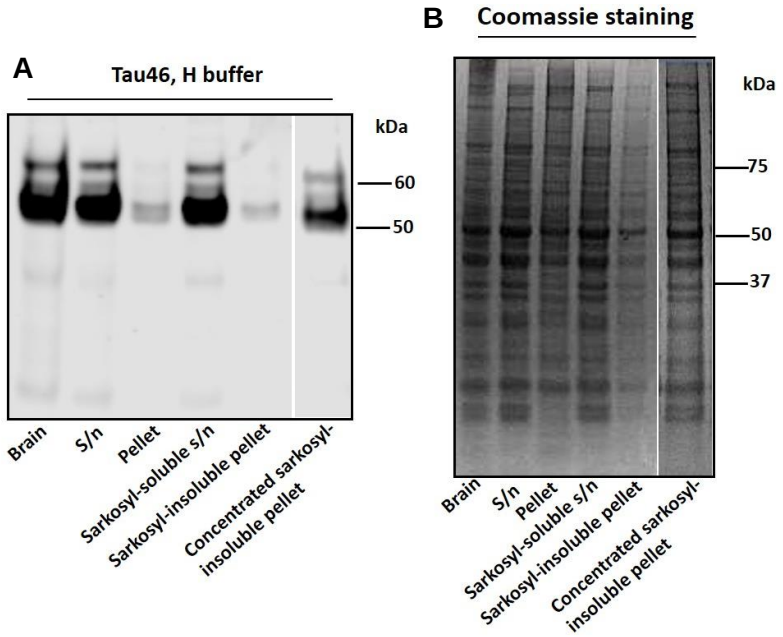

Figure 4.7 87V-VM mouse brain was homogenized according to Greenberg and Davies for the biochemical extraction of insoluble aggregated tau. A. Western blot analysis using Tau4 shows that three tau isoforms are detected at about 50 - 70 kDa and the concentration of the insoluble-tau fraction contains increased amount of insoluble tau. B. Gel was stained with Coomassie showing that the amount of total protein in the concentrated insoluble-tau fraction is not adequately low enabling the sample to be further analysed by MS, so an additional purification step is needed.

As a result, the additional purification of insoluble tau was achieved by extracting from the SDS-PAGE gel a region between 50 to 70 kDa that contains the three isoforms of mouse tau among other proteins of the same molecular weight and performing in-gel preparation and digestion of the proteins (for the whole list of proteins detected by MS in the insoluble-tau fraction from 50 to 70 kDa see Appendix IV; **Supplementary table 3**). In contrast to previous preparations, the proteins were denatured by SDS before gel electrophoresis but not reduced and alkylated aiming to increase the sensitivity of tau identification by MS. Six types of post-translational modifications occurring on insoluble endogenous tau under pathological conditions were identified including serine phosphorylation, threonine phosphorylation, arginine methylation, lysine methylation and lysine dimethylation (**Table 4.3**). The specific modified sites were assigned according to the longest isoform of mouse tau (430 amino acids mouse isoform) as well as the homologous longest human isoform (441 amino acids human isoform). Since tau peptides identified by MS were matched with the tau isoform found in the peripheral nervous system, which consists of 733 amino acids, some modified sites could not be matched with either the homologous mouse or human isoform due to absence of these sequences. One peptide was detected to include methionine oxidation at M250 being the same site that was found to be oxidized in the case of soluble tau. Again, whether it represents truly post-translational modification of tau or results from the preparation procedure was not able to be tested during this work, so it will not be considered as tau putative post-translational modification. The following data include analysis of tau peptides derived by in-gel digestion after being matched with the Uniprot database against both overall protein entries and tau entries only. Although the matching of the tryptic peptides with known entries indicates specific sites where post-translational modifications may occur, further analysis is needed to confirm these modifications.

Table 4.3 Endogenous post-translational modifications that have been detected on insoluble tau under pathological conditions. The tryptic peptides that were detected by mass spectrometry are listed, including both the modified and unmodified ones, along with the specific type and sites of post-translational modifications. The sites are numbered according to the mouse 430 isoform as well as the homologous human 441 isoform.

Peptides detected by MS	Post-translational modification	Modified residue (Mouse 430 isoform)	Modified residue (Human 441 isoform)
K.GTKEASLQEPPGKQPAAGLPGRPVSR.V	Threonine phosphorylation Lysine dimethylation Lysine trimethylation Serine phosphorylation	- - - -	- - - -
K.KAKTSTPSCAK.A	Lysine dimethylation Lysine methylation Serine phosphorylation Lysine dimethylation	K128 K130 - -	K141 K143 - -
K.GADGKTGAK.I	Lysine trimethylation	K135	K148
K.QMKLKGADGKTGAK.I	Methionine oxidation Lysine dimethylation Lysine dimethylation Lysine methylation Threonine phosphorylation Lysine trimethylation	- - - K135 T136 K139	- - - K148 T149 K150
R.SGYSSPGSPGTPGSR.S	-	-	-
R.SRTPSLPTPPTREPK.K	-	-	-
R.SRTPSLPTPPTREPK.K	Arginine methylation Serine phosphorylation Threonine phosphorylation Arginine methylation Lysine dimethylation	R200 S203 T209 R210 K213	R211 S214 T220 R221 K224
R.TPSLPTPPTREPK.K	-	-	-
R.LQTAPVPMPDLK.N	-	-	-
R.LQTAPVPMPDLK.N	Methionine oxidation	M239	M250
K.DRVQSKIGSLDNITHVPGGGNK.K	Serine phosphorylation Lysine dimethylation Lysine methylation	S341 K342 K358	S352 K353 K369
K.IGSLDNITHVPGGGNK.K	-	-	-

The modified sites detected in insoluble tau isolated from 87V-VM brain cluster in three distinct regions, at the end of the N'-terminal region, proline-

rich region and MBD, respectively (**Figure 4.8**). Two putative trimethylation sites have been detected to occur on aggregated tau, at K148 and K150, whereas tau can be possibly dimethylated at three different lysine residues (K141, K224 and K353) under pathological conditions, of which only K353 was shown to be dimethylated before by reductive methylation of recombinant tau[169]. Also, both lysine and arginine residues were found to be monomethylated. K148 and K369 were shown to be dimethylated and monomethylated, respectively, *in vitro* according to earlier studies[169]. Notably, despite that aggregated tau bears abnormal hyperphosphorylation on several sites throughout its sequence typically seen in tauopathies, insoluble tau extracted from 87V-VM brain seems to be slightly phosphorylated based on the mass spectrometric analysis performed up to date. Four phosphorylation sites were detected during this project to occur possibly on aggregated tau, including T149, S214, T220 and S352, all of which were identified previously under normal conditions. However, the pattern of site-directed post-translational modifications may vary between different species and pathologies. Since tau phosphorylation sites have been mostly assigned in AD, it is likely phosphorylation sites that have not been implicated in AD-related tau pathology to be pathogenic in other cases, including 87V-VM brains, and vice versa.

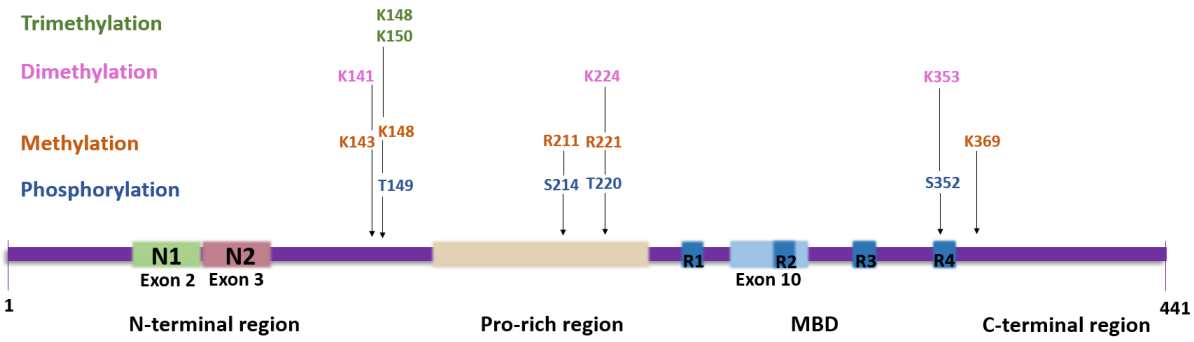

Figure 4.8 Putative post-translationally modified sites identified in insoluble aggregated tau extracted from 87V-VM mouse brain by MS. Modifications are shown on the longest human tau isoform.

Since the Greenberg and Davies protocol was successful in terms of extracting insoluble tau from 87V-VM brains for mass spectrometric analysis, further investigation of the protocol was performed. For this reason, a normal brain was homogenized accordingly and analysed by western blotting using both Tau46 and AT8 along with the 87V-VM brain. Also, anti-mouse secondary antibodies are able to recognize endogenous mouse immunoglobulins, even though their amount in brain is relatively low due to the presence of the blood brain barrier that blocks antibodies entrance into the brain. Therefore, being necessary to test whether there is any possible cross-reactivity, the samples were also analysed by western blotting using only secondary antibody (Ab_2).

As shown in **Figure 4.9**, incubation with Tau46 primary antibody identified three 4R tau isoforms at about 50 – 70 kDa in both normal and 87V-VM brains. The sarkosyl-insoluble pellet of normal brain contains remarkably low amount of tau, which is expected since normal brain does not contain insoluble aggregated tau theoretically. Compared to the sarkosyl-insoluble pellet from normal brain, the sarkosyl-insoluble pellet of the 87V-VM brain before being concentrated (see Figure 4.7) includes similarly low amount of insoluble tau. Only after concentration, insoluble tau could be detected by MS as it was discussed above. Moreover, incubation with secondary antibody exclusively revealed that there is some cross-reactivity, but it seems insignificant to take into consideration compared to the intense signal observed in other cases. Strangely, AT8 does not seem to react preferentially with tau derived from 87V-VM brains compared to normal tau. However, in the case of normal brain, tau bands detected by AT8 are likely to be present due to cross reactivity of the secondary antibody since both immunoblots are similar. On the other hand, this is not the case in the 87V-VM brains, where there was not detected any cross reactivity of the secondary antibody with tissue antibodies. Besides, inhibitors of phosphatases were not included in the homogenizing buffers leading possibly to the loss of all or some of the PHF-specific phosphorylation sites that are recognized by AT8 (S202, T205, S208). In agreement with this, these sites were not detected by MS to be modified in the insoluble-tau fraction from the 87V-VM brain.

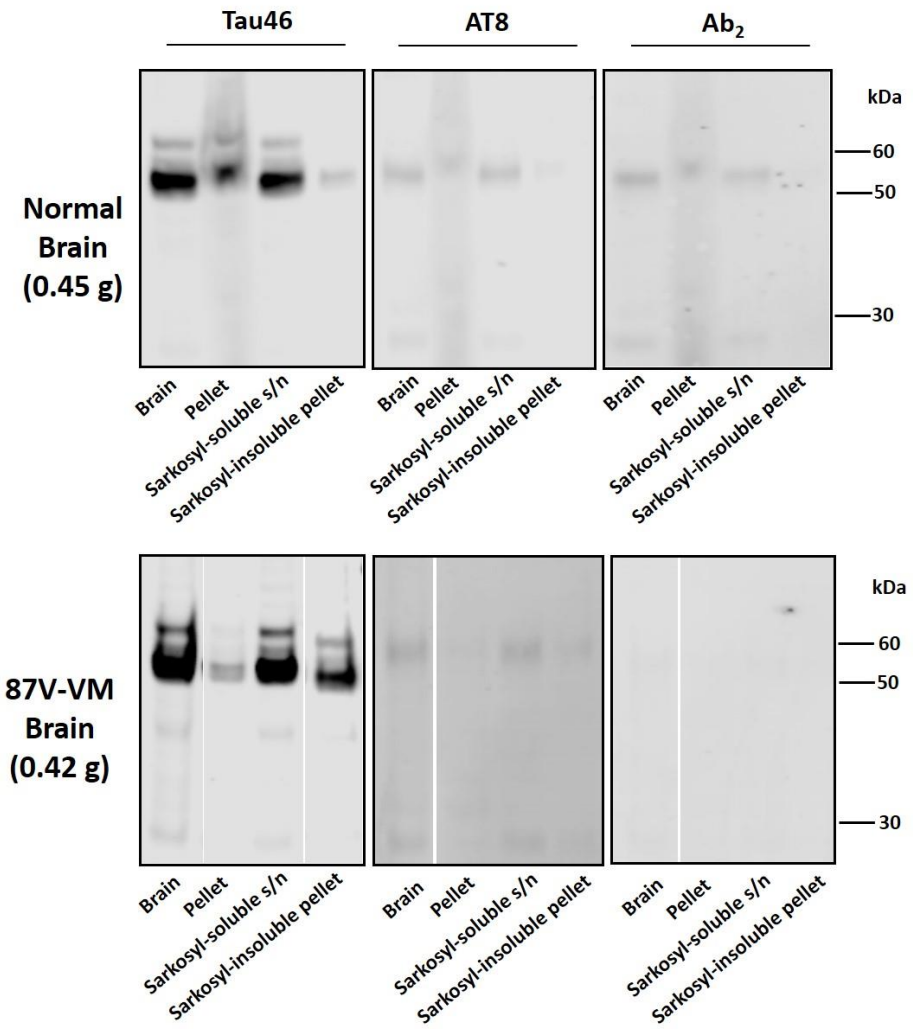

Figure 4.9 Normal and 87V-VM brains were homogenized according to Greenberg and Davies and analyzed by immunoblotting. By using Tau46, the immunoblot shows that all three 4R isoforms of mouse tau are detected at 50 – 70 kDa in both brains (left blots). Also, incubation with exclusively secondary antibody demonstrates some cross-reactivity with tissue immunoglobulins in the case of normal brain, but it can be considered negligible (right blots). AT8 does not seem to react preferably with tau derived from 87V-VM brains compared to normal tau (middle blots). The immunoblot that was generated by incubation with AT8 in the case of normal brain is similar to that showing the cross reactivity of the secondary antibody in contrast to the 87V-VM brain.

4.3 Phosphorylation state of soluble tau in 87V brains

As mentioned before (see 4.1.2 Extraction of soluble tau from 87V-VM mouse brain), the pool of soluble tau in 87V-VM brains extracted by treatment

with PCA may contain various tau proteins, including normal soluble tau properly folded, tau prior to aggregation and aggregated-derived tau given that PHF-tau was shown to display solubility in PCA[208]. By incubating with the AT8 primary antibody, western blot analysis showed that this soluble fraction contains phosphorylated tau on S202, T205 and S208 sites due to the fact that AT8 binds to a site-dependent phosphorylated epitope on tau protein[210]. AT8 is widely known to react specifically with PHF-tau in immunohistochemical studies. Also, it recognizes preferably PHF-tau on immunoblots, and to a lesser extent, normal tau isoforms, since both S202 and T205 are phosphorylated primarily in PHF-tau and less in tau from normal brains and S208 has been identified as a PHF phosphorylation site[209, 212, 213]. In addition, phosphorylation of S202 has been associated with the pathological shift of tau to an aggregated state, while double phosphorylation of S202/T205 was shown to trigger tau aggregation[212, 214].

Since abnormal hyperphosphorylation is considered to be the major trigger of tau malfunction in tauopathies and soluble hyperphosphorylated tau seems to have toxic properties, the phosphorylation state of soluble tau extracted from 87V-VM brain was explored during this project[13, 215]. For this reason, a normal and an 87V-VM mouse brain were homogenized in 1 % (v/v) PCA as previously described. Despite the obvious difference in their weight, this has been counterbalanced during the concentration of the soluble-tau fraction allowing further comparisons. The concentrated supernatant along with aliquots of the brain and pellet were analysed by western blotting using both Tau46 and AT8. Also, anti-mouse secondary antibodies are able to recognize endogenous mouse immunoglobulins, even though their amount in brain is relatively low due to the presence of the blood brain barrier that blocks antibodies entrance into the brain. As a result, being necessary to test whether there is any possible cross-reactivity, the samples were also analysed by western blotting using only secondary antibody (Ab_2).

As shown in **Figure 4.10**, the three 4R isoforms of mouse tau were detected by incubation with the primary antibodies Tau46 and AT8 in both normal and 87V-VM brain at about 50 – 70 kDa. Also, incubation with solely secondary antibody revealed that there is some cross-reactivity, but it seems insignificant to take into consideration compared to the intense signal observed in other cases. Notably, AT8 seems to react preferably with tau derived from 87V-VM brains compared to normal tau, which has remarkably lower signal almost

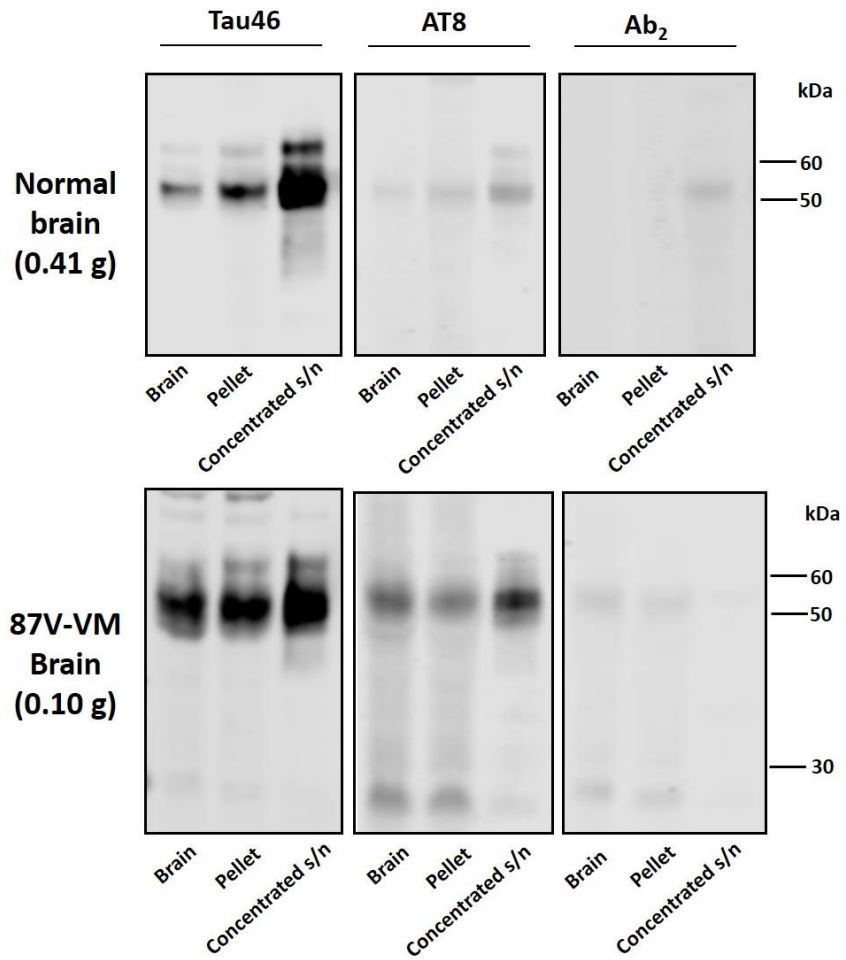

Figure 4.10 Phosphorylation, the most well studied tau post-translational modification, is differentiated between normal and 87V-VM brains. Western blot analysis using Tau46 shows that all three 4R isoforms of mouse tau are detected at 50 – 70 kDa in both brains (left blots). Also, incubation with solely secondary antibody demonstrates some cross-reactivity with tissue immunoglobulins, but it can be considered negligible (right blots). Soluble tau is phosphorylated in PHF-specific sites in the case of 87V-VM brain and, to a lesser extent, in normal brain, as results from western blotting using the AT8 primary antibody (middle blots). The difference in the brains weight was counterbalanced during the concentration of the soluble-tau fraction.

similar to being incubated with Ab_2. This argues that soluble tau in 87V-VM brains is possibly hyperphosphorylated in contrast to normal brains and precedes possibly tau aggregation, and/or biochemically confirms that filamentous aggregates being solubilized in PCA are abnormally hyperphosphorylated tau species typical for tauopathies. However, it has been proposed that AT8 exhibits high non-specificity and in combination with the

lack of tau negative and positive controls, it is more than necessary to further investigate the phosphorylation state of tau in 87V-VM brains[216].

4.4 Method development for quantifying tau post-translational modifications

One of the common features that characterizes tauopathies is the abnormal hyperphosphorylation of tau; however, different tau pathologies may vary depending on their phosphorylation pattern. Examining distinct patterns of phosphorylation and, by extension, of other post-translational modifications can be proved to be a useful tool for diagnosing tau neuropathological phenotypes. Previously, a quantitative method was established achieving to distinguish variable proteinase K-cleaved products of prion protein aiming ultimately to differentiate prion strains for diagnostic purposes[217]. For this reason, we took the first steps towards developing a similar biochemical method during this project based on mass spectrometric analysis for quantifying targeted phosphorylated peptides of tau existing in a pool of various tryptic peptides, which was achieved using a multiple reaction monitoring (MRM) process. According to the lists of tryptic peptides detected in the samples of purified tau, the peptide R.SGYSSPGSPGTPGSR.S was commonly detected in all three tau samples as detailed previously and is present in three different states: unphosphorylated, monophosphorylated at one of S198, S199 or S202 and diphosphorylated at either S198 and S202 or S199 and S202 (for the Mascot search results including the MS/MS spectra see Appendix V). It was, therefore, chosen to determine whether relative quantification of its variants may be possible on the crudely purified tau samples, in order to produce a ratio of different phosphorylation states in normal soluble tau that can be compared to respective ratios from soluble or insoluble aggregated tau extracted from 87V-VM brains and soluble tau extracted from mouse brain infected by a different prion strain (22F-VM).

Initially, the sample of soluble tau derived from normal brain was analysed by the Bruker AmaZon ETD mass spectrometer after being digested by trypsin, leading to the detection of all tryptic peptides included in the sample, as shown in **Figure 4.11**. Each state of the peptide of interest is characterized by a specific molecular mass and ionization state that is 697.3 Da, 2+ for non-

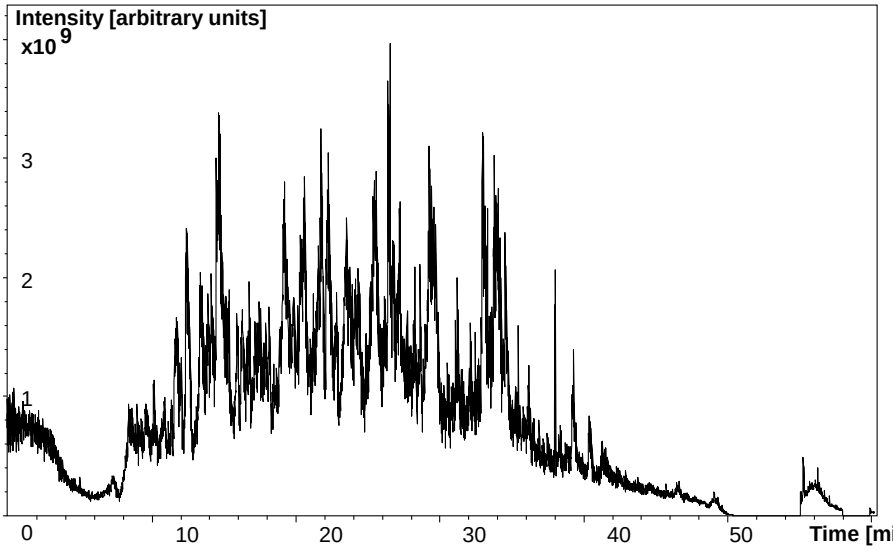

Figure 4.11 LC-MS/MS chromatogram of all digested peptides included in the sample of normal soluble tau.

phosphorylation, 737.3 Da, 2+ for monophosphorylation and 777.3 Da, 2+ for diphosphorylation. The same sample of normal soluble tau was analysed again, but this time the mass spectrometer was set to identify only the peptides that produce mass spectrometric signals of the preferable molecular mass in each case (**Figure 4.12**). These chromatograms show the presence of many signals from peptides that produce signals at m/z 697.3, 737.3 and 777.3, respectively. The isolation and subsequent quantification of these signals from the targeted tau peptides requires the identification of specific fragment ions for them. The ion fragmentation of the targeted peptides is based on the ratio m/z of y ions that seem to emerge from the C-terminal side of proline residues present in the peptides (**Table 4.4**), which are particularly susceptible to fragmentation due to their conformation. As a result, the LC-MS/MS spectra were collected for the fragmented tryptic peptides representing distinct phosphorylation patterns (**Figure 4.13**), all of which are characterized by the common presence of a fragment ion at m/z about 416.3. Based on this, extracted ion chromatograms that include the transitions 697.3→416.3, 737.3→416.3 and 777.3→416.3, respectively, were produced by processing the data demonstrated on Figure 4.12 (**Figure 4.14**). Each chromatogram was smoothed and integrated enabling to determine the area under the curve for

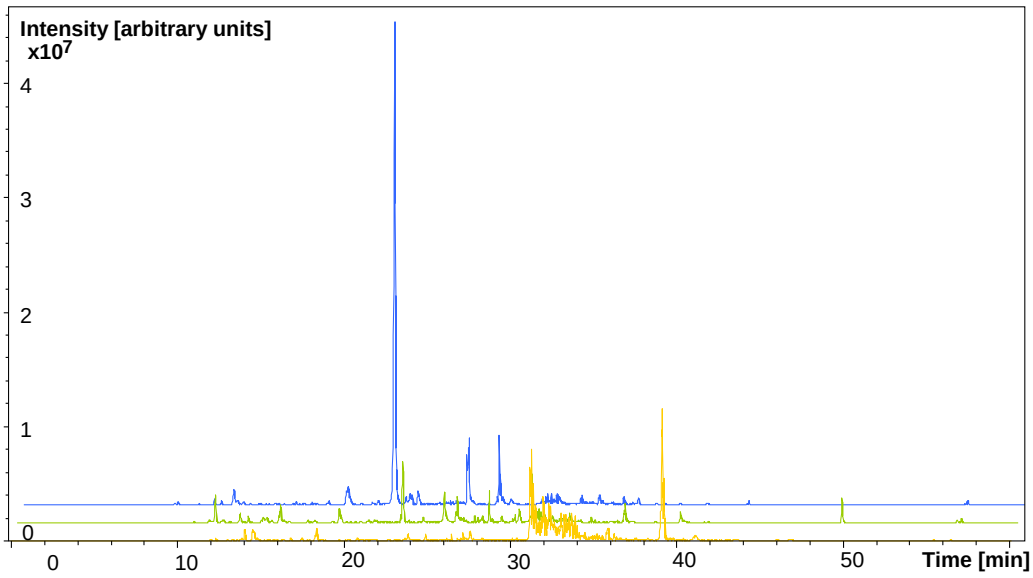

Figure 4.12 LC-MS/MS chromatograms of all digested peptides included in the sample of normal soluble tau that agree with the targeted molecular mass and ionization (blue for unphosphorylated state, 697.3 Da, 2+; green for monophosphorylated state, 737.3 Da, 2+; and orange for diphosphorylated state, 777.3 Da; 2+).

Table 4.4 MRM fragmentation ions for each peptide of certain phosphorylation state derived from normal soluble tau. The S4, S5, S8 represent the position of the putative phosphorylated serine residues on the peptide that correspond to S198, S199 and S202 on longest human tau isoform, respectively.

Peptide	Molecular mass (Da)	Ionization level	Phosphorylation state	y ion	Molecular mass of y ion (Da)
R.SGYSSPGS PGTPGSR.S	697.3	2+	0	PGSR	416.2
				PGTPGSR	671.3
				PGSPGTPGSR	912.4
R.SGYSSPGS PGTPGSR.S	737.3	2+	1	PGSR	416.2
				PGTPGSR	671.3
				PGSPGTPGSR	912.4 (S4 or S5) 894.4 (S8)
R.SGYSSPGS PGTPGSR.S	777.3	2+	2	PGSR	416.2
				PGTPGSR	671.3
				PGSPGTPGSR	894.4

the peptides in each phosphorylation state. As shown in Figure 4.14, in the case of normal soluble tau, two phosphorylation states were detected: unphosphorylated and monophosphorylated with the value of the integral to be 5969428.2 and 1503139.7, respectively. Although there is signal representing the diphosphorylated state, this was not above noise level, so as to be taken into consideration. Therefore, the above values produce a ratio of non-phosphorylation to monophosphorylation that is about 4 for normal soluble tau.

The same procedure that was followed for normal soluble tau can be repeated for different samples of purified tau, including soluble and insoluble tau isolated from 87V-VM brains as well as soluble tau derived from 22F-VM brain. In the case of soluble tau extracted from 87V-VM brain, two phosphorylation states were detected similarly to normal soluble tau: unphosphorylated and monophosphorylated with the value of the integral to be 27944402 and 5015785, respectively (**Figure 4.15**). No signal representing the diphosphorylated state above noise level was detected. Consequently, the above values produce a ratio of non-phosphorylation to monophosphorylation that is about 5.6 for soluble tau from 87V-VM brain. Similarly, analysis of the insoluble aggregated tau sample led to signals from unphosphorylated and monophosphorylated peptides (**Figure 4.16**). Although the signals from the unphosphorylated peptides are above noise level, the signals from the monophosphorylated peptides are too low to get reliable quantitation. Again, no signal representing the diphosphorylated state above noise level was detected. Lastly, in the case of soluble tau extracted from 22F-VM brain, all three phosphorylation states were detected: unphosphorylated, monophosphorylated and diphosphorylated with the value of the integral to be 942531.1, 270300.4 and 77090.2, respectively (**Figure 4.17**). Thereby, the above values produce a ratio of non-phosphorylation to monophosphorylation that is about 3.5 for soluble tau from 22F-VM brain. Since diphosphorylation failed to be detected in other cases, a ratio that involves diphosphorylation and either monophosphorylation or non-phosphorylation would not be helpful for further comparison.

Notably, the quantitation within an experiment should not be considered literally since variably phosphorylated peptides will fragment to generate the ion fragment 416.3 with different efficiencies and no normalization preceded quantification. Therefore, only between different experiments the relative

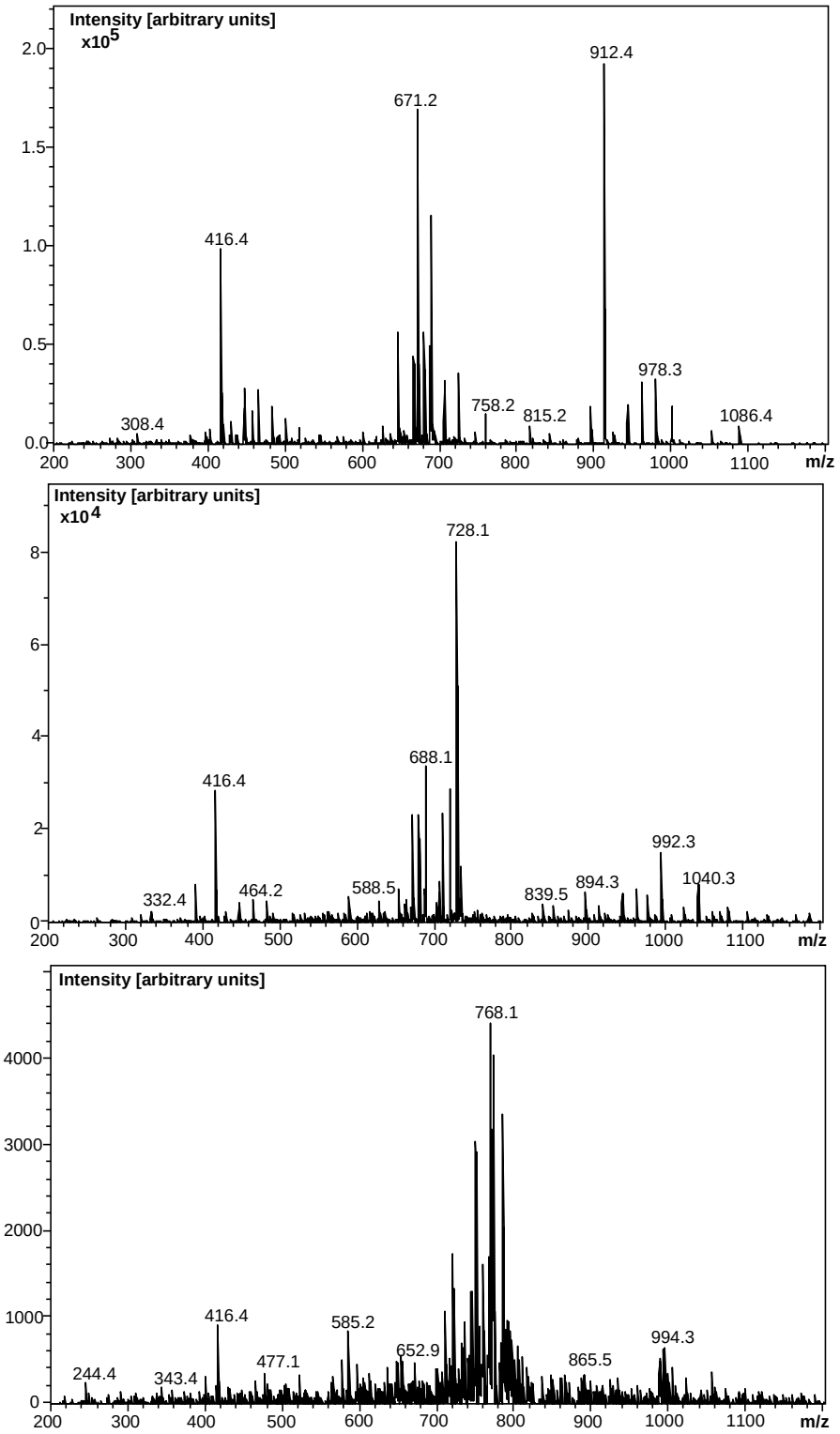

Figure 4.13 MS/MS spectra of unphosphorylated (top), monophosphorylated (middle) and diphosphorylated (bottom) peptides, respectively.

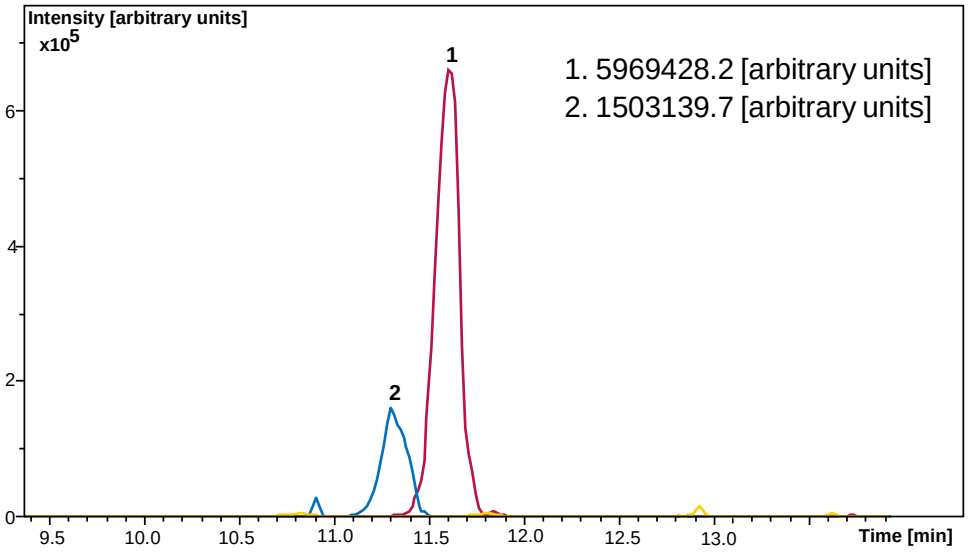

Figure 4.14 Smoothed and integrated extracted ion chromatograms of transitions from normal soluble tau. Chromatogram 1 (fuchsia) represents the unphosphorylated state of the targeted tau peptide and integration of the area under the curve gives a value of 5969428.2 [arbitrary units]. Respectively, chromatogram 2 (blue) represents the monophosphorylated state of the targeted tau peptide and integration of the area under the curve gives a value of 1503139.7 [arbitrary units].

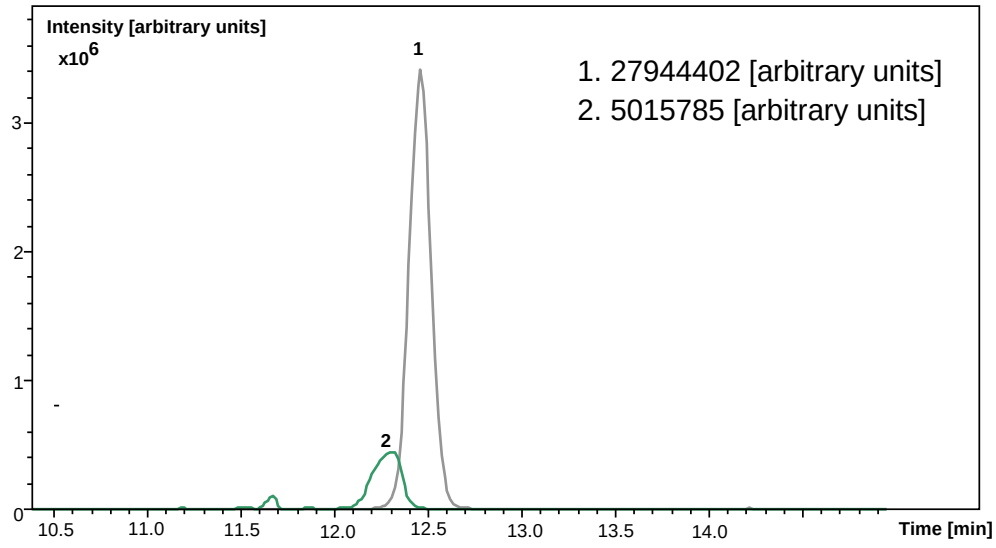

Figure 4.15 Smoothed and integrated extracted ion chromatograms of transitions from soluble tau extracted from 87V-VM brain. Chromatogram 1 (grey) represents the unphosphorylated state of the targeted tau peptide and integration of the area under the curve gives a value of 27944402 [arbitrary units]. Respectively, chromatogram 2 (green) represents the monophosphorylated state of the targeted tau peptide and integration of the area under the curve gives a value of 5015785 [arbitrary units].

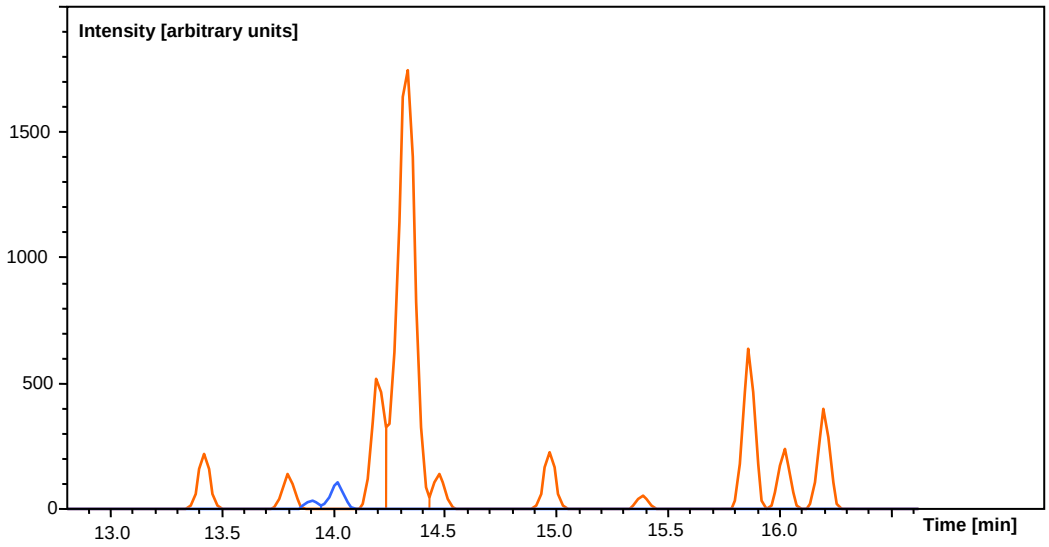

Figure 4.16 Smoothed, but not integrated extracted ion chromatograms of transitions from insoluble aggregated tau extracted from 87V-VM brain. The orange chromatogram represents the unphosphorylated state of the targeted tau peptide, whereas the blue chromatogram represents the monophosphorylated state of the targeted tau peptide.

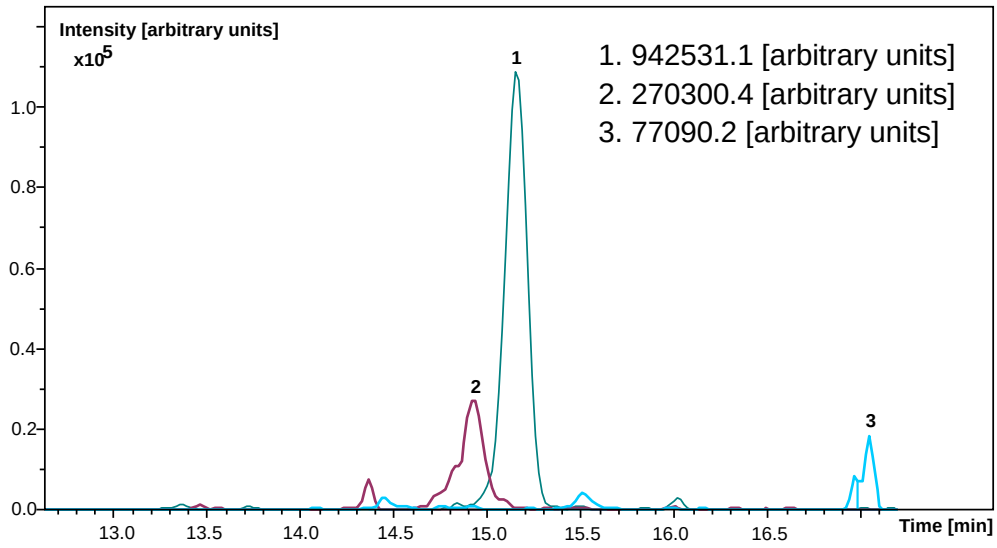

Figure 4.17 Smoothed and integrated extracted ion chromatograms of transitions from soluble tau extracted from 22F-VM brain. Chromatogram 1 (mint green) represents the unphosphorylated state of the targeted tau peptide and integration of the area under the curve gives a value of 942531.1 [arbitrary units]. Chromatogram 2 (purple) represents the monophosphorylated state of the targeted tau peptide and integration of the area under the curve gives a value of 270300.4 [arbitrary units]. Respectively, chromatogram 3 (turquoise) represents the diphosphorylated state of the targeted tau peptide and integration of the area under the curve gives a value of 77090.2 [arbitrary units].

quantification results that emerge after integration could be useful to examine the differences on the phosphorylation levels. In conclusion, the ratio of the unphosphorylated to monophosphorylated state was determined to be 4, 5.6 and 3.5 for soluble tau from normal, 87V-VM and 22F-VM brain, respectively. This suggests that the 87V-VM brains are less abundantly monophosphorylated possibly due to the presence of other post-translational modifications in the expense of phosphorylation. In agreement with this, a variety of post-translational modifications detected on soluble tau from 87V-VM brains has been displayed above that may prevent tau phosphorylation. On the other hand, soluble tau from 22F-VM brains seems to be relatively more monophosphorylated compared to the other cases. However, the above methodology requires validation by testing known abundances of phosphorylation states and reproducibility of the different measurements. Also, this methodology needs to be applied to various tau pathological cases before it is safely suggested that could be used as a diagnostic tool, whereas the sample preparation and the inclusion of other post-translational modifications would be important aspects.

5. Discussion and future perspectives

Tau is a highly soluble protein that undergoes several post-translational modifications that regulate both its subcellular localization and its physiological activity in the brain. In this study, using LC-MS, five types of post-translational modifications were identified occurring at 21 sites on crudely purified soluble endogenous tau under physiological conditions. Amongst them, 12 sites were found to be modified in wild-type or non-pathological transgenic mouse brains before. In contrast, one phosphorylation site, at S185, was found according to earlier studies in AD brain tissues exclusively. However, it is necessary to consider that the modification pattern of tau under normal conditions may vary between different species.

In addition, post-translational modifications of tau are likely to influence its misfolding and aggregation under pathological conditions in a site-dependent manner by altering the physicochemical properties of tau molecule. In 87V-VM mouse brains, tau aggregates were previously observed immunohistochemically in the vicinity of prion protein amyloid plaques proposing that prion dysfunction generates a pathogenic environment that promotes tau aggregation. In addition, the mouse brains used in this project were of relatively old age. In the brains of aged humans, tau lesions can be detected in a pathology called primary age-related tauopathy[218]. Although this type of tauopathy has not been detected in mouse brains, age is likely to be an additional factor underpinning tau pathology in 87V-VM brains. Using LC-MS, seven types of post-translational modifications were assigned to soluble tau crudely extracted from 87V-VM mouse brains occurring at 51 sites overall. Amongst these sites, 13 sites were previously detected under non-pathological conditions, whereas 22 sites were found under both normal and pathological conditions *in vivo*. In the case of insoluble aggregated tau extracted from 87V-VM brains, six types of post-translational modifications were found occurring at 14 sites merely.

Despite the obvious differences between the overall numbers of sites assigned to normal soluble tau, soluble and insoluble aggregated tau in 87V-VM brains, respectively, some post-translationally modified sites have been commonly identified. Nine modified sites are found in soluble tau in both normal and 87V-VM brains, including acetylated K281 and phosphorylated T181, S185, S199, S214, T217, T231, S412 and S416. This implies that these sites might not be required for tau transition to a pathological state and/or may play a physiological role in both cases given that soluble tau in 87V-VM brains may contain both pathologically differentiated as well as normally folded tau molecules. Respectively, soluble and insoluble aggregated tau from 87V-VM brains share seven common modified sites, which include trimethylated K148 and K150, methylated R211 and phosphorylated T149, S214, T220 and S352. These data suggest that these sites may facilitate tau pathology in 87V-VM brains, especially considering their absence from normal soluble tau. However, further investigation of tau post-translational modifications in normal brains is necessary in order to clarify if these sites are certainly absent from normal tau or failed to be detected during this project. Nevertheless, since only S214 was commonly found in all three distinct cases of purified tau, this argues that phosphorylation at S214 is possibly neutral in terms of its involvement in tau pathology in the 87V-VM brains. Of course, different post-translational modifications may characterize distinct tau pathologies.

Several post-translational modifications targeting lysine residues were chosen as fixed modifications during mass spectrometric analysis of tau samples. The detection of lysine residues in all samples that can be common targets of more than one type of modification proposes that it is likely tau post-translational modifications to compete each other for the same residues on tau in both health and pathology. Consequently, this crosstalk between tau lysine-directed modifications reveals a more complex regulation of tau biological activity under normal conditions as well as during misfolding and fibrillization, which begins to unfold as more modifications are mapped - and crucially quantified - and their role is investigated. Hence, further mass spectrometric investigation is needed for a more complete mapping of modified sites, in order to reveal the level of regulation they may serve in tau biology. Furthermore, many sites identified in this project appear to be distributed in the proline-rich region recommending that this region is possibly quite susceptible to modifications, which may control tau ability to

interact with other partners that are involved in intracellular signalling pathways[133].

Despite the presence of a few common residues, the distinct pattern of modified residues as was emerged in each of the three tau samples implies that different post-translational modifications control biochemically the state of tau in normal brains compared to 87V-VM brains bearing tau pathology. However, three aspects impose the need to further explore tau modified sites. Firstly, the investigation of tau post-translational modifications by MS can be a challenging process. Also, it is not known if the methods used for the biochemical extraction of tau from brain tissues during this project are suitable for preserving tau post-translational modifications especially considering the lack of inhibitors for the enzymes that catalyse the biochemical reactions in the homogenizing buffers. In addition, the abundance of modified peptides in combination with the stability of the modifications during mass spectrometric analysis are two parameters that can influence the detection of post-translational modifications[219]. Secondly, the assignment of specific sites, where detected modifications may occur, needs further confirmation, since the matching of tryptic peptides against known protein entries via Mascot 2.4 is merely indicative and, in a few cases, not even reliable. Assigned sites of interest could be additionally tested by fragmentation of the modified peptides by MS or western blotting using antibodies against site-dependent modified epitopes. Lastly, although soluble-tau extracted from 87V-VM brains reacts specifically with the AT8 primary antibody through a site-dependent phosphorylated epitope, the mass spectrometric analysis failed to detect the phosphorylated sites S202, T205 and S208. This indicates that the list of MS-detected modified sites on tau extracted from either normal or 87V-VM brain is not complete yet.

Concerning the methods used for the biochemical extraction of tau from mouse brains, the lack of positive controls cannot allow to estimate the purification and extraction level that has been achieved in each case. However, the fact that the samples collected during these methods were to be used for mass spectrometric analysis, their evaluation was based on the ability to detect post-translational modifications during the mass spectrometric analysis. Regarding the method used for the biochemical extraction of soluble tau, it achieved the highest possible enrichment and purity of soluble tau to be analysed subsequently by MS. On the other hand, whereas the method used

for the biochemical extraction of insoluble aggregated tau achieved the isolation of aggregated filamentous tau, the purity level was barely satisfying for further analysis by MS. Consistent with this, the number of post-translationally modified sites in the case of insoluble aggregated tau was relatively low compared to soluble tau, because the purity level affects the sensitivity of the MS to detect post-translational modifications, which is already a difficult task. Of course, an additional purification step during the extraction procedure would possibly cause the loss of some post-translational modifications. Instead, a further purification step was carried out during the in-gel preparation of the insoluble-tau sample for MS. However, since many methods were used for the isolation of insoluble aggregated tau and it was shown systematically that the amount of insoluble aggregated tau was low to be further analysed, it is quite likely the aggregated tau in 87V-VM brains to be present in low levels accordingly. For this reason, it would be useful to isolate specifically those brain tissues that were detected immunohistochemically to contain tau inclusions or increase the number of brains to be homogenized increasing, thus, the starting material and apply the same biochemical preparation for MS.

Site-specific post-translational modifications may preferentially affect tau biological activities under normal conditions as well as the properties of different pathological types of tau. Based on this, the initial steps for developing a methodology that quantifies certain post-translational modifications by LC-MS/MS, using a multiple reaction monitoring (MRM) process, were taken during this project. This methodology achieved to produce comparable ratios of different phosphorylation states (unphosphorylated to monophosphorylated) of a certain peptide for various tau samples allowing to examine the relative differentiation of tau phosphorylation between them. However, further development of this methodology is required in order to be able to reliably differentiate various tau properties.

Possible future objectives of the research that focuses on tau physiology and pathology in 87V-VM brains involve primarily the additional investigation of site-directed post-translational modifications occurring on tau clarifying, thus, distinct differences responsible for tau biological activity as well as misfolding. This could be processed by two possible ways. At first, as discussed above, certain regions in 87V-VM brains observed to include more densely tau

aggregates could be dissected and prepared for mass spectrometric analysis. This, thereby, could increase the total content of tau in the same volume unit, especially considering that 87V-VM brains may contain possibly low amount of aggregated tau. Similarly, more brains could be homogenized to increase the starting material. What is more, further optimization of the biochemical extraction of aggregated tau could be useful, in order to enhance both the harvest and purity of insoluble aggregated tau and the use of positive tau controls would allow the estimation of both parameters. Modified sites of interest, including those of high risk, could be quantified according to a methodology similar to this developed preliminarily during this project or could be explored in other ways aiming to reveal the underlying processes that they serve. For example, site-specific mutagenesis is one of the many possible approaches to study the impact of certain sites on tau biology. Lastly, it is worth investigating the impact of prion pathology on tau in terms of the interactions and processes that are involved in the development of tau aggregates in the case of 87V as well as different prion strains.

6. References

1. Kovacs, G.G. Molecular Pathological Classification of Neurodegenerative Diseases: Turning towards Precision Medicine. *Int J Mol Sci* **17** (2016).
2. Verkhratsky, A., Parpura, V., Pekna, M., Pekny, M. & Sofroniew, M. Glia in the pathogenesis of neurodegenerative diseases. *Biochem Soc Trans* **42**, 1291-301 (2014).
3. Jellinger, K.A. Basic mechanisms of neurodegeneration: a critical update. *J Cell Mol Med* **14**, 457-87 (2010).
4. Ramanan, V.K. & Saykin, A.J. Pathways to neurodegeneration: mechanistic insights from GWAS in Alzheimer's disease, Parkinson's disease, and related disorders. *Am J Neurodegener Dis* **2**, 145-75 (2013).
5. Herczenik, E. & Gebbink, M.F. Molecular and cellular aspects of protein misfolding and disease. *FASEB J* **22**, 2115-33 (2008).
6. Mahler, H.C., Friess, W., Grauschopf, U. & Kiese, S. Protein aggregation: pathways, induction factors and analysis. *J Pharm Sci* **98**, 2909-34 (2009).
7. Ferrer, I. et al. Glial and neuronal tau pathology in tauopathies: characterization of disease-specific phenotypes and tau pathology progression. *J Neuropathol Exp Neurol* **73**, 81-97 (2014).
8. Spillantini, M.G. et al. Familial multiple system tauopathy with presenile dementia: a disease with abundant neuronal and glial tau filaments. *Proc Natl Acad Sci U S A* **94**, 4113-8 (1997).
9. Hernandez, F. & Avila, J. Tauopathies. *Cell Mol Life Sci* **64**, 2219-33 (2007).
10. Gratuze, M., Cisbani, G., Cicchetti, F. & Planel, E. Is Huntington's disease a tauopathy? *Brain* **139**, 1014-25 (2016).
11. Spillantini, M.G. & Goedert, M. Tau pathology and neurodegeneration. *Lancet Neurol* **12**, 609-22 (2013).
12. Arendt, T., Stieler, J.T. & Holzer, M. Tau and tauopathies. *Brain Res Bull* **126**, 238-292 (2016).
13. Grundke-Iqbal, I. et al. Abnormal phosphorylation of the microtubule-associated protein tau (tau) in Alzheimer cytoskeletal pathology. *Proc Natl Acad Sci U S A* **83**, 4913-7 (1986).
14. Grundke-Iqbal, I. et al. Microtubule-associated protein tau. A component of Alzheimer paired helical filaments. *J Biol Chem* **261**, 6084-9 (1986).
15. Wisniewski, H.M. & Wen, G.Y. Substructures of paired helical filaments from Alzheimer's disease neurofibrillary tangles. *Acta Neuropathol* **66**, 173-6 (1985).
16. Goedert, M., Spillantini, M.G., Cairns, N.J. & Crowther, R.A. Tau proteins of Alzheimer paired helical filaments: abnormal phosphorylation of all six brain isoforms. *Neuron* **8**, 159-68 (1992).

17. Simic, G. et al. Tau Protein Hyperphosphorylation and Aggregation in Alzheimer's Disease and Other Tauopathies, and Possible Neuroprotective Strategies. *Biomolecules* **6**, 6 (2016).
18. Duyckaerts, C. et al. Modeling the relation between neurofibrillary tangles and intellectual status. *Neurobiol Aging* **18**, 267-73 (1997).
19. Komori, T. Tau-positive glial inclusions in progressive supranuclear palsy, corticobasal degeneration and Pick's disease. *Brain Pathol* **9**, 663-79 (1999).
20. Yoshida, M. Cellular tau pathology and immunohistochemical study of tau isoforms in sporadic tauopathies. *Neuropathology* **26**, 457-70 (2006).
21. Murray, M.E. et al. Clinicopathologic assessment and imaging of tauopathies in neurodegenerative dementias. *Alzheimers Res Ther* **6**, 1 (2014).
22. Spillantini, M.G. & Goedert, M. Tau protein pathology in neurodegenerative diseases. *Trends Neurosci* **21**, 428-33 (1998).
23. Lasagna-Reeves, C.A., Castillo-Carranza, D.L., Guerrero-Muoz, M.J., Jackson, G.R. & Kayed, R. Preparation and characterization of neurotoxic tau oligomers. *Biochemistry* **49**, 10039-41 (2010).
24. Clavaguera, F. et al. Transmission and spreading of tauopathy in transgenic mouse brain. *Nat Cell Biol* **11**, 909-13 (2009).
25. Lee, H.G. et al. Tau phosphorylation in Alzheimer's disease: pathogen or protector? *Trends Mol Med* **11**, 164-9 (2005).
26. Weingarten, M.D., Lockwood, A.H., Hwo, S.Y. & Kirschner, M.W. A protein factor essential for microtubule assembly. *Proc Natl Acad Sci U S A* **72**, 1858-62 (1975).
27. Dehmelt, L. & Halpain, S. The MAP2/Tau family of microtubule-associated proteins. *Genome Biol* **6**, 204 (2005).
28. Viereck, C., Tucker, R.P., Binder, L.I. & Matus, A. Phylogenetic conservation of brain microtubule-associated proteins MAP2 and tau. *Neuroscience* **26**, 893-904 (1988).
29. Cleveland, D.W., Spiegelman, B.M. & Kirschner, M.W. Conservation of microtubule associated proteins. Isolation and characterization of tau and the high molecular weight microtubule associated protein from chicken brain and from mouse fibroblasts and comparison to the corresponding mammalian brain proteins. *J Biol Chem* **254**, 12670-8 (1979).
30. RayChaudhuri, D. ZipA is a MAP-Tau homolog and is essential for structural integrity of the cytokinetic FtsZ ring during bacterial cell division. *EMBO J* **18**, 2372-83 (1999).
31. Goedert, M. et al. PTL-1, a microtubule-associated protein with tau-like repeats from the nematode Caenorhabditis elegans. *J Cell Sci* **109 (Pt 11)**, 2661-72 (1996).
32. McDermott, J.B., Aamodt, S. & Aamodt, E. ptl-1, a Caenorhabditis elegans gene whose products are homologous to the tau microtubule-associated proteins. *Biochemistry* **35**, 9415-23 (1996).
33. Heidary, G. & Fortini, M.E. Identification and characterization of the Drosophila tau homolog. *Mech Dev* **108**, 171-8 (2001).
34. Olesen, O.F., Kawabata-Fukui, H., Yoshizato, K. & Noro, N. Molecular cloning of XTP, a tau-like microtubule-associated protein from Xenopus laevis tadpoles. *Gene* **283**, 299-309 (2002).
35. Sundermann, F., Fernandez, M.P. & Morgan, R.O. An evolutionary roadmap to the microtubule-associated protein MAP Tau. *BMC Genomics* **17**, 264 (2016).
36. Trojanowski, J.Q., Schuck, T., Schmidt, M.L. & Lee, V.M. Distribution of tau proteins in the normal human central and peripheral nervous system. *J Histochem Cytochem* **37**, 209-15 (1989).
37. Binder, L.I., Frankfurter, A. & Rebhun, L.I. The distribution of tau in the mammalian central nervous system. *J Cell Biol* **101**, 1371-8 (1985).

38. LoPresti, P., Szuchet, S., Papasozomenos, S.C., Zinkowski, R.P. & Binder, L.I. Functional implications for the microtubule-associated protein tau: localization in oligodendrocytes. *Proc Natl Acad Sci U S A* **92**, 10369-73 (1995).
39. Dugger, B.N. et al. The Presence of Select Tau Species in Human Peripheral Tissues and Their Relation to Alzheimer's Disease. *J Alzheimers Dis* **54**, 1249 (2016).
40. Gu, Y., Oyama, F. & Ihara, Y. Tau is widely expressed in rat tissues. *J Neurochem* **67**, 1235-44 (1996).
41. Neve, R.L., Harris, P., Kosik, K.S., Kurnit, D.M. & Donlon, T.A. Identification of cDNA clones for the human microtubule-associated protein tau and chromosomal localization of the genes for tau and microtubule-associated protein 2. *Brain Res* **387**, 271-80 (1986).
42. Andreadis, A., Brown, W.M. & Kosik, K.S. Structure and novel exons of the human tau gene. *Biochemistry* **31**, 10626-33 (1992).
43. Baker, M. et al. Association of an extended haplotype in the tau gene with progressive supranuclear palsy. *Hum Mol Genet* **8**, 711-5 (1999).
44. Houlden, H. et al. Corticobasal degeneration and progressive supranuclear palsy share a common tau haplotype. *Neurology* **56**, 1702-6 (2001).
45. Caillet-Boudin, M.L., Buee, L., Sergeant, N. & Lefebvre, B. Regulation of human MAPT gene expression. *Mol Neurodegener* **10**, 28 (2015).
46. Poorkaj, P. et al. A genomic sequence analysis of the mouse and human microtubule-associated protein tau. *Mamm Genome* **12**, 700-12 (2001).
47. Sadot, E., Heicklen-Klein, A., Barg, J., Lazarovici, P. & Ginzburg, I. Identification of a tau promoter region mediating tissue-specific-regulated expression in PC12 cells. *J Mol Biol* **256**, 805-12 (1996).
48. Heicklen-Klein, A. & Ginzburg, I. Tau promoter confers neuronal specificity and binds Sp1 and AP-2. *J Neurochem* **75**, 1408-18 (2000).
49. Goedert, M., Wischik, C.M., Crowther, R.A., Walker, J.E. & Klug, A. Cloning and sequencing of the cDNA encoding a core protein of the paired helical filament of Alzheimer disease: identification as the microtubule-associated protein tau. *Proc Natl Acad Sci U S A* **85**, 4051-5 (1988).
50. Andreadis, A. Tau gene alternative splicing: expression patterns, regulation and modulation of function in normal brain and neurodegenerative diseases. *Biochim Biophys Acta* **1739**, 91-103 (2005).
51. Wang, Y., Loomis, P.A., Zinkowski, R.P. & Binder, L.I. A novel tau transcript in cultured human neuroblastoma cells expressing nuclear tau. *J Cell Biol* **121**, 257-67 (1993).
52. Drubin, D.G., Caput, D. & Kirschner, M.W. Studies on the expression of the microtubule-associated protein, tau, during mouse brain development, with newly isolated complementary DNA probes. *J Cell Biol* **98**, 1090-7 (1984).
53. Sadot, E., Marx, R., Barg, J., Behar, L. & Ginzburg, I. Complete sequence of 3'-untranslated region of Tau from rat central nervous system. Implications for mRNA heterogeneity. *J Mol Biol* **241**, 325-31 (1994).
54. Couchie, D. et al. Primary structure of high molecular weight tau present in the peripheral nervous system. *Proc Natl Acad Sci U S A* **89**, 4378-81 (1992).
55. Buee, L., Bussiere, T., Buee-Scherrer, V., Delacourte, A. & Hof, P.R. Tau protein isoforms, phosphorylation and role in neurodegenerative disorders. *Brain Res Brain Res Rev* **33**, 95-130 (2000).
56. Sergeant, N., Delacourte, A. & Buee, L. Tau protein as a differential biomarker of tauopathies. *Biochim Biophys Acta* **1739**, 179-97 (2005).

57. Goedert, M., Spillantini, M.G., Jakes, R., Rutherford, D. & Crowther, R.A. Multiple isoforms of human microtubule-associated protein tau: sequences and localization in neurofibrillary tangles of Alzheimer's disease. *Neuron* **3**, 519-26 (1989).
58. Andreadis, A., Broderick, J.A. & Kosik, K.S. Relative exon affinities and suboptimal splice site signals lead to non-equivalence of two cassette exons. *Nucleic Acids Res* **23**, 3585-93 (1995).
59. Hong, M. et al. Mutation-specific functional impairments in distinct tau isoforms of hereditary FTDP-17. *Science* **282**, 1914-7 (1998).
60. Lee, G., Neve, R.L. & Kosik, K.S. The microtubule binding domain of tau protein. *Neuron* **2**, 1615-24 (1989).
61. Takuma, H., Arawaka, S. & Mori, H. Isoforms changes of tau protein during development in various species. *Brain Res Dev Brain Res* **142**, 121-7 (2003).
62. D'Souza, I. & Schellenberg, G.D. Determinants of 4-repeat tau expression. Coordination between enhancing and inhibitory splicing sequences for exon 10 inclusion. *J Biol Chem* **275**, 17700-9 (2000).
63. Liu, F. & Gong, C.X. Tau exon 10 alternative splicing and tauopathies. *Mol Neurodegener* **3**, 8 (2008).
64. Hutton, M. et al. Association of missense and 5'-splice-site mutations in tau with the inherited dementia FTDP-17. *Nature* **393**, 702-5 (1998).
65. Wu, J.Y., Kar, A., Kuo, D., Yu, B. & Havlioglu, N. SRp54 (SFRS11), a regulator for tau exon 10 alternative splicing identified by an expression cloning strategy. *Mol Cell Biol* **26**, 6739-47 (2006).
66. Kondo, S. et al. Tra2 beta, SF2/ASF and SRp30c modulate the function of an exonic splicing enhancer in exon 10 of tau pre-mRNA. *Genes Cells* **9**, 121-30 (2004).
67. Broderick, J., Wang, J. & Andreadis, A. Heterogeneous nuclear ribonucleoprotein E2 binds to tau exon 10 and moderately activates its splicing. *Gene* **331**, 107-14 (2004).
68. Hernandez, F. et al. Glycogen synthase kinase-3 plays a crucial role in tau exon 10 splicing and intranuclear distribution of SC35. Implications for Alzheimer's disease. *J Biol Chem* **279**, 3801-6 (2004).
69. Smith, P.Y. et al. MicroRNA-132 loss is associated with tau exon 10 inclusion in progressive supranuclear palsy. *Hum Mol Genet* **20**, 4016-24 (2011).
70. D'Souza, I. & Schellenberg, G.D. Arginine/serine-rich protein interaction domain-dependent modulation of a tau exon 10 splicing enhancer: altered interactions and mechanisms for functionally antagonistic FTDP-17 mutations Delta280K AND N279K. *J Biol Chem* **281**, 2460-9 (2006).
71. Dickson, J.R., Kruse, C., Montagna, D.R., Finsen, B. & Wolfe, M.S. Alternative polyadenylation and miR-34 family members regulate tau expression. *J Neurochem* **127**, 739-49 (2013).
72. Cohen, J.E., Lee, P.R. & Fields, R.D. Systematic identification of 3'-UTR regulatory elements in activity-dependent mRNA stability in hippocampal neurons. *Philos Trans R Soc Lond B Biol Sci* **369** (2014).
73. Aronov, S., Marx, R. & Ginzburg, I. Identification of 3'UTR region implicated in tau mRNA stabilization in neuronal cells. *J Mol Neurosci* **12**, 131-45 (1999).
74. Behar, L., Marx, R., Sadot, E., Barg, J. & Ginzburg, I. cis-acting signals and trans-acting proteins are involved in tau mRNA targeting into neurites of differentiating neuronal cells. *Int J Dev Neurosci* **13**, 113-27 (1995).
75. Litman, P., Barg, J. & Ginzburg, I. Microtubules are involved in the localization of tau mRNA in primary neuronal cell cultures. *Neuron* **13**, 1463-74 (1994).
76. Larcher, J.C. et al. Ilf3 and NF90 associate with the axonal targeting element of Tau mRNA. *FASEB J* **18**, 1761-3 (2004).

77. Aronov, S., Aranda, G., Behar, L. & Ginzburg, I. Visualization of translated tau protein in the axons of neuronal P19 cells and characterization of tau RNP granules. *J Cell Sci* **115**, 3817-27 (2002).
78. Aronov, S., Aranda, G., Behar, L. & Ginzburg, I. Axonal tau mRNA localization coincides with tau protein in living neuronal cells and depends on axonal targeting signal. *J Neurosci* **21**, 6577-87 (2001).
79. Veo, B.L. & Krushel, L.A. Translation initiation of the human tau mRNA through an internal ribosomal entry site. *J Alzheimers Dis* **16**, 271-5 (2009).
80. Atlas, R., Behar, L., Elliott, E. & Ginzburg, I. The insulin-like growth factor mRNA binding-protein IMP-1 and the Ras-regulatory protein G3BP associate with tau mRNA and HuD protein in differentiated P19 neuronal cells. *J Neurochem* **89**, 613-26 (2004).
81. Atlas, R., Behar, L., Sapoznik, S. & Ginzburg, I. Dynamic association with polysomes during P19 neuronal differentiation and an untranslated-region-dependent translation regulation of the tau mRNA by the tau mRNA-associated proteins IMP1, HuD, and G3BP1. *J Neurosci Res* **85**, 173-83 (2007).
82. Morita, T. & Sobue, K. Specification of neuronal polarity regulated by local translation of CRMP2 and Tau via the mTOR-p70S6K pathway. *J Biol Chem* **284**, 27734-45 (2009).
83. Wang, J.Z. & Liu, F. Microtubule-associated protein tau in development, degeneration and protection of neurons. *Prog Neurobiol* **85**, 148-75 (2008).
84. Schweers, O., Schonbrunn-Hanebeck, E., Marx, A. & Mandelkow, E. Structural studies of tau protein and Alzheimer paired helical filaments show no evidence for beta-structure. *J Biol Chem* **269**, 24290-7 (1994).
85. Mukrasch, M.D. et al. Structural polymorphism of 441-residue tau at single residue resolution. *PLoS Biol* **7**, e34 (2009).
86. Mylonas, E. et al. Domain conformation of tau protein studied by solution small-angle X-ray scattering. *Biochemistry* **47**, 10345-53 (2008).
87. Jeganathan, S., von Bergen, M., Brutlach, H., Steinhoff, H.J. & Mandelkow, E. Global hairpin folding of tau in solution. *Biochemistry* **45**, 2283-93 (2006).
88. Mandelkow, E.M. & Mandelkow, E. Biochemistry and cell biology of tau protein in neurofibrillary degeneration. *Cold Spring Harb Perspect Med* **2**, a006247 (2012).
89. Mandelkow, E.M. et al. Tau domains, phosphorylation, and interactions with microtubules. *Neurobiol Aging* **16**, 355-62; discussion 362-3 (1995).
90. Guo, T., Noble, W. & Hanger, D.P. Roles of tau protein in health and disease. *Acta Neuropathol* **133**, 665-704 (2017).
91. Bullmann, T., Holzer, M., Mori, H. & Arendt, T. Pattern of tau isoforms expression during development in vivo. *Int J Dev Neurosci* **27**, 591-7 (2009).
92. Mandell, J.W. & Banker, G.A. The microtubule cytoskeleton and the development of neuronal polarity. *Neurobiol Aging* **16**, 229-37; discussion 238 (1995).
93. Papasozomenos, S.C. & Binder, L.I. Phosphorylation determines two distinct species of Tau in the central nervous system. *Cell Motil Cytoskeleton* **8**, 210-26 (1987).
94. Litman, P., Barg, J., Rindzoonski, L. & Ginzburg, I. Subcellular localization of tau mRNA in differentiating neuronal cell culture: implications for neuronal polarity. *Neuron* **10**, 627-38 (1993).
95. Tashiro, K., Hasegawa, M., Ihara, Y. & Iwatsubo, T. Somatodendritic localization of phosphorylated tau in neonatal and adult rat cerebral cortex. *Neuroreport* **8**, 2797-801 (1997).
96. Brady, R.M., Zinkowski, R.P. & Binder, L.I. Presence of tau in isolated nuclei from human brain. *Neurobiol Aging* **16**, 479-86 (1995).
97. Brandt, R., Leger, J. & Lee, G. Interaction of tau with the neural plasma membrane mediated by tau's amino-terminal projection domain. *J Cell Biol* **131**, 1327-40 (1995).

98. Farah, C.A. et al. Tau interacts with Golgi membranes and mediates their association with microtubules. *Cell Motil Cytoskeleton* **63**, 710-24 (2006).
99. Pooler, A.M., Phillips, E.C., Lau, D.H., Noble, W. & Hanger, D.P. Physiological release of endogenous tau is stimulated by neuronal activity. *EMBO Rep* **14**, 389-94 (2013).
100. Yamada, K. et al. Neuronal activity regulates extracellular tau in vivo. *J Exp Med* **211**, 387-93 (2014).
101. Zempel, H. et al. Axodendritic sorting and pathological missorting of Tau is isoform specific and determined by axon initial segment architecture. *J Biol Chem* (2017).
102. Liu, C. & Gotz, J. Profiling murine tau with 0N, 1N and 2N isoform-specific antibodies in brain and peripheral organs reveals distinct subcellular localization, with the 1N isoform being enriched in the nucleus. *PLoS One* **8**, e84849 (2013).
103. Hirokawa, N., Funakoshi, T., Sato-Harada, R. & Kanai, Y. Selective stabilization of tau in axons and microtubule-associated protein 2C in cell bodies and dendrites contributes to polarized localization of cytoskeletal proteins in mature neurons. *J Cell Biol* **132**, 667-79 (1996).
104. Lei, P. et al. Lithium suppression of tau induces brain iron accumulation and neurodegeneration. *Mol Psychiatry* **22**, 396-406 (2017).
105. Kadavath, H. et al. Tau stabilizes microtubules by binding at the interface between tubulin heterodimers. *Proc Natl Acad Sci U S A* **112**, 7501-6 (2015).
106. Goedert, M. & Jakes, R. Expression of separate isoforms of human tau protein: correlation with the tau pattern in brain and effects on tubulin polymerization. *EMBO J* **9**, 4225-30 (1990).
107. Chau, M.F. et al. The microtubule-associated protein tau cross-links to two distinct sites on each alpha and beta tubulin monomer via separate domains. *Biochemistry* **37**, 17692-703 (1998).
108. Gustke, N., Trinczek, B., Biernat, J., Mandelkow, E.M. & Mandelkow, E. Domains of tau protein and interactions with microtubules. *Biochemistry* **33**, 9511-22 (1994).
109. Kar, S., Fan, J., Smith, M.J., Goedert, M. & Amos, L.A. Repeat motifs of tau bind to the insides of microtubules in the absence of taxol. *EMBO J* **22**, 70-7 (2003).
110. Igaev, M. et al. A refined reaction-diffusion model of tau-microtubule dynamics and its application in FDAP analysis. *Biophys J* **107**, 2567-78 (2014).
111. Chen, J., Kanai, Y., Cowan, N.J. & Hirokawa, N. Projection domains of MAP2 and tau determine spacings between microtubules in dendrites and axons. *Nature* **360**, 674-7 (1992).
112. Drechsel, D.N., Hyman, A.A., Cobb, M.H. & Kirschner, M.W. Modulation of the dynamic instability of tubulin assembly by the microtubule-associated protein tau. *Mol Biol Cell* **3**, 1141-54 (1992).
113. Trinczek, B., Biernat, J., Baumann, K., Mandelkow, E.M. & Mandelkow, E. Domains of tau protein, differential phosphorylation, and dynamic instability of microtubules. *Mol Biol Cell* **6**, 1887-902 (1995).
114. Caceres, A. & Kosik, K.S. Inhibition of neurite polarity by tau antisense oligonucleotides in primary cerebellar neurons. *Nature* **343**, 461-3 (1990).
115. Knops, J. et al. Overexpression of tau in a nonneuronal cell induces long cellular processes. *J Cell Biol* **114**, 725-33 (1991).
116. Dixit, R., Ross, J.L., Goldman, Y.E. & Holzbaur, E.L. Differential regulation of dynein and kinesin motor proteins by tau. *Science* **319**, 1086-9 (2008).
117. Frandemiche, M.L. et al. Activity-dependent tau protein translocation to excitatory synapse is disrupted by exposure to amyloid-beta oligomers. *J Neurosci* **34**, 6084-97 (2014).

118. Ittner, L.M. et al. Dendritic function of tau mediates amyloid-beta toxicity in Alzheimer's disease mouse models. *Cell* **142**, 387-97 (2010).
119. Suzuki, M. & Kimura, T. Microtubule-associated tau contributes to intra-dendritic trafficking of AMPA receptors in multiple ways. *Neurosci Lett* **653**, 276-282 (2017).
120. Kimura, T. et al. Microtubule-associated protein tau is essential for long-term depression in the hippocampus. *Philos Trans R Soc Lond B Biol Sci* **369**, 20130144 (2014).
121. Greenwood, J.A. & Johnson, G.V. Localization and in situ phosphorylation state of nuclear tau. *Exp Cell Res* **220**, 332-7 (1995).
122. Thurston, V.C., Zinkowski, R.P. & Binder, L.I. Tau as a nucleolar protein in human nonneural cells in vitro and in vivo. *Chromosoma* **105**, 20-30 (1996).
123. Lefebvre, T. et al. Evidence of a balance between phosphorylation and O-GlcNAc glycosylation of Tau proteins--a role in nuclear localization. *Biochim Biophys Acta* **1619**, 167-76 (2003).
124. Camero, S. et al. Tau protein provides DNA with thermodynamic and structural features which are similar to those found in histone-DNA complex. *J Alzheimers Dis* **39**, 649-60 (2014).
125. Qi, H. et al. Nuclear magnetic resonance spectroscopy characterization of interaction of Tau with DNA and its regulation by phosphorylation. *Biochemistry* **54**, 1525-33 (2015).
126. Sultan, A. et al. Nuclear tau, a key player in neuronal DNA protection. *J Biol Chem* **286**, 4566-75 (2011).
127. Violet, M. et al. A major role for Tau in neuronal DNA and RNA protection in vivo under physiological and hyperthermic conditions. *Front Cell Neurosci* **8**, 84 (2014).
128. Sjoberg, M.K., Shestakova, E., Mansuroglu, Z., Maccioni, R.B. & Bonnefoy, E. Tau protein binds to pericentromeric DNA: a putative role for nuclear tau in nucleolar organization. *J Cell Sci* **119**, 2025-34 (2006).
129. Gauthier-Kemper, A. et al. The frontotemporal dementia mutation R406W blocks tau's interaction with the membrane in an annexin A2-dependent manner. *J Cell Biol* **192**, 647-61 (2011).
130. Georgieva, E.R., Xiao, S., Borbat, P.P., Freed, J.H. & Eliezer, D. Tau binds to lipid membrane surfaces via short amphipathic helices located in its microtubule-binding repeats. *Biophys J* **107**, 1441-52 (2014).
131. Pooler, A.M. & Hanger, D.P. Functional implications of the association of tau with the plasma membrane. *Biochem Soc Trans* **38**, 1012-5 (2010).
132. Ekinci, F.J. & Shea, T.B. Phosphorylation of tau alters its association with the plasma membrane. *Cell Mol Neurobiol* **20**, 497-508 (2000).
133. Lee, G. Tau and src family tyrosine kinases. *Biochim Biophys Acta* **1739**, 323-30 (2005).
134. Gomez-Ramos, A., Diaz-Hernandez, M., Rubio, A., Miras-Portugal, M.T. & Avila, J. Extracellular tau promotes intracellular calcium increase through M1 and M3 muscarinic receptors in neuronal cells. *Mol Cell Neurosci* **37**, 673-81 (2008).
135. Gomez-Ramos, A. et al. Characteristics and consequences of muscarinic receptor activation by tau protein. *Eur Neuropsychopharmacol* **19**, 708-17 (2009).
136. Petrucelli, L. et al. CHIP and Hsp70 regulate tau ubiquitination, degradation and aggregation. *Hum Mol Genet* **13**, 703-14 (2004).
137. David, D.C. et al. Proteasomal degradation of tau protein. *J Neurochem* **83**, 176-85 (2002).

138. Grune, T. et al. Tau protein degradation is catalyzed by the ATP/ubiquitin-independent 20S proteasome under normal cell conditions. *Arch Biochem Biophys* **500**, 181-8 (2010).
139. Martin, L., Latypova, X. & Terro, F. Post-translational modifications of tau protein: implications for Alzheimer's disease. *Neurochem Int* **58**, 458-71 (2011).
140. Gong, C.X. et al. Phosphorylation of microtubule-associated protein tau is regulated by protein phosphatase 2A in mammalian brain. Implications for neurofibrillary degeneration in Alzheimer's disease. *J Biol Chem* **275**, 5535-44 (2000).
141. Gong, C.X. et al. Dephosphorylation of microtubule-associated protein tau by protein phosphatase 5. *J Neurochem* **88**, 298-310 (2004).
142. Kanemaru, K., Takio, K., Miura, R., Titani, K. & Ihara, Y. Fetal-type phosphorylation of the tau in paired helical filaments. *J Neurochem* **58**, 1667-75 (1992).
143. Kopke, E. et al. Microtubule-associated protein tau. Abnormal phosphorylation of a non-paired helical filament pool in Alzheimer disease. *J Biol Chem* **268**, 24374-84 (1993).
144. Hanger, D.P., Seereeram, A. & Noble, W. Mediators of tau phosphorylation in the pathogenesis of Alzheimer's disease. *Expert Rev Neurother* **9**, 1647-66 (2009).
145. Alonso, A., Zaidi, T., Novak, M., Grundke-Iqbal, I. & Iqbal, K. Hyperphosphorylation induces self-assembly of tau into tangles of paired helical filaments/straight filaments. *Proc Natl Acad Sci U S A* **98**, 6923-8 (2001).
146. Wang, J.Z., Grundke-Iqbal, I. & Iqbal, K. Glycosylation of microtubule-associated protein tau: an abnormal posttranslational modification in Alzheimer's disease. *Nat Med* **2**, 871-5 (1996).
147. Liu, F., Zaidi, T., Iqbal, K., Grundke-Iqbal, I. & Gong, C.X. Aberrant glycosylation modulates phosphorylation of tau by protein kinase A and dephosphorylation of tau by protein phosphatase 2A and 5. *Neuroscience* **115**, 829-37 (2002).
148. Sato, Y., Naito, Y., Grundke-Iqbal, I., Iqbal, K. & Endo, T. Analysis of N-glycans of pathological tau: possible occurrence of aberrant processing of tau in Alzheimer's disease. *FEBS Lett* **496**, 152-60 (2001).
149. Liu, F., Iqbal, K., Grundke-Iqbal, I., Hart, G.W. & Gong, C.X. O-GlcNAcylation regulates phosphorylation of tau: a mechanism involved in Alzheimer's disease. *Proc Natl Acad Sci U S A* **101**, 10804-9 (2004).
150. Yuzwa, S.A., Cheung, A.H., Okon, M., McIntosh, L.P. & Vocadlo, D.J. O-GlcNAc modification of tau directly inhibits its aggregation without perturbing the conformational properties of tau monomers. *J Mol Biol* **426**, 1736-52 (2014).
151. Yuzwa, S.A. et al. Mapping O-GlcNAc modification sites on tau and generation of a site-specific O-GlcNAc tau antibody. *Amino Acids* **40**, 857-68 (2011).
152. Wang, A.C., Jensen, E.H., Rexach, J.E., Vinters, H.V. & Hsieh-Wilson, L.C. Loss of O-GlcNAc glycosylation in forebrain excitatory neurons induces neurodegeneration. *Proc Natl Acad Sci U S A* **113**, 15120-15125 (2016).
153. Nukina, N. & Ihara, Y. Proteolytic fragments of Alzheimer's paired helical filaments. *J Biochem* **98**, 1715-8 (1985).
154. Horowitz, P.M. et al. Early N-terminal changes and caspase-6 cleavage of tau in Alzheimer's disease. *J Neurosci* **24**, 7895-902 (2004).
155. Fasulo, L., Ugolini, G. & Cattaneo, A. Apoptotic effect of caspase-3 cleaved tau in hippocampal neurons and its potentiation by tau FTDP-mutation N279K. *J Alzheimers Dis* **7**, 3-13 (2005).
156. Garg, S., Timm, T., Mandelkow, E.M., Mandelkow, E. & Wang, Y. Cleavage of Tau by calpain in Alzheimer's disease: the quest for the toxic 17 kD fragment. *Neurobiol Aging* **32**, 1-14 (2011).

157. Basurto-Islas, G. et al. Accumulation of aspartic acid421- and glutamic acid391-cleaved tau in neurofibrillary tangles correlates with progression in Alzheimer disease. *J Neuropathol Exp Neurol* **67**, 470-83 (2008).
158. Wang, Y. & Mandelkow, E. Tau in physiology and pathology. *Nat Rev Neurosci* **17**, 5-21 (2016).
159. Garcia-Sierra, F., Ghoshal, N., Quinn, B., Berry, R.W. & Binder, L.I. Conformational changes and truncation of tau protein during tangle evolution in Alzheimer's disease. *J Alzheimers Dis* **5**, 65-77 (2003).
160. Mondragon-Rodriguez, S. et al. Cleavage and conformational changes of tau protein follow phosphorylation during Alzheimer's disease. *Int J Exp Pathol* **89**, 81-90 (2008).
161. Rohn, T.T. et al. Caspase-9 activation and caspase cleavage of tau in the Alzheimer's disease brain. *Neurobiol Dis* **11**, 341-54 (2002).
162. Min, S.W. et al. Acetylation of tau inhibits its degradation and contributes to tauopathy. *Neuron* **67**, 953-66 (2010).
163. Ding, H., Dolan, P.J. & Johnson, G.V. Histone deacetylase 6 interacts with the microtubule-associated protein tau. *J Neurochem* **106**, 2119-30 (2008).
164. Cook, C. et al. Acetylation of the KXGS motifs in tau is a critical determinant in modulation of tau aggregation and clearance. *Hum Mol Genet* **23**, 104-16 (2014).
165. Cohen, T.J., Friedmann, D., Hwang, A.W., Marmorstein, R. & Lee, V.M. The microtubule-associated tau protein has intrinsic acetyltransferase activity. *Nat Struct Mol Biol* **20**, 756-62 (2013).
166. Cohen, T.J. et al. The acetylation of tau inhibits its function and promotes pathological tau aggregation. *Nat Commun* **2**, 252 (2011).
167. Thomas, S.N. et al. Dual modification of Alzheimer's disease PHF-tau protein by lysine methylation and ubiquitylation: a mass spectrometry approach. *Acta Neuropathol* **123**, 105-17 (2012).
168. Morris, M. et al. Tau post-translational modifications in wild-type and human amyloid precursor protein transgenic mice. *Nat Neurosci* **18**, 1183-9 (2015).
169. Funk, K.E. et al. Lysine methylation is an endogenous post-translational modification of tau protein in human brain and a modulator of aggregation propensity. *Biochem J* **462**, 77-88 (2014).
170. Sinha, S. et al. Lysine-specific molecular tweezers are broad-spectrum inhibitors of assembly and toxicity of amyloid proteins. *J Am Chem Soc* **133**, 16958-69 (2011).
171. Babu, J.R., Geetha, T. & Wooten, M.W. Sequestosome 1/p62 shuttles polyubiquitinated tau for proteasomal degradation. *J Neurochem* **94**, 192-203 (2005).
172. Flach, K. et al. Axotrophin/MARCH7 acts as an E3 ubiquitin ligase and ubiquitinates tau protein in vitro impairing microtubule binding. *Biochim Biophys Acta* **1842**, 1527-38 (2014).
173. Wang, P. et al. Tau interactome mapping based identification of Otub1 as Tau deubiquitinase involved in accumulation of pathological Tau forms in vitro and in vivo. *Acta Neuropathol* (2017).
174. Morishima-Kawashima, M. et al. Ubiquitin is conjugated with amino-terminally processed tau in paired helical filaments. *Neuron* **10**, 1151-60 (1993).
175. Dorval, V. & Fraser, P.E. Small ubiquitin-like modifier (SUMO) modification of natively unfolded proteins tau and alpha-synuclein. *J Biol Chem* **281**, 9919-24 (2006).
176. Luo, H.B. et al. SUMOylation at K340 inhibits tau degradation through deregulating its phosphorylation and ubiquitination. *Proc Natl Acad Sci U S A* **111**, 16586-91 (2014).

177. Ledesma, M.D., Bonay, P., Colaco, C. & Avila, J. Analysis of microtubule-associated protein tau glycation in paired helical filaments. *J Biol Chem* **269**, 21614-9 (1994).
178. Ledesma, M.D., Bonay, P. & Avila, J. Tau protein from Alzheimer's disease patients is glycated at its tubulin-binding domain. *J Neurochem* **65**, 1658-64 (1995).
179. Yan, S.D. et al. Glycated tau protein in Alzheimer disease: a mechanism for induction of oxidant stress. *Proc Natl Acad Sci U S A* **91**, 7787-91 (1994).
180. Reynolds, M.R., Berry, R.W. & Binder, L.I. Site-specific nitration and oxidative dityrosine bridging of the tau protein by peroxynitrite: implications for Alzheimer's disease. *Biochemistry* **44**, 1690-700 (2005).
181. Horiguchi, T. et al. Nitration of tau protein is linked to neurodegeneration in tauopathies. *Am J Pathol* **163**, 1021-31 (2003).
182. Zhang, Y.J., Xu, Y.F., Chen, X.Q., Wang, X.C. & Wang, J.Z. Nitration and oligomerization of tau induced by peroxynitrite inhibit its microtubule-binding activity. *FEBS Lett* **579**, 2421-7 (2005).
183. Reynolds, M.R. et al. Tau nitration occurs at tyrosine 29 in the fibrillar lesions of Alzheimer's disease and other tauopathies. *J Neurosci* **26**, 10636-45 (2006).
184. Reyes, J.F., Geula, C., Vana, L. & Binder, L.I. Selective tau tyrosine nitration in non-AD tauopathies. *Acta Neuropathol* **123**, 119-32 (2012).
185. Reyes, J.F., Fu, Y., Vana, L., Kanaan, N.M. & Binder, L.I. Tyrosine nitration within the proline-rich region of Tau in Alzheimer's disease. *Am J Pathol* **178**, 2275-85 (2011).
186. Barelli, S. et al. Oxidation of proteins: Basic principles and perspectives for blood proteomics. *Proteomics Clin Appl* **2**, 142-57 (2008).
187. Schweers, O., Mandelkow, E.M., Biernat, J. & Mandelkow, E. Oxidation of cysteine-322 in the repeat domain of microtubule-associated protein tau controls the in vitro assembly of paired helical filaments. *Proc Natl Acad Sci U S A* **92**, 8463-7 (1995).
188. Guttmann, R.P., Erickson, A.C. & Johnson, G.V. Tau self-association: stabilization with a chemical cross-linker and modulation by phosphorylation and oxidation state. *J Neurochem* **64**, 1209-15 (1995).
189. Crowe, A. et al. Aminothienopyridazines and methylene blue affect Tau fibrillization via cysteine oxidation. *J Biol Chem* **288**, 11024-37 (2013).
190. Landino, L.M., Skreslet, T.E. & Alston, J.A. Cysteine oxidation of tau and microtubule-associated protein-2 by peroxynitrite: modulation of microtubule assembly kinetics by the thioredoxin reductase system. *J Biol Chem* **279**, 35101-5 (2004).
191. Lu, P.J., Wulf, G., Zhou, X.Z., Davies, P. & Lu, K.P. The prolyl isomerase Pin1 restores the function of Alzheimer-associated phosphorylated tau protein. *Nature* **399**, 784-8 (1999).
192. Kamah, A. et al. Isomerization and Oligomerization of Truncated and Mutated Tau Forms by FKBP52 are Independent Processes. *J Mol Biol* **428**, 1080-90 (2016).
193. Zhou, X.Z. et al. Pin1-dependent prolyl isomerization regulates dephosphorylation of Cdc25C and tau proteins. *Mol Cell* **6**, 873-83 (2000).
194. Watanabe, A., Takio, K. & Ihara, Y. Deamidation and isoaspartate formation in smeared tau in paired helical filaments. Unusual properties of the microtubule-binding domain of tau. *J Biol Chem* **274**, 7368-78 (1999).
195. Dan, A. et al. Extensive deamidation at asparagine residue 279 accounts for weak immunoreactivity of tau with RD4 antibody in Alzheimer's disease brain. *Acta Neuropathol Commun* **1**, 54 (2013).
196. Fischer, D. et al. Conformational changes specific for pseudophosphorylation at serine 262 selectively impair binding of tau to microtubules. *Biochemistry* **48**, 10047-55 (2009).

197. von Bergen, M. et al. Assembly of tau protein into Alzheimer paired helical filaments depends on a local sequence motif ((306)VQIVYK(311)) forming beta structure. *Proc Natl Acad Sci U S A* **97**, 5129-34 (2000).
198. Wegmann, S., Medalsy, I.D., Mandelkow, E. & Muller, D.J. The fuzzy coat of pathological human Tau fibrils is a two-layered polyelectrolyte brush. *Proc Natl Acad Sci U S A* **110**, E313-21 (2013).
199. Gillam, J.E. & MacPhee, C.E. Modelling amyloid fibril formation kinetics: mechanisms of nucleation and growth. *J Phys Condens Matter* **25**, 373101 (2013).
200. Zhong, Q., Congdon, E.E., Nagaraja, H.N. & Kuret, J. Tau isoform composition influences rate and extent of filament formation. *J Biol Chem* **287**, 20711-9 (2012).
201. Ivanovova, N., Handzusova, M., Hanes, J., Kontsekova, E. & Novak, M. High-yield purification of fetal tau preserving its structure and phosphorylation pattern. *J Immunol Methods* **339**, 17-22 (2008).
202. Cvjetkovic, A., Lotvall, J. & Lasser, C. The influence of rotor type and centrifugation time on the yield and purity of extracellular vesicles. *J Extracell Vesicles* **3** (2014).
203. Planel, E. et al. Acceleration and persistence of neurofibrillary pathology in a mouse model of tauopathy following anesthesia. *FASEB J* **23**, 2595-604 (2009).
204. Greenberg, S.G. & Davies, P. A preparation of Alzheimer paired helical filaments that displays distinct tau proteins by polyacrylamide gel electrophoresis. *Proc Natl Acad Sci U S A* **87**, 5827-31 (1990).
205. Hope, J., Multhaup, G., Reekie, L.J., Kimberlin, R.H. & Beyreuther, K. Molecular pathology of scrapie-associated fibril protein (PrP) in mouse brain affected by the ME7 strain of scrapie. *Eur J Biochem* **172**, 271-7 (1988).
206. Rappsilber, J., Mann, M. & Ishihama, Y. Protocol for micro-purification, enrichment, pre-fractionation and storage of peptides for proteomics using StageTips. *Nat Protoc* **2**, 1896-906 (2007).
207. Carrell, R.W. & Lomas, D.A. Conformational disease. *Lancet* **350**, 134-8 (1997).
208. Liu, W.K., Ksiezak-Reding, H. & Yen, S.H. Abnormal tau proteins from Alzheimer's disease brains. Purification and amino acid analysis. *J Biol Chem* **266**, 21723-7 (1991).
209. Goedert, M., Jakes, R. & Vanmechelen, E. Monoclonal antibody AT8 recognises tau protein phosphorylated at both serine 202 and threonine 205. *Neurosci Lett* **189**, 167-9 (1995).
210. Malia, T.J. et al. Epitope mapping and structural basis for the recognition of phosphorylated tau by the anti-tau antibody AT8. *Proteins* **84**, 427-34 (2016).
211. Noble, W. et al. Cdk5 is a key factor in tau aggregation and tangle formation in vivo. *Neuron* **38**, 555-65 (2003).
212. Biernat, J. et al. The switch of tau protein to an Alzheimer-like state includes the phosphorylation of two serine-proline motifs upstream of the microtubule binding region. *EMBO J* **11**, 1593-7 (1992).
213. Tomizawa, K., Omori, A., Ohtake, A., Sato, K. & Takahashi, M. Tau-tubulin kinase phosphorylates tau at Ser-208 and Ser-210, sites found in paired helical filament-tau. *FEBS Lett* **492**, 221-7 (2001).
214. Despres, C. et al. Identification of the Tau phosphorylation pattern that drives its aggregation. *Proc Natl Acad Sci U S A* (2017).
215. Sanchez-Mejias, E. et al. Soluble phospho-tau from Alzheimer's disease hippocampus drives microglial degeneration. *Acta Neuropathol* **132**, 897-916 (2016).
216. Petry, F.R. et al. Specificity of anti-tau antibodies when analyzing mice models of Alzheimer's disease: problems and solutions. *PLoS One* **9**, e94251 (2014).

217. Gielbert, A. et al. High-resolution differentiation of transmissible spongiform encephalopathy strains by quantitative N-terminal amino acid profiling (N-TAAP) of PK-digested abnormal prion protein. *J Mass Spectrom* **44**, 384-96 (2009).
218. Crary, J.F. et al. Primary age-related tauopathy (PART): a common pathology associated with human aging. *Acta Neuropathol* **128**, 755-66 (2014).
219. Olsen, J.V. & Mann, M. Status of large-scale analysis of post-translational modifications by mass spectrometry. *Mol Cell Proteomics* **12**, 3444-52 (2013).

Appendix I: Tau post-translational modifications – Biochemical reactions

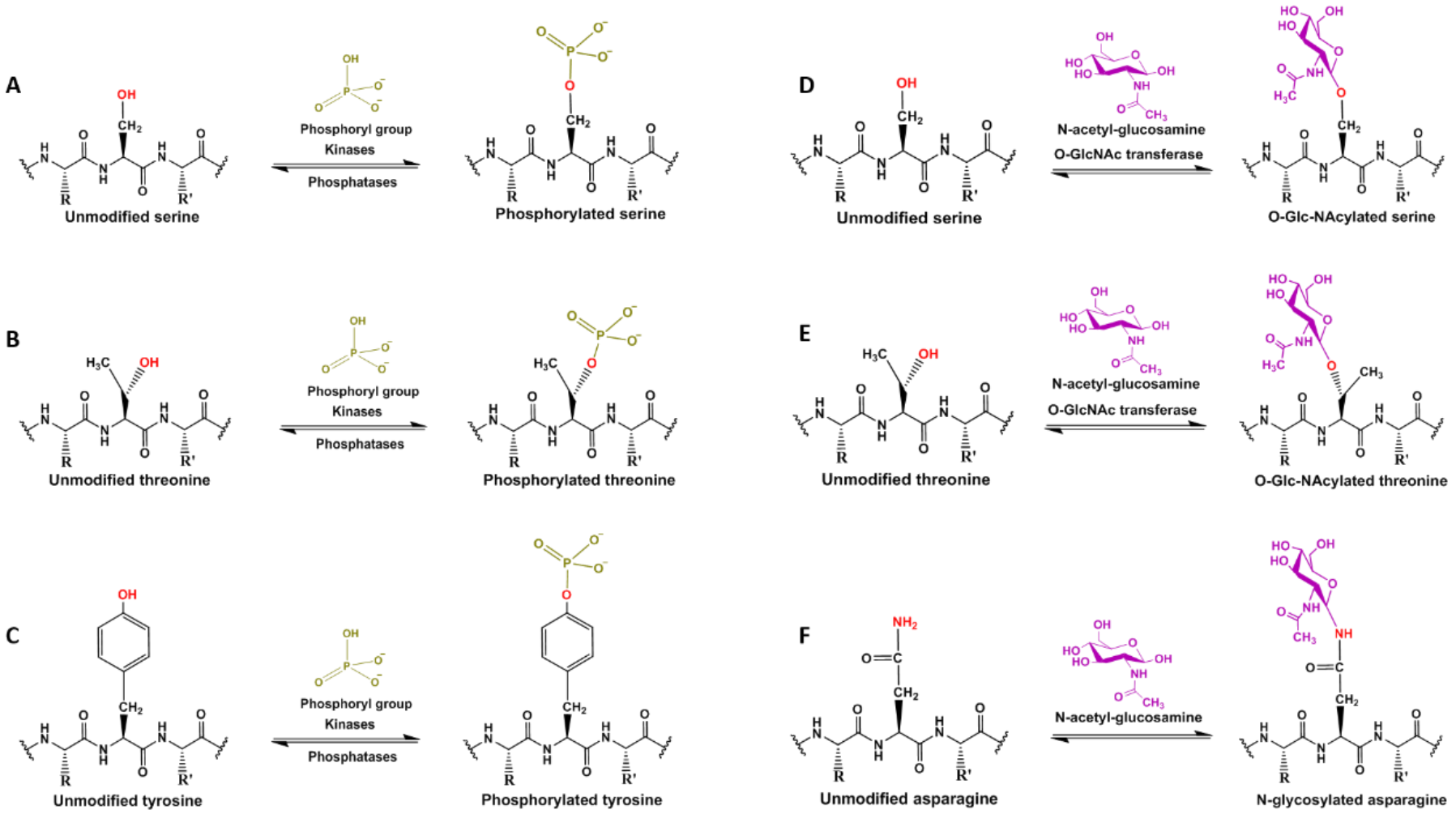
A
Unmodified serine
Phosphoryl group
Kinases
Phosphatases
Phosphorylated serine
B
Unmodified threonine
Phosphoryl group
Kinases
Phosphatases
Phosphorylated threonine
C
Unmodified tyrosine
Phosphoryl group
Kinases
Phosphatases
Phosphorylated tyrosine
D
Unmodified serine
N-acetyl-glucosamine
O-GlcNAc transferase
O-Glc-NAcylated serine
E
Unmodified threonine
N-acetyl-glucosamine
O-GlcNAc transferase
O-Glc-NAcylated threonine
F
Unmodified asparagine
N-acetyl-glucosamine
N-glycosylated asparagine

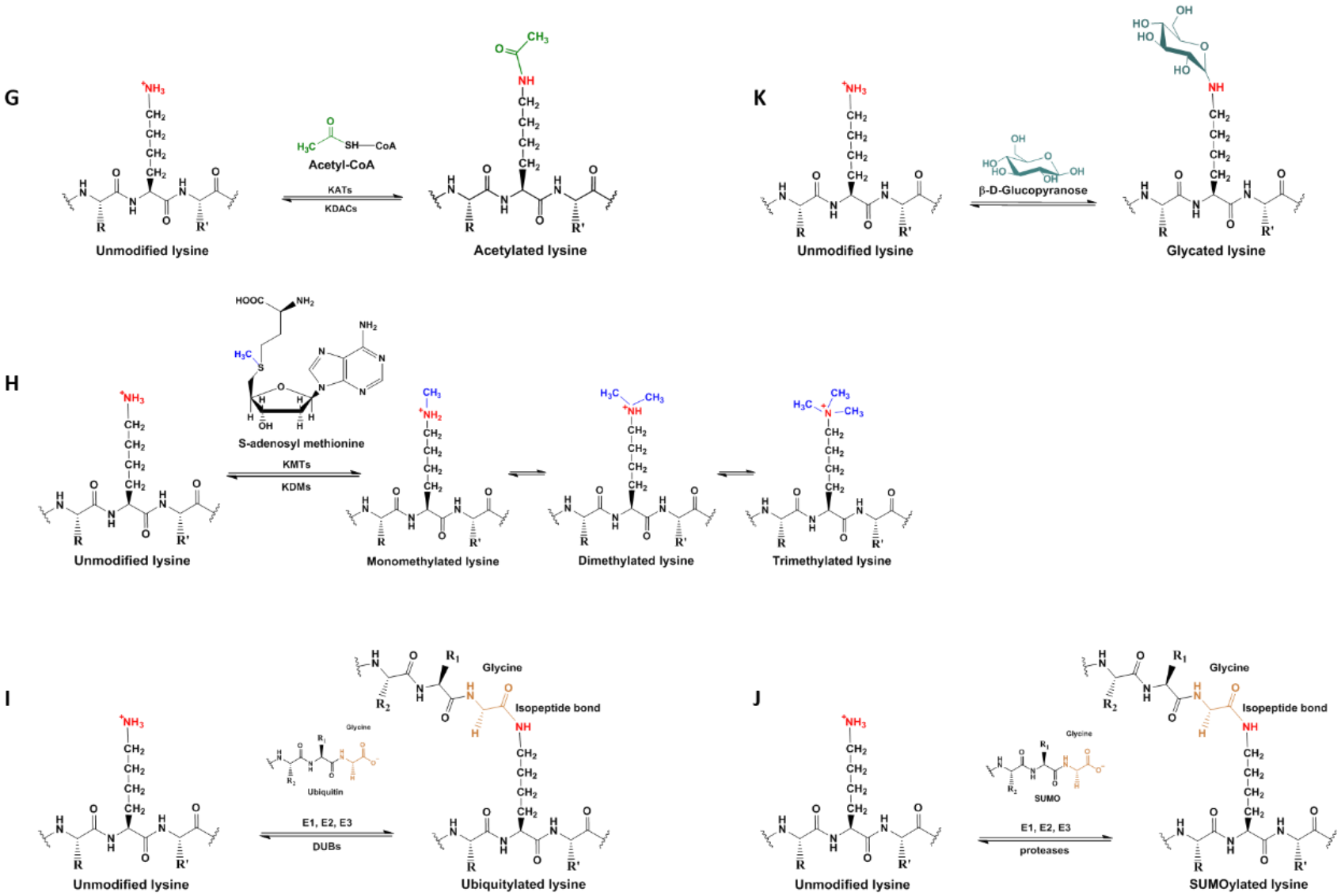
G
Unmodified lysine
Acetyl-CoA
KATs
KDACs
Acetylated lysine
K
Unmodified lysine
β-D-Glucopyranose
Glycated lysine
H
Unmodified lysine
S-adenosyl methionine
KMTs
KDMs
Monomethylated lysine
Dimethylated lysine
Trimethylated lysine
I
Unmodified lysine
Ubiquitin
Glycine
Isopeptide bond
E1, E2, E3
DUBs
Ubiquitylated lysine
J
Unmodified lysine
SUMO
Glycine
Isopeptide bond
E1, E2, E3
proteases
SUMOylated lysine

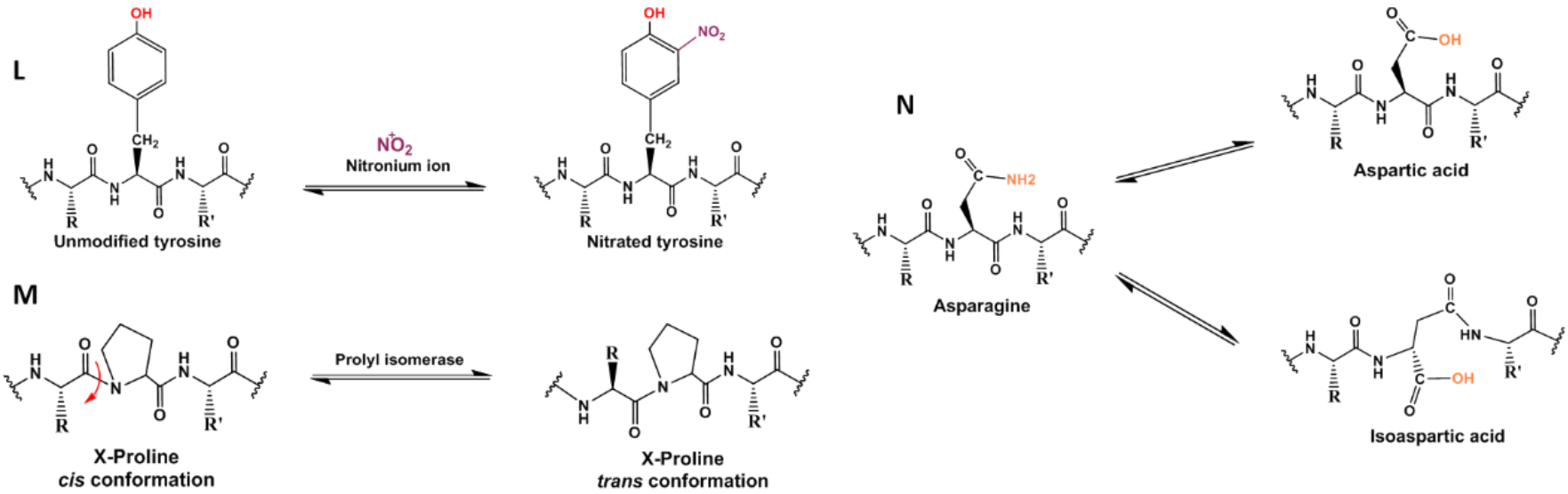

Supplementary figure 1 Several types of post-translational modifications have been detected on tau including (A, B, C) serine, threonine and tyrosine phosphorylation, (D, E) serine and threonine O-Glc-NAcylation, (F) asparagine N-glycosylation, (G, H, I, J, K) lysine acetylation, methylation, ubiquitylation, SUMOylation and glycation, (L) tyrosine nitration, (M) prolyl isomerization and (N) asparagine deamidation.

Appendix II: Review Article - Lysine-Directed Post-translational Modifications of Tau Protein in Alzheimer's Disease and Related Tauopathies

frontiers in Molecular Biosciences

REVIEW
published: 11 August 2017
doi: 10.3389/fmolb.2017.00056

Lysine-Directed Post-translational Modifications of Tau Protein in Alzheimer's Disease and Related Tauopathies

*Christiana Kontaxi, Pedro Piccardo and Andrew C. Gill **

Roslin Institute and Royal (Dick) School of Veterinary Sciences, University of Edinburgh, Edinburgh, United Kingdom

Tau is a microtubule-associated protein responsible mainly for stabilizing the neuronal microtubule network in the brain. Under normal conditions, tau is highly soluble and adopts an "unfolded" conformation. However, it undergoes conformational changes resulting in a less soluble form with weakened microtubule stabilizing properties. Altered tau forms characteristic pathogenic inclusions in Alzheimer's disease and related tauopathies. Although, tau hyperphosphorylation is widely considered to be the major trigger of tau malfunction, tau undergoes several post-translational modifications at lysine residues including acetylation, methylation, ubiquitylation, SUMOylation, and glycation. We are only beginning to define the site-specific impact of each type of lysine modification on tau biology as well as the possible interplay between them, but, like phosphorylation, these modifications are likely to play critical roles in tau's normal and pathobiology. This review summarizes the latest findings focusing on lysine post-translational modifications that occur at both endogenous tau protein and pathological tau forms in AD and other tauopathies. In addition, it highlights the significance of a site-dependent approach of studying tau post-translational modifications under normal and pathological conditions.

Keywords: tau, acetylation, methylation, ubiquitylation, SUMOylation, glycation, paired helical filaments, tauopathies

OPEN ACCESS

Edited by:
Laszlo Otvos,
OLPE, LLC, United States

Reviewed by:
Norelle Daly,
James Cook University, Australia
Sandor Lovas,
Creighton University, United States

****Correspondence:***
Andrew C. Gill
andrew.gill@roslin.ed.ac.uk

Specialty section:
This article was submitted to Chemical Biology, a section of the journal Frontiers in Molecular Biosciences

Received: *06 June 2017*
Accepted: *25 July 2017*
Published: *11 August 2017*

Citation:
Kontaxi C, Piccardo P and Gill AC (2017) Lysine-Directed Post-translational Modifications of Tau Protein in Alzheimer's Disease and Related Tauopathies. Front. Mol. Biosci. 4:56. doi: 10.3389/fmolb.2017.00056

INTRODUCTION

Neurodegenerative diseases of the central nervous system are characterized by selective loss of synapses and neurons, glial activation, progressive irreversible neural dysfunction, cognitive impairment and eventually death (Verkhratsky et al., 2014; Kovacs, 2016). Many neurodegenerative diseases are also known as conformational diseases- or proteinopathies-due to the presence of pathological forms of proteins that accumulate and deposit in the brain (Carrell and Lomas, 1997). For this reason, it has been assumed that the aggregation of misfolded proteins is the molecular cause of neurodegeneration. Proteins participating in aggregates lack their normal tertiary structure and, hence, they are incapable of serving their typical functions in living cells. The aberrantly-folded forms may also acquire a novel, neurotoxic role (Ballatore et al., 2007). A common class of neurodegenerative diseases includes the disorders associated with the filamentous inclusions of tau aggregates in nerve cells and glia, which are known collectively as tauopathies (Spillantini et al., 1997; Ferrer et al., 2014). One of the main pathological hallmarks

of Alzheimer's disease (AD) is the intraneuronal accumulation of neurofibrillary tangles (NFTs) consisting of misfolded tau protein and, therefore, AD is considered to be partly a tauopathy and is one of the most widely studied. Other tauopathies include progressive supranuclear palsy, frontotemporal dementia with parkinsonism-17, corticobasal degeneration, argyrophilic grain disease, Pick's disease and Huntington's disease (Hernandez and Avila, 2007; Gratuze et al., 2016).

Tau protein is a microtubule-associated protein (MAP) expressed abundantly in neurons and, to a lesser extent, in astrocytes and oligodendrocytes. In neurons, tau localizes predominantly to the axonal cytoplasm, but it can also be found in the nucleus and dendrites (Binder et al., 1985; Migheli et al., 1988; Loomis et al., 1990). Tau is responsible mainly for microtubule assembly and stabilization, thus maintaining the normal morphology of the neuronal cells and enabling axonal transport. Tau may also be involved in other activities such as neurogenesis and iron export (Lei et al., 2012; Pallas-Bazarra et al., 2016). It is encoded by the *MAPT* gene, which includes 16 exons located on the human chromosome 17 (Neve et al., 1986; Lee et al., 1988). Based on protein structure, tau can be divided into four regions: (i) a N-terminal projection region that protrudes from the microtubules to which tau is bound and is responsible for interacting with other, non-microtubular partners; (ii) a proline-rich region that contains seven PXXP motifs, which serve as binding sites for signaling proteins; (iii) a microtubule-binding domain (MBD) that contains three or four repeat regions, R1, R2, R3, and R4, which are essential for binding to microtubules through their conserved KXGS motifs, and the flanking regions between them; (iv) a C-terminal region (**Figure 1A**; Mandelkow et al., 1995). There is heterogeneity at the level of transcription due to alternative splicing of exon 10, resulting in the generation of two different tau isoforms; these isoforms are known as 3R or 4R depending on whether they contain three or four repeat regions within the MBD (Lee et al., 1989).

Under normal conditions, tau is highly soluble and is classed as an intrinsically disordered protein. It is believed to have little tendency for aggregation in this intrinsically disordered state (Schweers et al., 1994; Mukrasch et al., 2009), however, tau can undergo conformational changes resulting in altered physical and chemical properties, including a decrease of solubility. Thereby, conformationally-stable insoluble structures are formed as tau assembles into higher-polymerized aggregates that differ between different tauopathies (Yoshida, 2006). In AD, tau lesions include neurofibrillary tangles (NFTs) in neuronal cell bodies, neuropil threads in neurites and dystrophic neurites in neuritic plaques; in electron microscopy, tau assemblies form mainly paired helical filaments (PHFs) that consist of both 3R and 4R isoforms (**Figure 1B**). In contrast, 3R or 4R tau isoforms are preferentially accumulated in a variety of tauopathies, such as progressive supranuclear palsy and Pick's disease (Dickson et al., 2011). The processes underpinning the formation of tau aggregates are not completely understood, but appear to involve a variety of post-translational modifications occurring at many sites throughout tau, including phosphorylation, O-Glc-NAcylation, glycation, nitration, acetylation, methylation, SUMOylation, ubiquitylation, oxidation, and truncation (Martin et al., 2011).

Since the phosphorylation state of tau controls its intrinsic affinity for microtubules and given the fact that aggregated tau species have been shown to be hyperphosphorylated at several serine, threonine and tyrosine residues, numerous studies have focused on exploring tau phosphorylation (Grundke-Iqbal et al., 1986; Williamson et al., 2002). Conversely, tau modifications that extend to lysine residues have not yet been analyzed as extensively, but it is likely that they might be as important as phosphorylation in dictating the biophysical properties of tau, because they profoundly alter the charge of the protein. This review gives an overview of the latest findings concerning the lysine-directed tau post-translational modifications, which include acetylation, methylation, ubiquitylation, SUMOylation and glycation, and discusses the impact on tau biology of the possible cross-talk between them. It also emphasizes the need to achieve a complete understanding of the biological role of lysine site-specific modifications in both endogenous and aggregated tau, in order to shed light on the molecular events underlying the pathological transition of tau that characterizes tau-mediated neurodegeneration.

TAU ACETYLATION

Acetylation is a co- or post-translational modification that is best known for modifying the N-termini of eukaryotic proteins (around 85% of human proteins are believed to be N-terminally acetylated) as well as for modifying the side chains of specific lysine residues in histones, thereby altering chromatin structure and providing epigenetic control of transcription. As a result, the enzymes responsible for acetylating and deacetylating protein substrates at lysine residues are called histone acetyltransferases and histone deacetylases, respectively, but given the fact that a variety of other proteins except for histones can be acetylated the terms lysine acetyltransferase (KAT) and lysine deacetylase (KDAC) are more precise. The source of the acetyl group in protein acetylation reactions is acetyl-CoA and it has been demonstrated recently by Min et al. (2010), that lysine side chains of tau protein can be acetylated (**Figure 2A**). NMR analysis of recombinant human tau acetylated enzymatically *in vitro* has shown that tau displays an overall acetylation level of 6 ± 2 acetyl groups per molecule (Kamah et al., 2014). Tau can be acetylated by either the protein p300 or the CBP acetyltransferase, a CREB-binding protein and close homolog of the p300 acetyltransferase, and deacetylated by the NAD^+-dependent sirtuin 1 deacetylase (SIRT1; Min et al., 2010). A decrease in the levels of both SIRT1 mRNA and protein has been associated with enhanced PHF-tau accumulation in AD patients (Julien et al., 2009), thus indicating a negative correlation between the regulation of SIRT1 and tau accumulation. Moreover, histone deacetylase 6 (HDAC6), located mainly in the cytoplasm, has been shown to interact with tau in the MBD (Ding et al., 2008) suggesting that HDAC6 is another possible tau deacetylase, and Cook et al. found that HDAC6 could deacetylate tau on KXGS motifs (Cook et al., 2014). HDAC6 has also been shown to be involved in assisting the clearance of misfolded huntingtin through autophagic degradation by

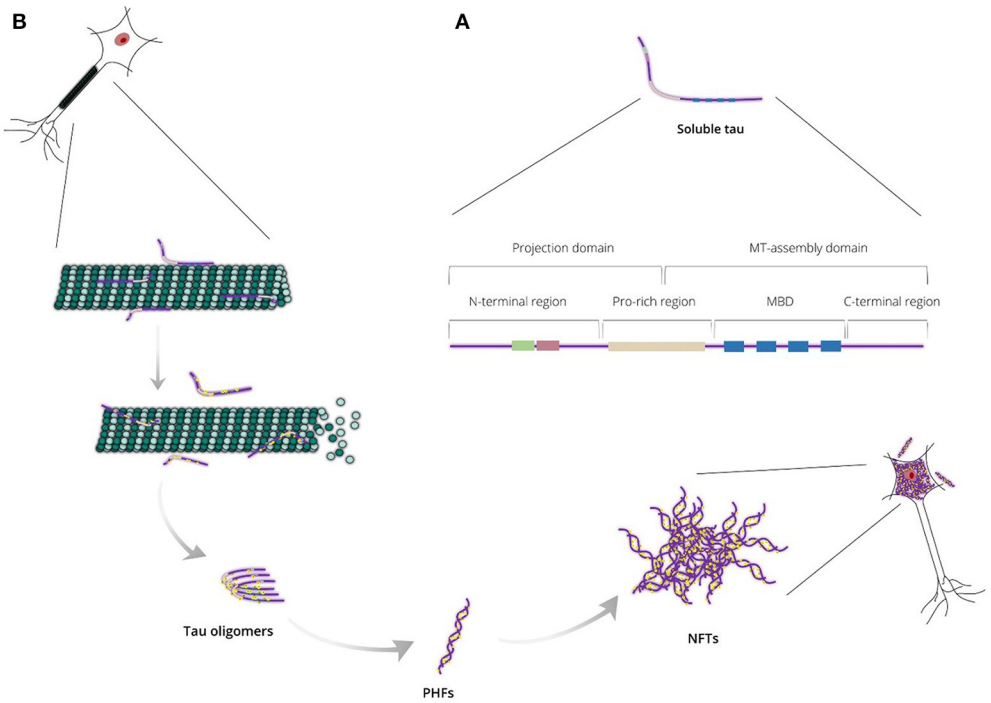

FIGURE 1 | (A) Endogenous tau is a highly soluble protein adopting an "unfolded" conformational state and consisting of two major domains: the projection domain that projects from microtubules and the microtubule (MT)-assembly domain that interacts with tubulin heterodimers. Tau can also be divided into four regions: the N-terminal region, the proline-rich (Pro-rich) region, the microtubule-binding domain (MBD) and the C-terminal region. **(B)** Tau is responsible mainly for stabilizing neuronal microtubules based on its phosphorylation state. Abnormal tau hyperphosphorylation weakens tau affinity for microtubules and, thus, releases tau in the cytosol and destabilizes the microtubule bundles. Unbound hyperphosphorylated tau assembles into pathogenic inclusions that deposit in brain tissues causing pathological phenotypes.

mediating the retrograde transport of autophagic components to huntingtin aggresomes (Iwata et al., 2005), supporting the notion that HDAC6 might act to protect neurons against abnormal tau rather than act only as a tau the deacetylase. In contrast to HDAC6, both p300 and SIRT1 are localized mainly in the nucleus (Michishita et al., 2005; Blanco-Garcia et al., 2009), whereas tau resides predominantly in the axonal cytoplasm (Binder et al., 1985); if they are to regulate tau acetylation exclusively and directly then the mechanisms underpinning the migration of these deacetylases to the cytosolic compartment of adult neurons need to be established.

Remarkably, tau also has intrinsic acetyltransferase activity and, hence, can catalyze its own acetylation by using cysteine residues in the MBD—C291 and C322 (all amino acid numbers in the manuscript refer to human tau) in the R2 and R3 repeats, respectively—as intermediates to enable transfer of the acetyl group from acetyl-CoA to certain lysine residues both intra- and inter-molecularly (Cohen et al., 2013). Different tau isoforms may have different tendency to undergo autoacetylation, with 4R isoforms displaying higher levels of autoacetylation compared to 3R isoforms, which lack the R2 repeat that includes C291 hence contain only the C322 residue (Cohen et al., 2016). Despite the intrinsically disordered nature of tau, both C291 and C322 residues participate in α-helical structures, which ensures a relatively ordered conformation and brings cysteine and lysine residues (C291 and K274, C322 and K340) into close proximity for the chemical reaction(s) to take place (Luo Y. et al., 2014). Since acetylated tau is unable to bind to microtubules (Cohen et al., 2011), it has been suggested that tau autoacetylation might serve as an autoinhibitory mechanism to prevent interaction between tau and microtubules (Cohen et al., 2013). Tau self-acetylation has also been shown to induce tau autoproteolysis, catalyzed by the same cysteine residues, during which about 17 kDa and 12 kDa C- and N-terminal fragments, respectively, are generated (Cohen et al., 2016). Mass spectrometry analysis of the N-terminal end of each fragment identified that the putative autocleavage sites on tau are located within the R2 and R4 repeats (Cohen et al., 2016).

Most lysine residues that are putative sites of acetylation are distributed in the MBD, whilst, a few are found in the N-terminal and C-terminal regions (**Figure 3A**). Proteomic studies revealed 23 lysine residues throughout the tau sequence that can potentially be acetylated by p300 *in vitro*, of which 13 lysines are found in the MBD (Min et al., 2010). NMR analysis assigned several lysine residues as potential CBP-catalyzed acetylation sites in accordance with previous mass spectrometric data, including two novel highly acetylated lysines, K240 and K294 (Kamah et al., 2014). Acetylation of K163, K174 and K180, located in the

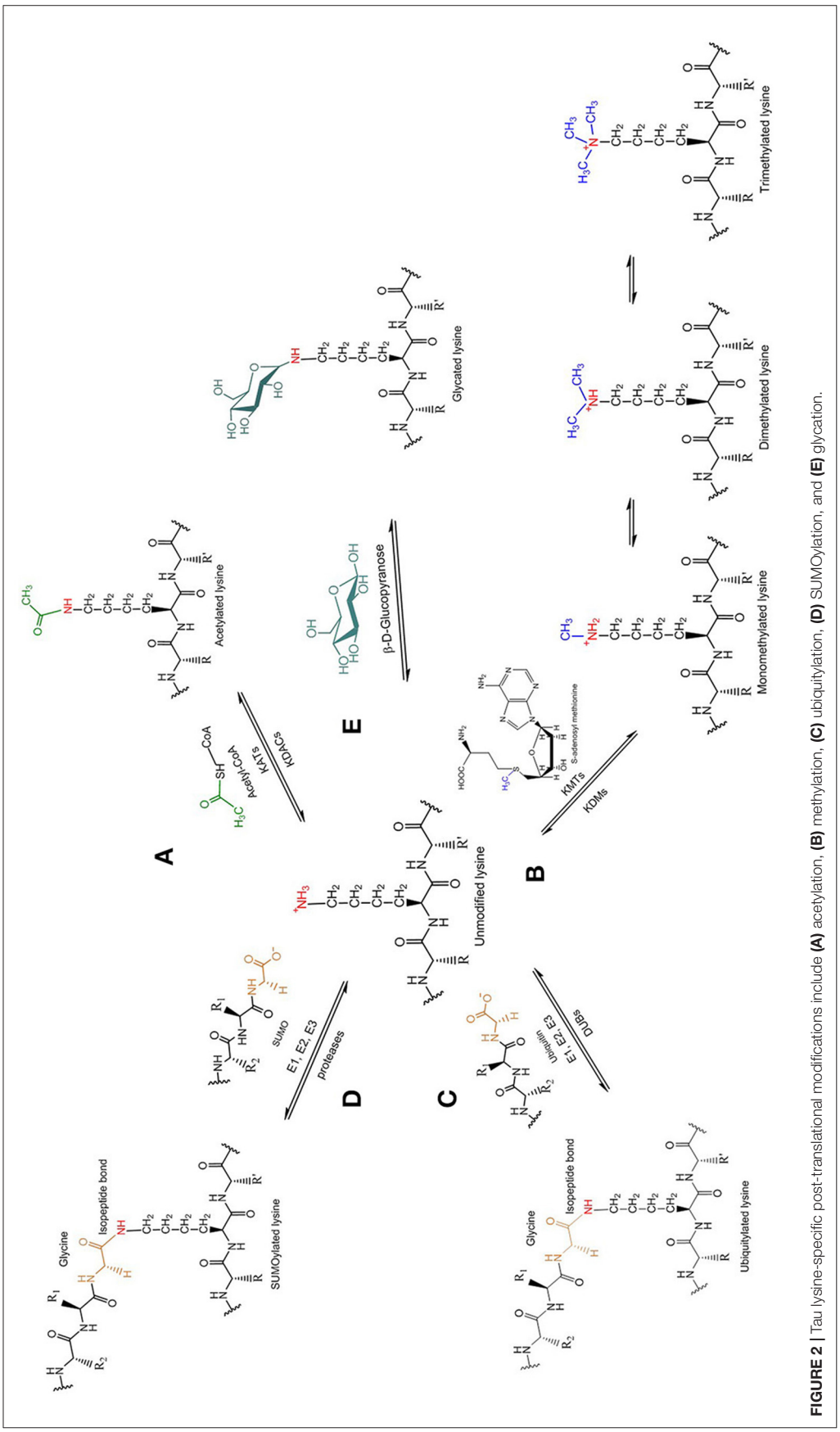

FIGURE 2 | Tau lysine-specific post-translational modifications include **(A)** acetylation, **(B)** methylation, **(C)** ubiquitylation, **(D)** SUMOylation, and **(E)** glycation.

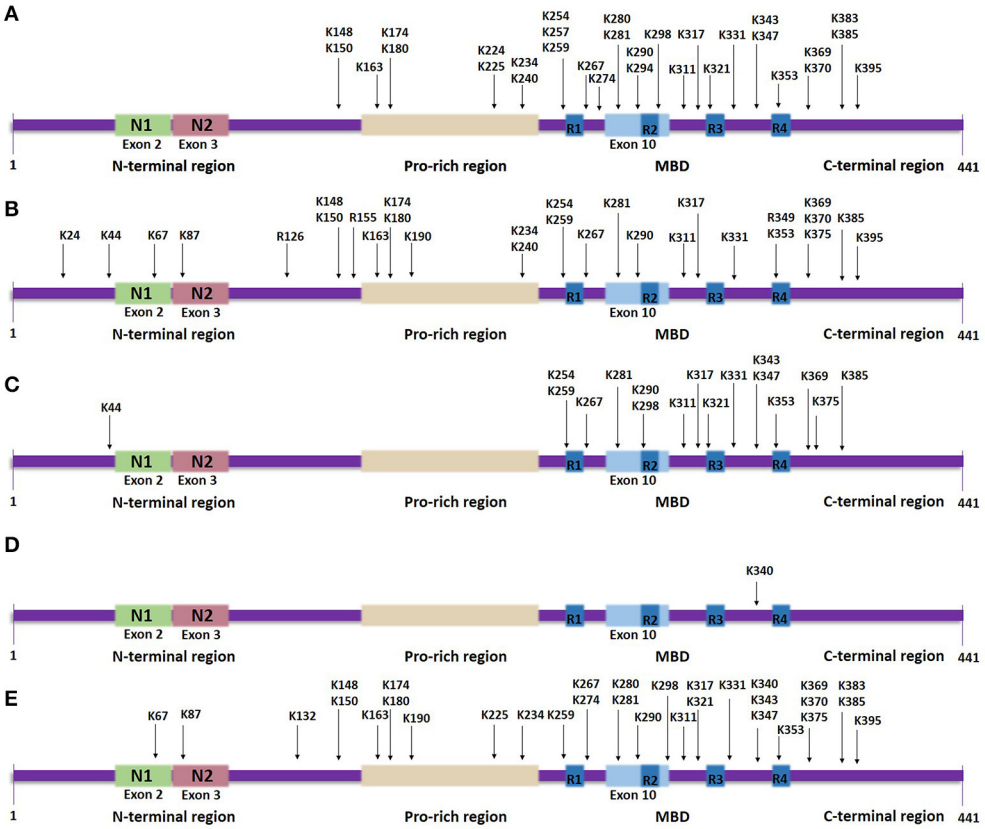

FIGURE 3 | Tau lysine-specific sites that are modified post-translationally based on the longest human tau isoform. The modified sites include the total number of sites that have been identified both *in vivo* and in vitro, in normal tau as well as in pathological states of tau. **(A)** Tau acetylation sites. **(B)** Tau methylation sites. **(C)** Tau ubiquitylation sites. **(D)** Tau SUMOylation site. **(E)** Tau glycation sites.

proline-rich region, has also been confirmed *in vivo* (Min et al., 2010). A further study detected K163 in the proline-rich region, K280 and K281 in the second repeat region and K369 in the MBD as the major sites of tau acetylation (Cohen et al., 2011). Recently, 13 putative lysine sites were discovered *in vivo* including K343 and K347 in the MBD (Morris et al., 2015)—acetylation in this region could affect the affinity of tau for microtubules.

Of the putative acetylation sites, K174, K274, K280, and K281 have received most attention concerning their significance in regulating tau function. Acetylation of K280 is of particular interest since it has been suggested to be a critical event for the formation of pathogenic tau based on data showing that this modification decreases microtubule binding and, also, precedes and possibly enhances tau fibrillization into PHFs (Irwin et al., 2012). Moreover, transgenic Drosophila models overexpressing a mutant form of human tau (K280Q) to mimic acetylation show increased phosphorylation at S262 and T212/S214 and enhanced tau levels, possibly due to either increased oligomerization or differential protein degradation, thus suggesting that acetylated K280 contributes to pathological events underlying tau toxicity (Gorsky et al., 2016). Conversely, examining the co-localization of acetylated K280 immunoreactivity with multiple tau epitopes in AD revealed a possible sequence of events, according to which tau hyperphosphorylation occurs before tau acetylation at K280, which is then followed by subsequent tau truncation (Irwin et al., 2012). Notably, immunohistopathological studies revealed that in normal brains K280 is not identified to be acetylated, whereas it is predominantly detected in NFTs and, to a lesser extent, in neuropil threads or pretangles (Cohen et al., 2011; Irwin et al., 2012). Acetylated K280 is detected in neuronal and glial inclusions in many tauopathies, such as argyrophilic grain disease, sporadic and familial AD, frontotemporal dementia with parkinsonism-17, corticobasal degeneration and progressive supranuclear palsy (Cohen et al., 2011; Irwin et al., 2012, 2013). However, Pick's disease is a 3R tauopathy and 3R tau isoforms lack exon 10, where K280 is located, so that a low degree of acetylated K280 was found only in a subset of 4R tau containing lesions (Irwin et al., 2013). This indicates that acetylation of K280 is not sufficient for causing tau-induced neurotoxicity.

In contrast to K280, acetylated K274, located in the first repeat region, was shown to be present in neuronal and glial inclusions of both 3R and 4R human tauopathies from a variety of sporadic as well as familial cases, with the exception of the 4R tauopathy argyrophilic grain disease (Grinberg et al., 2013). Pathological acetylation of K274, as well as K281, has been reported to cause downregulation of

the cytoskeletal protein network of the axon initial segment leading to destabilization of the microtubule barrier in this region and consequent somatodendritic mis-sorting of tau, which represents an early event of neurodegeneration (Sohn et al., 2016). Apart from enabling tau mislocalization, these modifications have been associated with synaptic dysfunction and memory deficits observed in AD brains (Tracy et al., 2016) with possible mechanisms involving the kidney/brain protein, a postsynaptic memory-associated protein. Specifically, primary hippocampal neurons expressing K274/K281-specific acetylation-mimic mutants failed to recruit AMPA receptors to the postsynaptic surface of spines, whilst activity-dependent postsynaptic actin polymerization was disrupted; site-specific acetylated tau was shown to disturb the postsynaptic distribution of kidney/brain protein, which contributes to impaired actin polymerization and trafficking of AMPA receptors in the postsynaptic membrane (Tracy et al., 2016). Lastly, another significant residue that can be acetylated is K174 found in the proline-rich region. Pseudoacetylation at K174 (K174Q) was reported to attenuate tau clearance resulting in increased tau accumulation and was sufficient to induce behavioral deficits *in vivo*, such as memory and learning impairments. Thus, acetylation of K174 is likely to be an additional key modification regulating tau-induced toxicity (Min et al., 2015).

The finding that tau can be acetylated gave rise to further research studies examining the impact of these modifications on tau physiopathology. In general, acetylation that is elevated by cellular stress, such as Aβ accumulation (Min et al., 2010), seems to affect tau biology via two different processes. The first involves the dysregulation of tau homeostasis due to prevention of degradation mediated by the ubiquitin-proteasome system (UPS; Min et al., 2010). Most of the putative acetylated lysine residues that are distributed in the MBD can also be polyubiquitylated (see below) to mark tau for degradation (Morris et al., 2015). Hence, acetylation of lysines can prevent their polyubiquitylation resulting in insufficient turnover of both endogenous and hyperphosphorylated tau (Min et al., 2010). Primary cultured neurons lacking SIRT1 activity that, as a result, show enhanced acetylated tau levels, also have impaired tau turnover (Min et al., 2010). Similarly, inadequate turnover of hyperphosphorylated tau is observed when tau also becomes hyperacetylated (Min et al., 2010). Impaired clearance of tau is believed to be one of the major factors that leads to tau accumulation by increasing the pool of tau available for aggregation by maintaining proteins that should be normally degraded.

The second mechanism by which acetylation is suggested to change tau function is through the impairment of tau-microtubule interactions (Cohen et al., 2011), since acetylation neutralizes the positive charge of lysine residues in the MBD, thereby disabling tau binding to negative charges on the microtubule surface (Luo Y. et al., 2014). Of course, the release of tau from microtubules might act collaboratively with impaired tau degradation in enhancing tau pathological accumulation. Nevertheless, whether acetylation facilitates tau fibrillization remains to be elucidated. However, acetylation of KXGS motifs (K259, K290, K312, and K353) has been reported to prevent tau phosphorylation at these same motifs and decreases aggregation of recombinant tau *in vitro* (Cohen et al., 2011; Cook et al., 2014). Furthermore, KXGS motifs are hypoacetylated in AD brains and in a mouse model of tauopathy (Cook et al., 2014). This discovery implies that acetylation of particularly KXGS motifs is an event possibly occurring merely in normal tau, but its role needs further investigation. In any case, the fact that other MAP proteins, such as MAP2, which share highly conserved repeats with tau, undergo lysine acetylation in the MBD and cysteine-dependent autoacetylation indicates that acetylation might be a conserved regulatory mechanism of MAP activity in governing cytoskeletal dynamics (Hwang et al., 2016).

TAU METHYLATION

Methylation refers to the enzymatic addition of one or more methyl groups to protein substrates. Typically, the methyl group derives from S-adenosyl methionine and it is added to the terminal amino group of lysine or arginine side chains of the target protein. Depending on the residue that is modified, lysine methyltransferases (KMTs) and protein arginine methyltransferases, respectively, are responsible for methylating the protein substrates; accordingly, the reverse reaction can be catalyzed by several lysine demethylases (KDMs), but no arginine demethylases are yet known. Lysine methylation of tau (**Figure 2B**) is a relatively recent discovery that, to date, has not received the same attention as acetylation. Mass spectrometric analysis of PHFs derived from AD brains showed that several lysine residues, distributed in the projection domain and MBD of tau protein, can be methylated (Thomas et al., 2012). So far, the specific enzymes involved in tau methylation have not been identified.

Lysine methylation has been detected in tau protein isolated from both pathological and normal brains (**Figure 3B**). In human AD brains, aggregated tau is monomethylated at seven lysine residues found in the proline-rich region and the R1 and R2 repeats within the MBD, of which K180 and K267 appear to be more frequently methylated, in contrast to K290 that displays the lowest level of methylation (Thomas et al., 2012). Later studies showed that endogenous tau from cognitively-normal human brains can be monomethylated as well as dimethylated at different lysine residues (Funk et al., 2014; Morris et al., 2015). Extracted soluble tau is methylated at up to 11 sites, more than found to be modified in PHF-tau, and which are distributed throughout the sequence, whilst *in vitro* reductive methylation of recombinant tau led to detection of 23 methylated lysines (Funk et al., 2014). Furthermore, not only lysine residues, but the arginine residues R126, R155, and R349 were detected as possible sites of monomethylation in normal mouse tau and in a mouse model of AD (Morris et al., 2015). Tau modified by the addition of three methyl groups at a single site—tri-methylation—has not yet been found in either healthy or pathological states.

Since K254 was found to be mainly methylated and, to a lesser extent, ubiquitylated (see below) in PHF-tau, it has been suggested that methylation may block UPS-mediated degradation of tau leading to a further enhancement of tau levels in the cell (Thomas et al., 2012). At the same time, phosphorylation of S262, which reduces tau affinity for

microtubules, is found more frequently in the presence of methylated K267 in PHF-tau (Thomas et al., 2012). This suggests that lysine methylation, apart from preventing degradation by the UPS, might result in abnormal phosphorylation of tau. In addition, most of the potentially methylated sites of PHF-tau are subject to acetylation as well, suggesting that these modifications might compete for the same site-specific lysine residues on pathological tau. K163, K174 and K180 were identified *in vivo* as possible sites of both acetylation and methylation (Min et al., 2010; Thomas et al., 2012), thus signifying the importance to explore the competing factors that may govern tau pathological modifications. However, significant putative acetylated sites, such as K280 and K281, have not yet been detected as being methylated (Thomas et al., 2012).

Immunohistochemical studies using a combination of a polyclonal antibody, that recognizes methylated tau epitopes, and antibodies specific for epitopes present on PHF-tau demonstrated that methylated tau is highly colocalized with NFTs especially in late-stage AD brains (Thomas et al., 2012). Given that the regions found to be potentially methylated in pathological tau are essential for interactions with microtubules and other partners, lysine methylation may serve to suppress tau binding to these partners. Moreover, lysine residues have been shown to participate in electrostatic interactions facilitating abnormal protein aggregation (Sinha et al., 2011) and, as a result, it has been suggested that methylation of lysine residues possibly enables interactions between tau molecules, playing thus an important role in tau self-assembly and NFT formation. This is further supported by the discovery that lysine methylation of other non-histone proteins, such as the transcription factor p53, affects both protein-protein interactions and protein stability (West and Gozani, 2011). In contrast, although the impact of lysine methylation on endogenous tau activity remains unknown, recombinant tau methylated *in vitro* via reductive methylation appeared to have low tendency for aggregation and the modifications actually promoted tubulin assembly (Funk et al., 2014), indicating that methylation of tau might have a protecting role against abnormal aggregation of the protein. However, the specificity of a chemically-induced modification is generally low, making it difficult to interpret its effects on tau. Therefore, an extensive investigation of the site-dependent lysine methylation observed *in vivo* would contribute to the understanding of this modification in tau biology.

TAU UBIQUITYLATION

Ubiquitylation involves the formation of an isopeptide bond between the C-terminal carboxyl group of the small regulatory protein ubiquitin and the ε-amino group present in lysine side chains of proteins (**Figure 2C**). Sequential addition of more than one ubiquitin molecule by ubiquitin-chain elongation factors (E4 polyubiquitin ligases) can result in the generation of long polyubiquitin chains, which differ in terms of the specific lysine residue that is used to form an isopeptide bond to the C-terminal glycine of the next ubiquitin molecule defining, therefore, the type of polyubiquitin linkage. In general, it is polyubiquitylation rather than the attachment of a single ubiquitin that acts to induce the proteolytic degradation of targeted proteins in the cytoplasm by the UPS, but different types of polyubiquitin linkage affect the fate of the modified protein in various ways. Whereas, K48-polyubiquitylated proteins are degraded by the UPS pathway with the help of Rad23 proteins, which stimulate their binding to the proteasome (Nathan et al., 2013), K63-polyubiquitylated proteins are directed to the lysosomal-autophagic pathway. K63 polyubiquitin chains were shown to interact selectively with the cellular factor ESCRT0 (*Endosomal Sorting Complex Required for Transport*), which prevents the binding to the 26s proteasome (Nathan et al., 2013), permitting K63-polyubiquitylated proteins to serve different functions, such as receptor endocytosis, intracellular signaling and DNA repair (Mukhopadhyay and Riezman, 2007; Ikeda and Dikic, 2008).

Ubiquitylation takes place in three successive stages, each of them involving a distinct enzyme: an E1 ubiquitin activating enzyme that catalyzes the ATP-dependent ubiquitin activation, an E2 ubiquitin conjugating enzyme onto which activated ubiquitin is transferred through a transesterification reaction and, finally, an E3 ubiquitin ligase essential for catalyzing the formation of the isopeptide bond between ubiquitin's terminal glycine and the target protein. Amongst these, the E3 ubiquitin ligase primarily defines the specific protein substrate that will be ubiquitylated.

Enzymes Regulating Tau Ubiquitylation

Several E3 ligases have been reported to ubiquitylate tau, including the C-terminus of the Hsc70-interacting protein (CHIP), TNF receptor-associated factor 6 (TRAF6) and axotrophin/MARCH7 (Petrucelli et al., 2004; Babu et al., 2005; Flach et al., 2014), whereas other E3 ubiquitin ligases, such as parkin and Cbl, failed to ubiquitylate hyperphosphorylated tau (Petrucelli et al., 2004; Shimura et al., 2004). CHIP was shown to ubiquitylate tau *in vivo* and *in vitro* by associating with tau's MBD and the nearby proline-rich region, thereby promoting the proteasome-mediated degradation of soluble tau (Petrucelli et al., 2004). CHIP has intrinsic E3 ubiquitin ligase activity via a U-box domain, and ubiquitylates tau through K48 or K63 linkages (Petrucelli et al., 2004). Two types of E2 ubiquitin conjugating enzymes, UbcH5a and Ubc13-Uev1a, have been identified to interact with CHIP, but it is likely that the sequential interaction of Ubc13-Uev1a with other E2 enzymes is responsible particularly for ubiquitylating tau with K63 polyubiquitin chains (Xu et al., 2008). It has also been reported that hyperphosphorylated tau derived from AD brains can be polyubiquitylated by use of HbcH5B as an E2 enzyme (Shimura et al., 2004). CHIP might mediate tau degradation in both physiological and diseased conditions regardless of its phosphorylation state (Zhang et al., 2008), however, tau hyperphosphorylation was shown to be a recognition requirement for ubiquitylation by the CHIP-Hsc70 complex in the presence of HbcH5B (Shimura et al., 2004).

CHIP interacts directly with the molecular chaperone Hsp70/Hsp90 and increased Hsp70 activity in HEK293 cells was found to weaken CHIP activity, thereby suppressing CHIP-mediated tau ubiquitylation; given that Hsp70 interacts with tau this suggests an antagonistic relationship between the two

interacting partners (Petrucelli et al., 2004). A quantitative analysis of CHIP in human and mouse brains revealed that the levels of CHIP and Hsp70 appear to be increased in AD compared with normal controls (Sahara et al., 2005). Also, in several human tauopathies, CHIP localized to tau neuronal and glial lesions, with 3R tauopathies displaying more CHIP immunoreactivity than 4R or 3R + 4R tauopathies (Petrucelli et al., 2004). Increased accumulation of aggregated tau species was observed in a cell culture system overexpressing CHIP (Petrucelli et al., 2004). In contrast, insoluble tau accumulation has been increased in a mouse model lacking CHIP (Sahara et al., 2005). These data suggest that the CHIP-Hsp70 complex might be a key molecular assembly affecting tau pathogenic events, but its role needs further investigation.

CHIP may also affect abnormal tau levels indirectly via two possible processes. Firstly, it has been demonstrated that CHIP ubiquitylates and controls the levels of HDAC6, a deacetylase of the molecular chaperone Hsp90, and enhanced levels of HDAC6 have been associated with augmented tau accumulation (Cook et al., 2012). The second pathway involves a different stress-induced substrate of CHIP, the cellular kinase Akt, which prevents CHIP-induced tau ubiquitylation and its subsequent degradation by regulating the CHIP-Hsp90 complex directly, competing with tau for binding to CHIP or promoting tau hyperphosphorylation at S262/S356, a tau species that is not recognized by the CHIP-Hsp90 complex (Dickey et al., 2008).

Another candidate E3 ubiquitin ligase for tau is TRAF6, which ubiquitylates tau via K63 linkages, apparently inducing tau degradation through the UPS pathway (Babu et al., 2005). Although, K63 polyubiquitylation has not been associated with proteolytic degradation of substrates by the UPS, the 26s proteasome is capable of binding and degrading K63-polyubiquitylated proteins *in vitro* in a similarly way to proteins modified by K48-polyubiquitin chains (Hofmann and Pickart, 2001). In aggregates extracted from AD brains TRAF6 was shown to be colocalized with the ubiquitin-associating protein sequestosome 1/p62, a cellular protein responsible for interacting with the proteasomal subunit Rpt1 (Babu et al., 2005). p62 interacts with the K63 polyubiquitin chain of tau through its UBA domain (Babu et al., 2005), so is suggested to be an essential intermediate of TRAF6-mediated tau degradation.

Recently, by use of yeast-two-hybrid systems it was shown that axotrophin/MARCH7 is a tau-interacting protein and, also, has E3 ligase activity via its C-terminal RING-variant domain in the presence of the E2 enzymes UbcH5b/c, UbcH6 and, to a lesser extent, UbcH13 (Flach et al., 2014). Axotrophin is able to induce tau monoubiquitylation *in vitro* with tau isoforms being preferentially modified at multiple sites, including some located in the MBD, which led to weakened tau binding to microtubules (Flach et al., 2014). In AD brain tissues, axotrophin was observed to colocalize with tau aggregates in different cellular compartments, such as the cell soma or dendrites, in contrast to normal brains and tau knockout mice, where axotrophin was found predominantly in the nucleus implying that tau affects the intracellular sorting of axotrophin (Flach et al., 2014).

Ubiquitylation is a reversible process with specific deubiquitinases (DUBs), catalyzing the cleavage of the isopeptide bond. So far, only Otub1, a cysteine protease deubiquitinating enzyme, has been reported to deubiquitinate endogenous tau in mouse brains and prevent tau degradation by removing K48 polyubiquitin chains (Wang et al., 2017). Using primary neurons derived from a tau transgenic mice model, it was shown that Otub1 expression leads to increased total tau levels confirming the role of Otub1 as a tau deubiquitinating enzyme and suggesting that impairment of Otub1 expression could result in impaired tau clearance (Wang et al., 2017). Furthermore, Otub1 was shown to contribute directly to tau pathology, since Otub1 expression in primary neurons leads to enhanced tau aggregation and increased levels of oligomeric tau forms (Wang et al., 2017), which might be important given that tau oligomers have emerged as the pathogenic species in tauopathies (Lasagna-Reeves et al., 2010).

Putative Ubiquitylated Sites on Tau

Mass spectrometric analysis of soluble PHF-tau immunopurified from AD brains revealed three putative ubiquitylated lysine residues: K254 and K353 located in the R1 and R4 repeat sequences, respectively, and K311 found in the flanking region between the R2 and R3 repeat sequences (**Figure 3C**; Cripps et al., 2006). K290, another lysine residue located within the MBD, was detected to be ubiquitylated in a mouse model of AD (Morris et al., 2015). Endogenous murine tau is ubiquitylated at 15 possible lysine residues, which are distributed mostly throughout the MBD region, except for K44 that is found in the N-terminal region (Morris et al., 2015); some of these residues are subject to methylation as well. For example, K254 from PHF-tau isolated from late-stage AD regions is either ubiquitylated or methylated, with the latter strongly dominating (Thomas et al., 2012). Moreover, to date all of the lysine residues discovered to be possibly ubiquitylated are sites that could be acetylated as well. These discoveries suggest that some modifications occur at the expense of others indicating even more strongly the importance to clarify the site-specific biochemical cross talk between competing post-translational modifications. Furthermore, mass spectrometric data identified three types of polyubiquitin linkage through which PHF-tau is modified, K6, K11 and, predominantly, K48 linkages (Cripps et al., 2006), whereas soluble tau can also be ubiquitylated via K63 polyubiquitin conjugation (Petrucelli et al., 2004). Notably, coexpression of K63 ubiquitin with a disease-associated tau mutant in SH-SY5Y neuroblastoma cells enhanced the formation of ubiquitin-enriched tau-positive inclusions (Tan et al., 2008).

The Effect of Ubiquitylation on Tau Biology

The studies concerning the role of tau ubiquitylation in its degradation are rather controversial. Tau can be proteolytically processed by the proteasome through an ubiquitin-dependent process, but, since tau is a natively unfolded protein, it was shown that normal tau degradation might not require its preceding ubiquitylation at all (David et al., 2002; Petrucelli et al., 2004; Grune et al., 2010). At the same time, the contribution of tau ubiquitylation in tau pathology has not been completely clarified. Ubiquitin was identified as a protein component of PHFs, NFTs and neurites associated with senile plaques in the brains of

patients with AD (Mori et al., 1987; Perry et al., 1987), which appeared to include more ubiquitin compared to normal controls (Riederer et al., 2009). However, given that pre-tangles were not immunostained by an anti-ubiquitin antibody, this suggests that ubiquitin might be linked to fibrillary inclusions only after their formation (Bancher et al., 1991; Garcia-Sierra et al., 2012). Similarly, the ends of neuropil threads, which represent newly formed regions, are characterized by the absence of anti-ubiquitin immunostaining (Iwatsubo et al., 1992). Moreover, abnormal hyperphosphorylation and N-terminal cleavage of tau was shown to precede both the formation as well as the ubiquitylation of tau neurofibrillary inclusions in AD brains (Bancher et al., 1991; Morishima-Kawashima et al., 1993). In contrast, it was reported that both monoubiquitylation and polyubiquitylation contribute to the formation of insoluble protein inclusions present in neurodegenerative diseases (Dickey et al., 2006; Tan et al., 2008) and, as mentioned above, increased aggregation of tau was detected in a cell culture overexpressing CHIP (Petrucelli et al., 2004) implying that ubiquitylation enhances the formation of these aggregates.

Since tau was identified as the ubiquitin-targeted protein in PHFs (Morishima-Kawashima et al., 1993), this has raised questions about the insufficient clearance of pathological fibrillary inclusions of tau. Apart from inaccessibility of the ubiquitylated tau aggregates by the cellular quality control system, the inhibitory binding of PHF-tau to proteasomes is responsible for the proteasomal impairment observed in AD brains (Keck et al., 2003). Additionally, most ubiquitin found in PHFs from AD brains occurs as a monoubiquitylated form, whereas only a small proportion of ubiquitin forms polyubiquitin chains (Morishima-Kawashima et al., 1993), making it difficult to induce UPS-mediated proteolysis of tau aggregates. Another aspect demanding further investigation is the role of the autophagic pathway in removing insoluble tau structures since truncated tau present in AD brains is reported to be preferentially cleared by the autophagic pathway (Rissman et al., 2004; Dolan and Johnson, 2010).

Since impaired tau clearance is widely considered to be a critical factor causing tau accumulation in neurons, many therapeutic approaches targeting tau pathology aim to promote either ubiquitylation or degradation of tau protein. Long-term administration of lithium to murine models of AD-like tauopathies reduces tau lesions primarily by enhancing their ubiquitylation (Nakashima et al., 2005), whereas synthesis of molecules that bring tau and E3 ubiquitin ligases together aims to enhance tau polyubiquitylation and degradation (Chu et al., 2016). Lastly, specific RNA aptamers of USP14, a proteasome-associated deubiquitylating enzyme, inhibited the deubiquitylating activity of this enzyme facilitating the proteasomal degradation of tau *in vitro* (Lee et al., 2015).

TAU SUMOYLATION

SUMOylation is another modification in which a small protein is post-translationally attached to the target protein. An ubiquitin-like protein, the small ubiquitin-like modifier (SUMO), is transferred enzymatically to the terminal amino group of lysine side chains of the target protein forming an isopeptide bond in a way similar to ubiquitylation (**Figure 2D**). Three main SUMO isoforms are expressed in cells, SUMO1, SUMO2, and SUMO3, of which SUMO2 and SUMO3 are more similar to each other than to SUMO1 (Sarge and Park-Sarge, 2009).

Analysis of immunoreactive tau species derived from HEK293 cells expressing tau and different His-tagged SUMO isoforms showed that tau is preferentially monoSUMOylated by SUMO1 and, to a lesser extent, by SUMO2 and SUMO3 (Dorval and Fraser, 2006). Like ubiquitin, SUMO is conjugated by an ATP-dependent enzymatic cascade involving an E1 activating enzyme, an E2 SUMO-conjugating enzyme and an E3-type SUMO ligase. The AOS1-UBA2 complex acts as an E1 activating enzyme, whilst Ubch9 has E2 SUMO-conjugating activity (Desterro et al., 1997; Gong et al., 1999), although there is as yet no direct evidence that they are responsible for tau SUMOylation. Like ubiquitylation, SUMOylation is a reversible process, since specific proteases, called SENPs, can rapidly remove SUMO from their substrates. Although the SENP3 protease was reported to be downregulated in AD tissues (Weeraratna et al., 2007), as with SUMOylation enzymes, no particular proteases have been identified specifically to deSUMOylate tau.

Lysine residues that are targeted for SUMOylation are part of the consensus motif ΨKX(E/D), where Ψ and X represent a hydrophobic residue and any amino acid, respectively, (Dorval and Fraser, 2006). Tau contains two such motifs, VK340SE and AK385TD, however, the examination of SUMOylation at these lysine sites by generating the tau mutants K340R and K385R showed that only K340R displays altered SUMOylation levels indicating that K340, located within the MBD, is the major SUMOylation site on tau (**Figure 3D**; Dorval and Fraser, 2006). Another study that also used the K340R mutation showed that the effect of tau SUMOylation on HEK293 cells co-transfected with SUMO1 and tau K340R is eliminated, confirming that K340 is indeed a putative SUMOylation site (Luo H. B. et al., 2014). Between valine and alanine, valine displays higher hydrophobicity, potentially explaining why the motif VK340SE might form a more appropriate environment than AK385TD for facilitating the SUMOylation of the included lysine residue.

Tau is available for SUMOylation only after its release from microtubules (Dorval and Fraser, 2006) suggesting that SUMOylation is a post-translational modification that does not target the endogenous tau pool but, consequently, is likely to be involved exclusively in tau pathogenic processes. This agrees with evidence showing that tau hyperphosphorylation, which is the main trigger of tau unbinding from microtubules, facilitates SUMOylation by SUMO1 in HEK293 cells (Luo H. B. et al., 2014). Although hyperphosphorylation possibly precedes SUMOylation, there is increased evidence that tau SUMOylation reciprocally enhances tau hyperphosphorylation at several AD-related sites, such as T231 and S262 (Luo H. B. et al., 2014). SUMOylation also modulates tau ubiquitylation; SUMOylation of hyperphosphorylated tau at K340 inhibits its ubiquitylation and the subsequent proteasome-dependent degradation (Luo H. B. et al., 2014). In contrast, inhibition of the proteasome pathway stimulates tau ubiquitylation, whereas tau

SUMOylation is eliminated (Dorval and Fraser, 2006). Possible reasons explaining why tau SUMOylation affects ubiquitylation and *vice versa* is that conjugation of a polypeptide group may inhibit the attachment of another large molecule to the neighboring lysine residues by steric factors or that these two tau modifications compete for the same lysine residues on tau, even though the only putative SUMOylated site, K340, was not identified to be ubiquitylated. SUMOylation could be a factor contributing to the impaired clearance of tau under pathological conditions by upregulating the pool of pathogenic tau in the cytosol and enhancing tau aggregation due to the decreased solubility of SUMOylated tau (Luo H. B. et al., 2014).

Immunohistochemical analysis of brains from APP transgenic mice, a model of AD, revealed that SUMO1 co-localizes with hyperphosphorylated tau in neurites associated with amyloid plaques suggesting that tau SUMOylation is a downstream effect mediated by pathological Aβ amyloid plaques (Takahashi et al., 2008). In agreement with this observation, rat primary hippocampal neurons displayed increasing levels of tau SUMOylation when treated with increasing concentrations of Aβ peptides (Luo H. B. et al., 2014). In the Tg2576 murine model of AD, SUMO1 protein conjugation was elevated both in the cortex and hippocampus (Nistico et al., 2014). Conversely, NFTs found in the brains of AD patients and hyperphosphorylated tau inclusions from mutant tau transgenic mouse brains were both negative for SUMO1 immunoreactivity (Takahashi et al., 2008). In progressive supranuclear palsy brain tissues, SUMO1 colocalizes within perinuclear tau-positive inclusions in oligodendrocytes and labels lysosomes in oligodendrocytes containing tau inclusions, in contrast to those where tau aggregates are absent (Wong et al., 2013). This finding indicates that SUMOylation might be involved in the autophagy-lysosome pathway in tauopathies, but this remains to be elucidated. What is more, increased SUMO1 levels were determined by ELISA in blood plasma derived from both dementia and mild cognitive impairment patients compared to healthy samples suggesting that SUMO1 could serve as an AD biomarker (Cho et al., 2015). Recently, a SUMO1 transgenic mouse model with SUMO1 overexpression in neurons was generated, in which increased levels of SUMO1 eliminated basal synaptic transmission, impaired presynaptic function and reduced spine density, which resulted in learning and memory deficits (Matsuzaki et al., 2015). Since tau is an important SUMO1 target in the cytoplasm and dendritic spines it would be intriguing if hyper-SUMOylation of tau underpinned these deficits, although there are clearly other molecular targets that require follow up.

TAU GLYCATION

Glycation (or non-enzymatic glycosylation) defines the non-specific reaction in which reducing sugars, especially glucose, are non-enzymatically linked to proteins by condensation of a sugar aldehyde or ketone group with terminal amino groups of lysine side chains (**Figure 2E**). As a result, glycation depends on both the availability of free lysine amino groups along the polypeptide chain and the concentration of sugar. The glycation products are subject to further changes that lead to the formation of the advanced glycation end products (AGEs) by developing irreversible cross-links with other proteins over a long period of time (Eble et al., 1983). Although, the formation of AGEs does not involve enzymes, there are several enzyme systems that antagonize AGEs production, like the NADPH-dependent aldose reductase and the aldehyde dehydrogenase (Li J. et al., 2012).

Non enzymatic glycation is one of the modifications detected in PHF-tau purified from human AD brains *in vivo*, but not in soluble tau (**Figure 3E**; Ledesma et al., 1994). It occurs preferentially at the MBD of PHF-tau (Ledesma and Avila, 1995); lysines present at the R3 repeat were initially identified to be glycated *in vitro* (Ledesma et al., 1994), but later studies confirmed immunologically that glycation takes place *in vivo* within the MBD (Ledesma and Avila, 1995). 13 lysine residues, located throughout the polypeptide chain, were also identified as being glycated *in vitro* (Nacharaju et al., 1997); although most of these sites were detected in both 3R and 4R isoforms, K280 and K281 are absent in the case of 3R tau and this difference seems enough to cause slower glycation of 3R compared to 4R isoforms (Nacharaju et al., 1997; Liu et al., 2016). Recently, mass spectrometry analysis revealed 19 novel sites of glycation occurring on recombinant full length tau (Liu et al., 2016).

Since tau has been shown to be glycated within the MBD and glycated tau appears to have reduced affinity for microtubules *in vitro*, it has been suggested that glycation blocks tau-microtubule interactions, thereby assisting tau hyperphosphorylation (Ledesma et al., 1994). The region of tau containing the MBD was shown to participate in its self-association (Ledesma and Avila, 1995), implying that glycation indirectly facilitates the aggregation of tau or stabilizes the aggregated tau species. On the other hand, since glycated PHF-tau has higher tendency for aggregation compared to non-glycated soluble tau, it is likely that glycation stimulates the aggregation of PHFs into more complex structures and stabilizes the assembled formations (Ledesma et al., 1994, 1996; Ko et al., 1999). This suggestion is supported by the observed crosslinking between AGE-modified proteins, which represents an additional factor contributing to the insolubility and resistance against proteolytic degradation that are characteristic of tau aggregates. However, tau glycation enhances, but is not able to trigger, aggregation *in vitro* (Necula and Kuret, 2004). In addition, glycation has different impacts on aggregation propensity depending on the tau isoform that is modified, with the full length tau isoform displaying more extensive aggregation when glycated (Liu et al., 2016).

By immunoelectron microscopy, AGEs were found to colocalize with PHF-tau in NFTs of sporadic AD (Yan et al., 1994). Intracellular AGE-positive deposits were found to correlate positively both with age in normal and AD cases and with the stage of the disease in AD patients (Luth et al., 2005). AGEs may be involved in several processes underlying tau pathogenesis; neurons carrying AGE-positive NFTs also bear intracellular reactive oxygen intermediates (Yan et al., 1994). Moreover, it has been found that the introduction of glycated recombinant tau into neuroblastoma cells is able to generate oxygen free radicals causing neuronal dysfunction by inducing

oxidative stress (Yan et al., 1994). Further studies demonstrated that AGEs may be involved in the tau-associated pathogenesis of AD via reactive oxygen intermediates by activating NF-kB-induced transcription, which leads to increased expression of the cytokine IL-6, and by enhancing the synthesis of the amyloid precursor protein, which, as a consequence, promotes the release of the Aβ peptides under stress conditions (Yan et al., 1995). By using reactive carbonyl compounds, which are elevated under conditions of oxidative stress, enhanced formation of AGE-modified tau tangles was observed *in vivo* (Kuhla et al., 2007). AGEs can also cause cellular toxicity through their receptor (RAGE). In a mouse model of AD, tau is colocalized with RAGE in the hippocampus and cortex (Choi et al., 2014) and RAGE has been associated with AGE-induced tau hyperphosphorylation as well as synapse dysfunction and spatial memory impairment in rats (Li X. H. et al., 2012). Lastly, apart from AD, tau-positive inclusions were also AGE-positive in the case of Pick's disease as well as in other neurodegenerative diseases (Sasaki et al., 1998).

CONCLUSION

Lysine residues of tau are common targets for different post-translational modifications including acetylation, methylation, ubiquitylation, SUMOylation, and glycation. As a result, it is likely that modification of a target lysine blocks or controls other possible modifications occurring at the same site. Although, the identification of possible sites found to be modified is unlikely yet to be complete, the overlap between each type of post-translational modification in terms of all lysine sites that have been discovered so far is obvious, implying that certain lysine modifications compete for the same site on tau. At the same time, the high content of lysine residues in tau provides sufficient targets to be modified emphasizing the importance of lysine post-translational modification in normal tau biology as well as the mechanisms of misfolding and cellular toxicity elicited by it pathogenic isoform(s). Significantly, the sites modified *in vitro* might differ from those identified in *in vivo* systems, whereas the species, neuronal subtype and pathological state could promote different site-specific modifications as well as certain combinations of modified lysine sites. Therefore, methodical mapping of the lysine residues that can be modified both on endogenous and abnormal tau under different pathological conditions is crucial. The impact of each type of post-translational modification on normal tau or related to pathological states of tau is likely to be site-dependent and the potential for cross-talk of these modifications is high—this fact guides the direction for future scientific research in order to unravel fully the biochemical mechanisms underpinning tau biology.

AUTHOR CONTRIBUTIONS

CK performed the review, wrote the first draft of the manuscript and prepared publication-ready figures. PP and AG supervised the work, and edited the manuscript into final form. All authors agreed the final version of the manuscript.

FUNDING

PP and AG are supported, in part, by Institute Strategic Programme Grants (BB/J004332/1 and BB/P013759/1) from the BBSRC, UK to the Roslin Institute.

REFERENCES

Babu, J. R., Geetha, T., and Wooten, M. W. (2005). Sequestosome 1/p62 shuttles polyubiquitinated tau for proteasomal degradation. *J. Neurochem.* 94, 192–203. doi: 10.1111/j.1471-4159.2005.03181.x

Ballatore, C., Lee, V. M., and Trojanowski, J. Q. (2007). Tau-mediated neurodegeneration in Alzheimer's disease and related disorders. *Nat. Rev. Neurosci.* 8, 663–672. doi: 10.1038/nrn2194

Bancher, C., Grundke-Iqbal, I., Iqbal, K., Fried, V. A., Smith, H. T., and Wisniewski, H. M. (1991). Abnormal phosphorylation of tau precedes ubiquitination in neurofibrillary pathology of Alzheimer disease. *Brain Res.* 539, 11–18. doi: 10.1016/0006-8993(91)90681-K

Binder, L. I., Frankfurter, A., and Rebhun, L. I. (1985). The distribution of tau in the mammalian central nervous system. *J. Cell Biol.* 101, 1371–1378. doi: 10.1083/jcb.101.4.1371

Blanco-Garcia, N., Asensio-Juan, E., de la Cruz, X., and Martinez-Balbas, M. A. (2009). Autoacetylation regulates P/CAF nuclear localization. *J. Biol. Chem.* 284, 1343–1352. doi: 10.1074/jbc.M806075200

Carrell, R. W., and Lomas, D. A. (1997). Conformational disease. *Lancet* 350, 134–138. doi: 10.1016/S0140-6736(97)02073-4

Cho, S. J., Yun, S. M., Lee, D. H., Jo, C., Ho Park, M., Han, C., et al. (2015). Plasma SUMO1 protein is elevated in Alzheimer's disease. *J. Alzheimers. Dis.* 47, 639–643. doi: 10.3233/JAD-150103

Choi, B. R., Cho, W. H., Kim, J., Lee, H. J., Chung, C., Jeon, W. K., et al. (2014). Increased expression of the receptor for advanced glycation end products in neurons and astrocytes in a triple transgenic mouse model of Alzheimer's disease. *Exp. Mol. Med.* 46:e75. doi: 10.1038/emm.2013.147.

Chu, T. T., Gao, N., Li, Q. Q., Chen, P. G., Yang, X. F., Chen, Y. X., et al. (2016). Specific knockdown of endogenous tau protein by peptide-directed ubiquitin-proteasome degradation. *Cell Chem. Biol.* 23, 453–461. doi: 10.1016/j.chembiol.2016.02.016

Cohen, T. J., Constance, B. H., Hwang, A. W., James, M., and Yuan, C. X. (2016). Intrinsic tau acetylation is coupled to auto-proteolytic tau fragmentation. *PLoS ONE* 11:e0158470. doi: 10.1371/journal.pone.0158470

Cohen, T. J., Friedmann, D., Hwang, A. W., Marmorstein, R., and Lee, V. M. (2013). The microtubule-associated tau protein has intrinsic acetyltransferase activity. *Nat. Struct. Mol. Biol.* 20, 756–762. doi: 10.1038/nsmb.2555

Cohen, T. J., Guo, J. L., Hurtado, D. E., Kwong, L. K., I., Mills, Trojanowski, J. Q., et al. (2011). The acetylation of tau inhibits its function and promotes pathological tau aggregation. *Nat. Commun.* 2:252. doi: 10.1038/ncomms1255

Cook, C., Carlomagno, Y., Gendron, T. F., Dunmore, J., Scheffel, K., Stetler, C., et al. (2014). Acetylation of the KXGS motifs in tau is a critical determinant in modulation of tau aggregation and clearance. *Hum. Mol. Genet.* 23, 104–116. doi: 10.1093/hmg/ddt402

Cook, C., Gendron, T. F., Scheffel, K., Carlomagno, Y., Dunmore, J., DeTure, M., et al. (2012). Loss of HDAC6, a novel CHIP substrate, alleviates abnormal tau accumulation. *Hum. Mol. Genet.* 21, 2936–2945. doi: 10.1093/hmg/dds125

Cripps, D., Thomas, S. N., Jeng, Y., Yang, F., Davies, P., and Yang, A. J. (2006). Alzheimer disease-specific conformation of hyperphosphorylated paired helical filament-Tau is polyubiquitinated through Lys-48, Lys-11, and Lys-6 ubiquitin conjugation. *J. Biol. Chem.* 281, 10825–10838. doi: 10.1074/jbc.M512786200

David, D. C., Layfield, R., Serpell, L., Narain, Y., Goedert, M., and Spillantini, M. G. (2002). Proteasomal degradation of tau protein. *J. Neurochem.* 83, 176–185. doi: 10.1046/j.1471-4159.2002.01137.x

Desterro, J. M., Thomson, J., and Hay, R. T. (1997). Ubch9 conjugates SUMO but not ubiquitin. *FEBS Lett.* 417, 297–300. doi: 10.1016/S0014-5793(97)01305-7

Dickey, C. A., Koren, J., Zhang, Y. J., Xu, Y. F., Jinwal, U. K., Birnbaum, M. J., et al. (2008). Akt and CHIP coregulate tau degradation through coordinated interactions. *Proc. Natl. Acad. Sci. U.S.A.* 105, 3622–3627. doi: 10.1073/pnas.0709180105

Dickey, C. A., Yue, M., Lin, W. L., Dickson, D. W., Dunmore, J. H., Lee, W. C., et al. (2006). Deletion of the ubiquitin ligase CHIP leads to the accumulation, but not the aggregation, of both endogenous phospho- and caspase-3-cleaved tau species. *J. Neurosci.* 26, 6985–6996. doi: 10.1523/JNEUROSCI.0746-06.2006

Dickson, D. W., Kouri, N., Murray, M. E., and Josephs, K. A. (2011). Neuropathology of frontotemporal lobar degeneration-tau (FTLD-tau). *J. Mol. Neurosci.* 45, 384–389. doi: 10.1007/s12031-011-9589-0

Ding, H., Dolan, P. J., and Johnson, G. V. (2008). Histone deacetylase 6 interacts with the microtubule-associated protein tau. *J. Neurochem.* 106, 2119–2130. doi: 10.1111/j.1471-4159.2008.05564.x

Dolan, P. J., and Johnson, G. V. (2010). A caspase cleaved form of tau is preferentially degraded through the autophagy pathway. *J. Biol. Chem.* 285, 21978–21987. doi: 10.1074/jbc.M110.110940

Dorval, V., and Fraser, P. E. (2006). Small ubiquitin-like modifier (SUMO) modification of natively unfolded proteins tau and alpha-synuclein. *J. Biol. Chem.* 281, 9919–9924. doi: 10.1074/jbc.M510127200

Eble, A. S., Thorpe, S. R., and Baynes, J. W. (1983). Nonenzymatic glucosylation and glucose-dependent cross-linking of protein. *J. Biol. Chem.* 258, 9406–9412.

Ferrer, I., Lopez-Gonzalez, I., Carmona, M., Arregui, L., Dalfo, E., Torrejon-Escribano, B., et al. (2014). Glial and neuronal tau pathology in tauopathies: characterization of disease-specific phenotypes and tau pathology progression. *J. Neuropathol. Exp. Neurol.* 73, 81–97. doi: 10.1097/NEN.0000000000000030

Flach, K., Ramminger, E., Hilbrich, I., Arsalan-Werner, A., Albrecht, F., Herrmann, L., et al. (2014). Axotrophin/MARCH7 acts as an E3 ubiquitin ligase and ubiquitinates tau protein *in vitro* impairing microtubule binding. *Biochim. Biophys. Acta* 1842, 1527–1538. doi: 10.1016/j.bbadis.2014.05.029

Funk, K. E., Thomas, S. N., Schafer, K. N., Cooper, G. L., Liao, Z., Clark, D. J., et al. (2014). Lysine methylation is an endogenous post-translational modification of tau protein in human brain and a modulator of aggregation propensity. *Biochem. J.* 462, 77–88. doi: 10.1042/BJ20140372

Garcia-Sierra, F., Jarero-Basulto, J. J., Kristofikova, Z., Majer, E., Binder, L. I., and Ripova, D. (2012). Ubiquitin is associated with early truncation of tau protein at aspartic acid(421) during the maturation of neurofibrillary tangles in Alzheimer's disease. *Brain Pathol.* 22, 240–250. doi: 10.1111/j.1750-3639.2011.00525.x

Gong, L., Li, B., Millas, S., and Yeh, E. T. (1999). Molecular cloning and characterization of human AOS1 and UBA2, components of the sentrin-activating enzyme complex. *FEBS Lett.* 448, 185–189. doi: 10.1016/S0014-5793(99)00367-1

Gorsky, M. K., Burnouf, S., Dols, J., Mandelkow, E., and Partridge, L. (2016). Acetylation mimic of lysine 280 exacerbates human tau neurotoxicity *in vivo*. *Sci. Rep.* 6:22685. doi: 10.1038/srep22685

Gratuze, M., Cisbani, G., Cicchetti, F., and Planel, E. (2016). Is Huntington's disease a tauopathy? *Brain* 139(Pt 4), 1014–1025. doi: 10.1093/brain/aww021

Grinberg, L. T., Wang, X., Wang, C., Sohn, P. D., Theofilas, P., Sidhu, M., et al. (2013). Argyrophilic grain disease differs from other tauopathies by lacking tau acetylation. *Acta Neuropathol.* 125, 581–593. doi: 10.1007/s00401-013-1080-2

Grundke-Iqbal, I., Iqbal, K., Tung, Y. C., Quinlan, M., Wisniewski, H. M., and Binder, L. I. (1986). Abnormal phosphorylation of the microtubule-associated protein tau (tau) in Alzheimer cytoskeletal pathology. *Proc. Natl. Acad. Sci. U.S.A.* 83, 4913–4917. doi: 10.1073/pnas.83.13.4913

Grune, T., Botzen, D., Engels, M., Voss, P., Kaiser, B., Jung, T., et al. (2010). Tau protein degradation is catalyzed by the ATP/ubiquitin-independent 20S proteasome under normal cell conditions. *Arch. Biochem. Biophys.* 500, 181–188. doi: 10.1016/j.abb.2010.05.008

Hernandez, F., and Avila, J. (2007). Tauopathies. *Cell. Mol. Life Sci.* 64, 2219–2233. doi: 10.1007/s00018-007-7220-x

Hofmann, R. M., and Pickart, C. M. (2001). *In vitro* assembly and recognition of Lys-63 polyubiquitin chains. *J. Biol. Chem.* 276, 27936–27943. doi: 10.1074/jbc.M103378200

Hwang, A. W., Trzeciakiewicz, H., Friedmann, D., Yuan, C. X., Marmorstein, R., Lee, V. M., et al. (2016). Conserved lysine acetylation within the microtubule-binding domain regulates map2/tau family members. *PLoS ONE* 11:e0168913. doi: 10.1371/journal.pone.0168913

Ikeda, F., and Dikic, I. (2008). Atypical ubiquitin chains: new molecular signals. 'Protein Modifications: Beyond the Usual Suspects' review series. *EMBO Rep.* 9, 536–542. doi: 10.1038/embor.2008.93.

Irwin, D. J., Cohen, T. J., Grossman, M., Arnold, S. E., McCarty-Wood, E., Van Deerlin, V. M., et al. (2013). Acetylated tau neuropathology in sporadic and hereditary tauopathies. *Am. J. Pathol.* 183, 344–351. doi: 10.1016/j.ajpath.2013.04.025

Irwin, D. J., Cohen, T. J., Grossman, M., Arnold, S. E., Xie, S. X., Lee, V. M., et al. (2012). Acetylated tau, a novel pathological signature in Alzheimer's disease and other tauopathies. *Brain* 135(Pt. 3), 807–818. doi: 10.1093/brain/aws013

Iwata, A., Riley, B. E., Johnston, J. A., and Kopito, R. R. (2005). HDAC6 and microtubules are required for autophagic degradation of aggregated huntingtin. *J. Biol. Chem.* 280, 40282–40292. doi: 10.1074/jbc.M508786200

Iwatsubo, T., Hasegawa, M., Esaki, Y., and Ihara, Y. (1992). Lack of ubiquitin immunoreactivities at both ends of neuropil threads. Possible bidirectional growth of neuropil threads. *Am. J. Pathol.* 140, 277–282.

Julien, C., Tremblay, C., Emond, V., Lebbadi, M., Salem N. Jr., Bennett, D. A., et al. (2009). Sirtuin 1 reduction parallels the accumulation of tau in Alzheimer disease. *J. Neuropathol. Exp. Neurol.* 68, 48–58. doi: 10.1097/NEN.0b013e3181922348

Kamah, A., Huvent, I., Cantrelle, F. X., Qi, H., Lippens, G., Landrieu, I., et al. (2014). Nuclear magnetic resonance analysis of the acetylation pattern of the neuronal Tau protein. *Biochemistry* 53, 3020–3032. doi: 10.1021/bi500006v

Keck, S., Nitsch, R., Grune, T., and Ullrich, O. (2003). Proteasome inhibition by paired helical filament-tau in brains of patients with Alzheimer's disease. *J. Neurochem.* 85, 115–122. doi: 10.1046/j.1471-4159.2003.01642.x

Ko, L. W., Ko, E. C., Nacharaju, P., Liu, W. K., Chang, E., Kenessey, A., et al. (1999). An immunochemical study on tau glycation in paired helical filaments. *Brain Res.* 830, 301–313. doi: 10.1016/S0006-8993(99)01415-8

Kovacs, G. G. (2016). Molecular pathological classification of neurodegenerative diseases: turning towards precision medicine. *Int. J. Mol. Sci.* 17:189. doi: 10.3390/ijms17020189

Kuhla, B., Haase, C., Flach, K., Luth, H. J., Arendt, T., and Munch, G. (2007). Effect of pseudophosphorylation and cross-linking by lipid peroxidation and advanced glycation end product precursors on tau aggregation and filament formation. *J. Biol. Chem.* 282, 6984–6991. doi: 10.1074/jbc.M609521200

Lasagna-Reeves, C. A., Castillo-Carranza, D. L., Guerrero-Muoz, M. J., Jackson, G. R., and Kayed, R. (2010). Preparation and characterization of neurotoxic tau oligomers. *Biochemistry* 49, 10039–10041. doi: 10.1021/bi1016233

Ledesma, M. D., Bonay, P., and Avila, J. (1995). Tau protein from Alzheimer's disease patients is glycated at its tubulin-binding domain. *J. Neurochem.* 65, 1658–1664.

Ledesma, M. D., Bonay, P., Colaco, C., and Avila, J. (1994). Analysis of microtubule-associated protein tau glycation in paired helical filaments. *J. Biol. Chem.* 269, 21614–21619.

Ledesma, M. D., Medina, M., and Avila, J. (1996). The *in vitro* formation of recombinant tau polymers: effect of phosphorylation and glycation. *Mol. Chem. Neuropathol.* 27, 249–258. doi: 10.1007/BF02815107

Lee, G., Cowan, N., and Kirschner, M. (1988). The primary structure and heterogeneity of tau protein from mouse brain. *Science* 239, 285–288. doi: 10.1126/science.3122323

Lee, G., Neve, R. L., and Kosik, K. S. (1989). The microtubule binding domain of tau protein. *Neuron* 2, 1615–1624. doi: 10.1016/0896-6273(89)90050-0

Lee, J. H., Shin, S. K., Jiang, Y., Choi, W. H., Hong, C., Kim, D. E., et al. (2015). Facilitated tau degradation by usp14 aptamers via enhanced proteasome activity. *Sci. Rep.* 5:10757. doi: 10.1038/srep10757

Lei, P., Ayton, S., Finkelstein, D. I., Spoerri, L., Ciccotosto, G. D., Wright, D. K., et al. (2012). Tau deficiency induces parkinsonism with dementia by impairing APP-mediated iron export. *Nat. Med.* 18, 291–295. doi: 10.1038/nm.2613

Li, J., Liu, D., Sun, L., Lu, Y., and Zhang, Z. (2012). Advanced glycation end products and neurodegenerative diseases: mechanisms and perspective. *J. Neurol. Sci.* 317, 1–5. doi: 10.1016/j.jns.2012.02.018

Li, X. H., Lv, B. L., Xie, J. Z., Liu, J., Zhou, X. W., and Wang, J. Z. (2012). AGEs induce Alzheimer-like tau pathology and memory deficit

via RAGE-mediated GSK-3 activation. *Neurobiol. Aging* 33, 1400–1410. doi: 10.1016/j.neurobiolaging.2011.02.003

Liu, K., Liu, Y., Li, L., Qin, P., Iqbal, J., Deng, Y., et al. (2016). Glycation alter the process of tau phosphorylation to change tau isoforms aggregation property. *Biochim. Biophys. Acta* 1862, 192–201. doi: 10.1016/j.bbadis.2015.12.002

Loomis, P. A., Howard, T. H., Castleberry, R. P., and Binder, L. I. (1990). Identification of nuclear tau isoforms in human neuroblastoma cells. *Proc. Natl. Acad. Sci. U.S.A.* 87, 8422–8426. doi: 10.1073/pnas.87.21.8422

Luo, H. B., Xia, Y. Y., Shu, X. J., Liu, Z. C., Feng, Y., Liu, X. H., et al. (2014). SUMOylation at K340 inhibits tau degradation through deregulating it s phosphorylation and ubiquitination. *Proc. Natl. Acad. Sci. U.S.A.* 111, 16586–16591. doi: 10.1073/pnas.1417548111

Luo, Y., Ma, B., Nussinov, R., and Wei, G. (2014). Structural insight into tau protein's paradox of intrinsically disordered behavior, self-acetylation activity, and aggregation. *J. Phys. Chem. Lett.* 5, 3026–3031. doi: 10.1021/jz501457f

Luth, H. J., Ogunlade, V., Kuhla, B., Kientsch-Engel, R., Stahl, W. J., Webster, J., et al. (2005). Age- and stage-dependent accumulation of advanced glycation end products in intracellular deposits in normal and Alzheimer's disease brains. *Cereb. Cortex* 15, 211–220. doi: 10.1093/cercor/bhh123

Mandelkow, E. M., Biernat, J., Drewes, G., Gustke, N., Trinczek, B., and Mandelkow, E. (1995). Tau domains, phosphorylation, and interactions with microtubules. *Neurobiol. Aging 16*, 355–362. discussion: 362–363. doi: 10.1016/0197-4580(95)00025-A

Martin, L., Latypova, X., and Terro, F. (2011). Post-translational modifications of tau protein: implications for Alzheimer's disease. *Neurochem. Int.* 58, 458–471. doi: 10.1016/j.neuint.2010.12.023

Matsuzaki, S., Lee, L., Knock, E., Srikumar, T., Sakurai, M., Hazrati, L. N., et al. (2015). SUMO1 affects synaptic function, spine density and memory. *Sci. Rep.* 5:10730. doi: 10.1038/srep10730.

Michishita, E., Park, J. Y., Burneskis, J. M., Barrett, J. C., and Horikawa, I. (2005). Evolutionarily conserved and nonconserved cellular localizations and functions of human SIRT proteins. *Mol. Biol. Cell* 16, 4623–4635. doi: 10.1091/mbc.E05-01-0033

Migheli, A., Butler, M., Brown, K., and Shelanski, M. L. (1988). Light and electron microscope localization of the microtubule-associated tau protein in rat brain. *J. Neurosci.* 8, 1846–1851.

Min, S. W., Chen, X., Tracy, T. E., Li, Y., Zhou, Y., Wang, C., et al. (2015). Critical role of acetylation in tau-mediated neurodegeneration and cognitive deficits. *Nat. Med.* 21, 1154–1162. doi: 10.1038/nm.3951

Min, S. W., Cho, S. H., Zhou, Y., Schroeder, S., Haroutunian, V., Seeley, W. W., et al. (2010). Acetylation of tau inhibits its degradation and contributes to tauopathy. *Neuron* 67, 953–966. doi: 10.1016/j.neuron.2010.08.044

Mori, H., Kondo, J., and Ihara, Y. (1987). Ubiquitin is a component of paired helical filaments in Alzheimer's disease. *Science* 235, 1641–1644. doi: 10.1126/science.3029875

Morishima-Kawashima, M., Hasegawa, M., Takio, K., Suzuki, M., Titani, K., and Ihara, Y. (1993). Ubiquitin is conjugated with amino-terminally processed tau in paired helical filaments. *Neuron* 10, 1151–1160. doi: 10.1016/0896-6273(93)90063-W

Morris, M., Knudsen, G. M., Maeda, S., Trinidad, J. C., Ioanoviciu, A., Burlingame, A. L., et al. (2015). Tau post-translational modifications in wild-type and human amyloid precursor protein transgenic mice. *Nat. Neurosci.* 18, 1183–1189. doi: 10.1038/nn.4067

Mukhopadhyay, D., and Riezman, H. (2007). Proteasome-independent functions of ubiquitin in endocytosis and signaling. *Science* 315, 201–205. doi: 10.1126/science.1127085

Mukrasch, M. D., Bibow, S., Korukottu, J., Jeganathan, S., Biernat, J., Griesinger, C., et al. (2009). Structural polymorphism of 441-residue tau at single residue resolution. *PLoS Biol.* 7:e34. doi: 10.1371/journal.pbio.1000034

Nacharaju, P., Ko, L., and Yen, S. H. (1997). Characterization of *in vitro* glycation sites of tau. *J. Neurochem.* 69, 1709–1719. doi: 10.1046/j.1471-4159.1997.69041709.x

Nakashima, H., Ishihara, T., Suguimoto, P., Yokota, O., Oshima, E., Kugo, A., et al. (2005). Chronic lithium treatment decreases tau lesions by promoting ubiquitination in a mouse model of tauopathies. *Acta Neuropathol.* 110, 547–556. doi: 10.1007/s00401-005-1087-4

Nathan, J. A., Kim, H. T., Ting, L., Gygi, S., and Goldberg, A. L. (2013). Why do cellular proteins linked to K63-polyubiquitin chains not associate with proteasomes? *EMBO J.* 32, 552–565. doi: 10.1038/emboj.2012.354

Necula, M., and Kuret, J. (2004). Pseudophosphorylation and glycation of tau protein enhance but do not trigger fibrillization *in vitro*. *J. Biol. Chem.* 279, 49694–49703. doi: 10.1074/jbc.M405527200

Neve, R. L., Harris, P., Kosik, K. S., Kurnit, D. M., and Donlon, T. A. (1986). Identification of cDNA clones for the human microtubule-associated protein tau and chromosomal localization of the genes for tau and microtubule-associated protein 2. *Brain Res.* 387, 271–280. doi: 10.1016/0169-328X(86)90033-1

Nistico, R., Ferraina, C., Marconi, V., Blandini, F., Negri, L., Egebjerg, J., et al. (2014). Age-related changes of protein SUMOylation balance in the AbetaPP Tg2576 mouse model of Alzheimer's disease. *Front. Pharmacol.* 5:63. doi: 10.3389/fphar.2014.00063.

Pallas-Bazarra, N., Jurado-Arjona, J., Navarrete, M., Esteban, J. A., Hernandez, F., Avila, J., et al. (2016). Novel function of Tau in regulating the effects of external stimuli on adult hippocampal neurogenesis. *EMBO J.* 35, 1417–1436. doi: 10.15252/embj.201593518

Perry, G., Friedman, R., Shaw, G., and Chau, V. (1987). Ubiquitin is detected in neurofibrillary tangles and senile plaque neurites of Alzheimer disease brains. *Proc. Natl. Acad. Sci. U.S.A.* 84, 3033–3036. doi: 10.1073/pnas.84.9.3033

Petrucelli, L., Dickson, D., Kehoe, K., Taylor, J., Snyder, H., Grover, A., et al. (2004). CHIP and Hsp70 regulate tau ubiquitination, degradation and aggregation. *Hum. Mol. Genet.* 13, 703–714. doi: 10.1093/hmg/ddh083

Riederer, I. M., Schiffrin, M., Kovari, E., Bouras, C., and Riederer, B. M. (2009). Ubiquitination and cysteine nitrosylation during aging and Alzheimer's disease. *Brain Res. Bull.* 80, 233–241. doi: 10.1016/j.brainresbull.2009.04.018

Rissman, R. A., Poon, W. W., Blurton-Jones, M., Oddo, S., Torp, R., Vitek, M., et al. (2004). Caspase-cleavage of tau is an early event in Alzheimer disease tangle pathology. *J. Clin. Invest.* 114, 121–130. doi: 10.1172/JCI200420640

Sahara, N., Murayama, M., Mizoroki, T., Urushitani, M., Imai, Y., Takahashi, R., et al. (2005). *In vivo* evidence of CHIP up-regulation attenuating tau aggregation. *J. Neurochem.* 94, 1254–1263. doi: 10.1111/j.1471-4159.2005.03272.x

Sarge, K. D., and Park-Sarge, O. K. (2009). Sumoylation and human disease pathogenesis. *Trends Biochem. Sci.* 34, 200–205. doi: 10.1016/j.tibs.2009.01.004

Sasaki, N., Fukatsu, R., Tsuzuki, K., Hayashi, Y., Yoshida, T., Fujii, N., et al. (1998). Advanced glycation end products in Alzheimer's disease and other neurodegenerative diseases. *Am. J. Pathol.* 153, 1149–1155. doi: 10.1016/S0002-9440(10)65659-3

Schweers, O., Schonbrunn-Hanebeck, E., Marx, A., and Mandelkow, E. (1994). Structural studies of tau protein and Alzheimer paired helical filaments show no evidence for beta-structure. *J. Biol. Chem.* 269, 24290–24297.

Shimura, H., Schwartz, D., Gygi, S. P., and Kosik, K. S. (2004). CHIP-Hsc70 complex ubiquitinates phosphorylated tau and enhances cell survival. *J. Biol. Chem.* 279, 4869–4876. doi: 10.1074/jbc.M305838200

Sinha, S., Lopes, D. H., Du, Z., Pang, E. S., Shanmugam, A., Lomakin, A., et al. (2011). Lysine-specific molecular tweezers are broad-spectrum inhibitors of assembly and toxicity of amyloid proteins. *J. Am. Chem. Soc.* 133, 16958–16969. doi: 10.1021/ja206279b

Sohn, P. D., Tracy, T. E., Son, H. I., Zhou, Y., Leite, R. E., Miller, B. L., et al. (2016). Acetylated tau destabilizes the cytoskeleton in the axon initial segment and is mislocalized to the somatodendritic compartment. *Mol. Neurodegener.* 11:47. doi: 10.1186/s13024-016-0109-0

Spillantini, M. G., Goedert, M., Crowther, R. A., Murrell, J. R., Farlow, M. R., and Ghetti, B. (1997). Familial multiple system tauopathy with presenile dementia: a disease with abundant neuronal and glial tau filaments. *Proc. Natl. Acad. Sci. U.S.A.* 94, 4113–4118. doi: 10.1073/pnas.94.8.4113

Takahashi, K., Ishida, M., Komano, H., and Takahashi, H. (2008). SUMO-1 immunoreactivity co-localizes with phospho-tau in APP transgenic mice but not in mutant Tau transgenic mice. *Neurosci. Lett.* 441, 90–93. doi: 10.1016/j.neulet.2008.06.012

Tan, J. M., Wong, E. S., Kirkpatrick, D. S., Pletnikova, O., Ko, H. S., Tay, S., et al. (2008). Lysine 63-linked ubiquitination promotes the formation and autophagic clearance of protein inclusions associated with neurodegenerative diseases. *Hum. Mol. Genet.* 17, 431–439. doi: 10.1093/hmg/ddm320

Thomas, S. N., Funk, K. E., Wan, Y., Liao, Z., Davies, P., Kuret, J., et al. (2012). Dual modification of Alzheimer's disease PHF-tau protein by lysine methylation and ubiquitylation: a mass spectrometry approach. *Acta Neuropathol.* 123, 105–117. doi: 10.1007/s00401-011-0893-0

Tracy, T. E., Sohn, P. D., Minami, S. S., Wang, C., Min, S. W., Li, Y., et al. (2016). Acetylated tau obstructs KIBRA-mediated signaling in synaptic plasticity and promotes tauopathy-related memory loss. *Neuron* 90, 245–260. doi: 10.1016/j.neuron.2016.03.005

Verkhratsky, A., Parpura, V., Pekna, M., Pekny, M., and Sofroniew, M. (2014). Glia in the pathogenesis of neurodegenerative diseases. *Biochem. Soc. Trans.* 42, 1291–1301. doi: 10.1042/BST20140107

Wang, P., Joberty, G., Buist, A., Vanoosthuyse, A., Stancu, I. C., Vasconcelos, B., et al. (2017). Tau interactome mapping based identification of Otub1 as tau deubiquitinase involved in accumulation of pathological tau forms *in vitro* and *in vivo*. *Acta Neuropathol.* 133, 731–749. doi: 10.1007/s00401-016-1663-9

Weeraratna, A. T., Kalehua, A., Deleon, I., Bertak, D., Maher, G., Wade, M. S., et al. (2007). Alterations in immunological and neurological gene expression patterns in Alzheimer's disease tissues. *Exp. Cell Res.* 313, 450–461. doi: 10.1016/j.yexcr.2006.10.028

West, L. E., and Gozani, O. (2011). Regulation of p53 function by lysine methylation. *Epigenomics* 3, 361–369. doi: 10.2217/epi.11.21

Williamson, R., Scales, T., Clark, B. R., Gibb, G., Reynolds, C. H., Kellie, S., et al. (2002). Rapid tyrosine phosphorylation of neuronal proteins including tau and focal adhesion kinase in response to amyloid-beta peptide exposure: involvement of Src family protein kinases. *J. Neurosci.* 22, 10–20. Available online at: http://www.jneurosci.org/content/22/1/10.long

Wong, M. B., Goodwin, J., Norazit, A., Meedeniya, A. C., Richter-Landsberg, C.,Gai, W., et al. (2013). SUMO-1 is associated with a subset of lysosomes in glial protein aggregate diseases. *Neurotox. Res.* 23, 1–21. doi: 10.1007/s12640-012-9358-z

Xu, Z., Kohli, E., Devlin, K. I., Bold, M., Nix, J. C., and Misra, S. (2008). Interactions between the quality control ubiquitin ligase CHIP and ubiquitin conjugating enzymes. *BMC Struct. Biol.* 8:26. doi: 10.1186/1472-6807-8-26

Yan, S. D., Chen, X., Schmidt, A. M., Brett, J., Godman, G., Zou, Y. S., et al. (1994). Glycated tau protein in Alzheimer disease: a mechanism for induction of oxidant stress. *Proc. Natl. Acad. Sci. U.S.A.* 91, 7787–7791. doi: 10.1073/pnas.91.16.7787

Yan, S. D., Yan, S. F., Chen, X., Fu, J., Chen, M., Kuppusamy, P., et al. (1995). Non-enzymatically glycated tau in Alzheimer's disease induces neuronal oxidant stress resulting in cytokine gene expression and release of amyloid beta-peptide. *Nat. Med.* 1, 693–699. doi: 10.1038/nm0795-693

Yoshida, M. (2006). Cellular tau pathology and immunohistochemical study of tau isoforms in sporadic tauopathies. *Neuropathology* 26, 457–470. doi: 10.1111/j.1440-1789.2006.00743.x

Zhang, Y. J., Xu, Y. F., Liu, X. H., Li, D., Yin, J., Liu, Y. H., et al. (2008). Carboxyl terminus of heat-shock cognate 70-interacting protein degrades tau regardless its phosphorylation status without affecting the spatial memory of the rats. *J. Neural. Transm.* 115, 483–491. doi: 10.1007/s00702-007-0857-7

Conflict of Interest Statement: The authors declare that the research was conducted in the absence of any commercial or financial relationships that could be construed as a potential conflict of interest.

Appendix III: Determining the suitable boiling time for Western blot analysis of tau protein

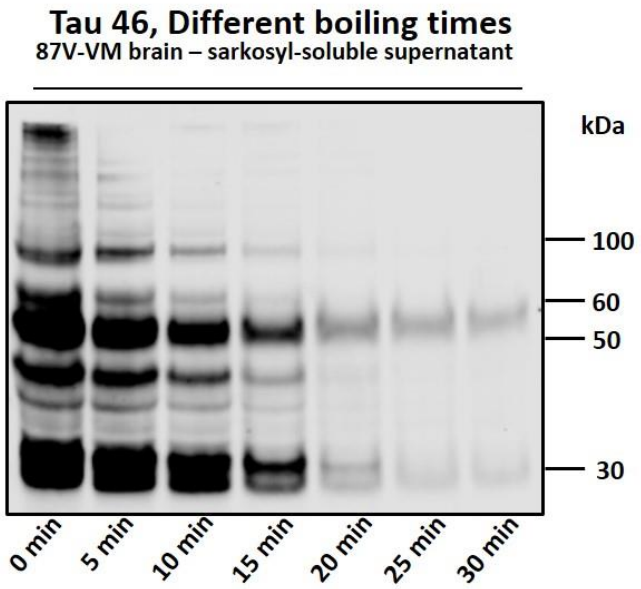

Supplementary figure 2 The sarkosyl-soluble fraction that derived from an 87V-VM mouse brain was boiled for different times before running on a gel. Western blot analysis incubating with the primary antibody Tau46 showed that the boiling time does not affect the migration of tau isoforms on the gel and, in addition, the most suitable boiling duration for western blot is 10 min.

Appendix IV: Proteomic analysis of tau samples

Supplementary table 1 List of proteins detected by MS in the sample of normal soluble tau (in-solution preparation).

UniProtKB entry	Protein full name	Molecular mass (Da)
E9Q4K7	Kinesin-like protein	204,575
Q5NCI0	Up-regulator of cell proliferation	104,683
Q8C0C0	Zinc fingers and homeoboxes protein 2	92,259
O70494	Transcription factor Sp3	82,362
A0A0A0MQC7	Microtubule-associated protein	76,259
O88935	Synapsin-1	74,097
P07724	Serum albumin	68,693
Q0VGU4	MCG18019	68,232
A2AVX1	Breast carcinoma-amplified sequence 1 homolog	61,162
Q3TEA8	Heterochromatin protein 1-binding protein 3	60,867
Q8VC30	Bifunctional ATP-dependent dihydroxyacetone kinase/FAD-AMP lyase (cyclizing)	59,691
Q9Z2D6	Methyl-CpG-binding protein 2	52,307
P0C7L0	WAS/WASL-interacting protein family member 3	49,453
A0A0A0MQA3	Alpha-1-antitrypsin 1-1	48,796
Q00897	Alpha-1-antitrypsin 1-4	45,998
Q9CY58	Plasminogen activator inhibitor 1 RNA-binding protein	44,714
Q60980	Krueppel-like factor 3	38,561
A2BI12	PC4 and SFRS1-interacting protein	36,968
P47911	60S ribosomal protein L6	33,510
D3YXH0	Immunoglobulin superfamily member 5	32,628
Q792Y8	MCG15081	26,119
A0A087WNP6	Protein CDV3	24,196
P06837	Neuromodulin	23,632
Q7TQD2	Tubulin polymerization-promoting protein	23,575
Q9DD18	D-tyrosyl-tRNA(Tyr) deacylase 1	23,384
F6RT34	Myelin basic protein (Fragment)	23,197
Q9DCT8	Cysteine-rich protein 2 OS=Mus musculus GN=Crip2 PE=1 SV=1	22,727
P43276	Histone H1.5	22,576
P43277	Histone H1.3	22,100
Q91XV3	Brain acid soluble protein 1	22,087
D3Z7Q5	Programmed cell death protein 5	21,985
P43274	Histone H1.4	21,977
Q60829	Protein phosphatase 1 regulatory subunit 1B	21,781
O09114	Prostaglandin-H2 D-isomerase	21,066
A2A6Q8	Myosin light chain 4 (Fragment)	21,045
P10922	Histone H1.0	20,861
P55821	Stathmin-2	20,828

Q60648	Ganglioside GM2 activator	20,824
Q3UHX2	28 kDa heat- and acid-stable phosphoprotein	20,605
B1AZQ0	Proenkephalin-A (Fragment)	20,132
O54693-4	Isoform TAB of Ectodysplasin-A	19,297
Q9CRB6	Tubulin polymerization-promoting protein family member 3	18,965
E0CX65	Tyrosine-protein phosphatase non-receptor type substrate 1	18,890
B1AXW5	Peroxiredoxin-1 (Fragment)	18,870
P63089	Pleiotrophin	18,869
Q9ERT9	Protein phosphatase 1 regulatory subunit 1A	18,718
A2AP78	High mobility group protein B3 (Fragment)	18,311
P62983	Ubiquitin-40S ribosomal protein S27a	17,951
Q8BP67	60S ribosomal protein L24	17,779
P62751	60S ribosomal protein L23a	17,695
D3Z1N9	MCG9889	17,587
F6ZIA4	Myelin basic protein (Fragment)	17,109
F6RWW8	Myelin basic protein (Fragment)	16,479
D5MCW4	Protein CutA	16,453
P97825	Hematological and neurological expressed 1 protein	16,081
D3Z4A4	Peroxiredoxin-2 (Fragment)	15,977
P08228	Superoxide dismutase [Cu-Zn]	15,943
P02089	Hemoglobin subunit beta-2	15,878
P02088	Hemoglobin subunit beta-1	15,840
P62267	40S ribosomal protein S23	15,808
P84086	Complexin-2	15,394
P63040	Complexin-1	15,122
Q91VB8	Alpha globin 1	15,112
D3YUT3	40S ribosomal protein S19 (Fragment)	14,896
P11404	Fatty acid-binding protein, heart	14,819
O55042	Alpha-synuclein	14,485
Q642K5	40S ribosomal protein S30	14,416
P52760	Ribonuclease UK114	14,255
Q6GSS7	Histone H2A type 2-A	14,095
Q91ZZ3	Beta-synuclein	14,052
Q6ZWY9	Histone H2B type 1-C/E/G	13,906
P62852	40S ribosomal protein S25	13,742
Q9D1R9	60S ribosomal protein L34	13,293
P62889	60S ribosomal protein L30	12,784
Q9Z1P6	NADH dehydrogenase [ubiquinone] 1 alpha subcomplex subunit 7	12,576
P83882	60S ribosomal protein L36a	12,441
D3YWA4	PEST proteolytic signal-containing nuclear protein	12,097

Q9QUH0	Glutaredoxin-1	11,871
D3Z1Z8	Stathmin (Fragment)	11,729
Q9D0J8	Parathymosin	11,430
G3UW55	MCG14937	11,426
Q9CQX8	28S ribosomal protein S36, mitochondrial	11,101
B1ARW4	NADH dehydrogenase [ubiquinone] iron-sulfur protein 5 (Fragment)	10,909
E9QAD6	ATP synthase-coupling factor 6, mitochondrial (Fragment)	10,473
P56391	Cytochrome c oxidase subunit 6B1	10,071
P31786	Acyl-CoA-binding protein	10,000
D3Z794	Small ubiquitin-related modifier 2	8,111
P63248	cAMP-dependent protein kinase inhibitor alpha	7,960
Q6W8Q3	Purkinje cell protein 4-like protein 1	7,502
P60761	Neurogranin	7,496
P20065-2	Isoform Short of Thymosin beta-4	5,053
Q6ZWY8	Thymosin beta-10	5,026
G3UWG1	MCG115977	-

Supplementary table 2 List of proteins detected by MS in the sample of soluble tau extracted from 87V-VM brain (in-solution preparation).

UniProtKB entry	Protein full name	Molecular mass (Da)
Q8K4E0	Alstrom syndrome protein 1 homolog	360,215
E9PVX6	Protein Mki67	350,864
Q62261	Spectrin beta chain, non-erythrocytic 1	274,223
A2A7F4	MCG122876	217,389
Q5HZJ0	Ribonuclease 3	158,828
Q8CH77-3	Isoform 3 of Neuron navigator 1	129,744
O70318	Band 4.1-like protein 2	109,940
E9PZ43	Microtubule-associated protein	97,796
Q7TSJ2	Microtubule-associated protein 6	96,450
B2RPU8	MCG130675	84,267
P0CG50	Polyubiquitin-C	82,550
O88935	Synapsin-1	74,097
P07724	Serum albumin	68,693
Q0VGU4	MCG18019	68,232
Q80YN3	Breast carcinoma-amplified sequence 1 homolog	67,378
Q4W8U9	Scg2 protein	66,366
O08553	Dihydropyrimidinase-related protein 2	62,278
Q3TEA8	Heterochromatin protein 1-binding protein 3	60,867
Q99JF8	PC4 and SFRS1-interacting protein	59,697

Q9EQW4	Cytochrome P450, CYP3A	57,617
Q9Z2D6-2	Isoform B of Methyl-CpG-binding protein 2	53,576
Q3U422	NADH dehydrogenase [ubiquinone] flavoprotein 3, mitochondrial	50,499
P0C7L0	WAS/WASL-interacting protein family member 3	49,453
Q9JL35	High mobility group nucleosome-binding domain-containing protein 5	45,344
P10637-2	Isoform Tau-A of Microtubule-associated protein tau	44,893
P10637-5	Isoform Tau-D of Microtubule-associated protein tau	38,961
Q6DFY2	Opioid binding protein/cell adhesion molecule-like	37,156
Q80Y39	Uncharacterized protein C10orf62 homolog	34,025
D3YXH0	Immunoglobulin superfamily member 5	32,628
Q8R5L1	Complement component 1 Q subcomponent-binding protein, mitochondrial	31,025
P26645	Myristoylated alanine-rich C-kinase substrate	29,661
Q9CR68	Cytochrome b-c1 complex subunit Rieske, mitochondrial	29,368
A0A087WRY3	Nuclear ubiquitous casein and cyclin-dependent kinase substrate 1	26,184
P63158	High mobility group protein B1	24,894
Q4VAA2-2	Isoform 2 of Protein CDV3	24,338
P06837	Neuromodulin	23,632
Q7TQD2	Tubulin polymerization-promoting protein	23,575
Q9D1J3	SAP domain-containing ribonucleoprotein	23,533
Q9DD18	D-tyrosyl-tRNA(Tyr) deacylase 1	23,384
Q9DCL8	Protein phosphatase inhibitor 2	23,119
Q9DCT8	Cysteine-rich protein 2	22,727
Q8CHP5	Partner of Y14 and mago	22,690
P43276	Histone H1.5	22,576
E0CXA0	Hepatoma-derived growth factor (Fragment)	22,115
P43277	Histone H1.3	22,100
Q91XV3	Brain acid soluble protein 1	22,087
Q8CCT4	Transcription elongation factor A protein-like 5	22,038
P43274	Histone H1.4	21,977
P43275	Histone H1.1	21,785
Q60829	Protein phosphatase 1 regulatory subunit 1B	21,781
P10922	Histone H1.0	20,861
Q60648	Ganglioside GM2 activator	20,824
Q3UHX2	28 kDa heat- and acid-stable phosphoprotein	20,605
Q80ZM5	H1 histone family, member X	20,151
B1AZQ0	Proenkephalin-A (Fragment)	20,132
Q9R0P4	Small acidic protein	20,046
A2AEC2	Transcription elongation factor A protein-like 3 (Fragment)	19,926

Q9CRB6	Tubulin polymerization-promoting protein family member 3	18,965
E0CX65	Tyrosine-protein phosphatase non-receptor type substrate 1	18,890
B1AXW5	Peroxiredoxin-1 (Fragment)	18,870
Q64288	Olfactory marker protein	18,867
Q9ERT9	Protein phosphatase 1 regulatory subunit 1A	18,718
P04370-5	Isoform 5 of Myelin basic protein	18,488
P01831	Thy-1 membrane glycoprotein	18,080
Q8BP67	60S ribosomal protein L24	17,779
P62751	60S ribosomal protein L23a	17,695
D3YVR4	LDLR chaperone MESD (Fragment)	17,347
Q9JMG1	Endothelial differentiation-related factor 1	16,369
A2AA85	SUZ domain-containing protein 1 (Fragment)	16,277
P97825	Hematological and neurological expressed 1 protein	16,081
P08228	Superoxide dismutase [Cu-Zn]	15,943
P07309	Transthyretin	15,776
A8DUK4	Beta-globin	15,748
Q3TM89	PEST proteolytic signal-containing nuclear protein	15,562
P27661	Histone H2AX	15,143
P63040	Complexin-1	15,122
Q91VB8	Alpha globin 1	15,112
Q9JKC6	Cell cycle exit and neuronal differentiation protein 1	14,987
D3YUT3	40S ribosomal protein S19 (Fragment)	14,896
O55042	Alpha-synuclein	14,485
P11031	Activated RNA polymerase II transcriptional coactivator p15	14,427
Q642K5	40S ribosomal protein S30	14,416
P52760	Ribonuclease UK114	14,255
P04370-8	Isoform 8 of Myelin basic protein	14,211
Q91ZZ3	Beta-synuclein	14,052
Q8R1M2	Histone H2A.J	14,045
P10854	Histone H2B type 1-M	13,936
P62852	40S ribosomal protein S25	13,742
P60840	Alpha-endosulfine	13,335
Q9Z0F7	Gamma-synuclein	13,160
P52503	NADH dehydrogenase [ubiquinone] iron-sulfur protein 6, mitochondrial	13,020
Q9Z1P6	NADH dehydrogenase [ubiquinone] 1 alpha subcomplex subunit 7	12,576
P97450	ATP synthase-coupling factor 6, mitochondrial	12,496
P56212	cAMP-regulated phosphoprotein 19	12,293
P26350	Prothymosin alpha	12,254
P32848	Parvalbumin alpha	11,931

Q8BK30	NADH dehydrogenase [ubiquinone] flavoprotein 3, mitochondrial	11,813
D3Z1Z8	Stathmin (Fragment)	11,729
P10639	Thioredoxin	11,675
P99027	60S acidic ribosomal protein P2	11,651
P17095	High mobility group protein HMG-I/HMG-Y	11,614
Q9DAM7	Transmembrane protein 263	11,549
Q9D0J8	Parathymosin	11,430
G3UW55	MCG14937	11,426
Q9CQX8	28S ribosomal protein S36, mitochondrial	11,101
Q64433	10 kDa heat shock protein, mitochondrial	10,963
P17095-1	Isoform HMG-Y of High mobility group protein HMG-I/HMG-Y	10,617
P56212-2	Isoform ARPP-16 of cAMP-regulated phosphoprotein 19	10,605
Q91VW3	SH3 domain-binding glutamic acid-rich-like protein 3	10,477
Q9D0M5	Dynein light chain 2, cytoplasmic	10,350
P56391	Cytochrome c oxidase subunit 6B1	10,071
P31786	Acyl-CoA-binding protein	10,000
Q5XK38	Hmgn2 protein	9,609
G3UWI9	SMT3 suppressor of mif two 3 homolog 3 (Yeast), isoform CRA_c	9,373
H3BLI9	TSC22 domain family protein 1	9,358
P61961	Ubiquitin-fold modifier 1	9,118
P29595	NEDD8	8,972
Q9D115	Zinc finger protein 706	8,498
Q9JJI8	60S ribosomal protein L38	8,204
D3Z794	Small ubiquitin-related modifier 2	8,111
P63248	cAMP-dependent protein kinase inhibitor alpha	7,960
D6RFU4	Myosin light chain 4	7,957
Q6W8Q3	Purkinje cell protein 4-like protein 1	7,502
P60761	Neurogranin	7,496
O08997	Copper transport protein ATOX1	7,338
A2AF31	Protein Tmsb15b2	5,247
P20065-2	Isoform Short of Thymosin beta-4	5,053
Q6ZWY8	Thymosin beta-10	5,026
G3UWG1	MCG115977	-
F7D425	cAMP-regulated phosphoprotein 21 (Fragment)	-

Supplementary table 3 List of proteins detected by MS in the sample of insoluble aggregated tau extracted from 87V-VM brain (in-gel preparation).

UniProtKB entry	Protein full name	Molecular mass (Da)
A0A0A0MQC7	Microtubule-associated protein	76,259
Q6P1J1	Crmp1 protein	74,221
O88935	Synapsin-1	74,097
P20029	78 kDa glucose-regulated protein	72,422
P63017	Heat shock cognate 71 kDa protein	70,871
P07724	Serum albumin	68,693
P50516	V-type proton ATPase catalytic subunit A	68,326
P40142	Transketolase	67,63
O08599	Syntaxin-binding protein 1	67,569
Q76MZ3	Serine/threonine-protein phosphatase 2A 65 kDa regulatory subunit A alpha isoform	65,323
Q64332	Synapsin-2	63,373
P06745	Glucose-6-phosphate isomerase	62,767
O08553	Dihydropyrimidinase-related protein 2	62,278
Q3TT92	Dihydropyrimidinase-related protein 3	61,78
Q9EQF6	Dihydropyrimidinase-related protein 5	61,516
P08551	Neurofilament light polypeptide	61,508
Q9D0F9	Phosphoglucomutase-1	61,418
P26443	Glutamate dehydrogenase 1, mitochondrial	61,337
E9Q6Q4	Protein Rap1gds1	60,793
P28652	Calcium/calmodulin-dependent protein kinase type II subunit beta	60,461
P63328	Serine/threonine-protein phosphatase 2B catalytic subunit alpha isoform	58,644
G3UYZ1	Immunoglobulin superfamily member 8	58,132
P52480	Pyruvate kinase PKM	57,845
P62814	V-type proton ATPase subunit B, brain isoform	56,551
P56480	ATP synthase subunit beta, mitochondrial	56,300
P46660	Alpha-internexin	55,383
F8WIS9	Calcium/calmodulin-dependent protein kinase type II subunit alpha	55,347
D3Z6F5	ATP synthase subunit alpha	54,595
P11798	Calcium/calmodulin-dependent protein kinase type II subunit alpha	54,115
H3BL49	T-complex protein 1 subunit theta	53,083
A0A0A0MQA5	Tubulin alpha-4A chain (Fragment)	52,905
Q6P1B9	Bin1 protein	52,764
Q9CZU6	Citrate synthase, mitochondrial	51,737
A0A0A6YW88	CaM kinase-like vesicle-associated protein	51,675
O89053	Coronin-1A	50,989

E9Q1G8	Septin-7	50,649
Q61644	Protein kinase C and casein kinase substrate in neurons protein 1	50,575
P50396	Rab GDP dissociation inhibitor alpha	50,522
P62631	Elongation factor 1-alpha 2	50,454
Q9ERD7	Tubulin beta-3 chain	50,419
P68369	Tubulin alpha-1A chain	50,136
P10126	Elongation factor 1-alpha 1	50,114
Q9CWF2	Tubulin beta-2B chain	49,953
Q7TMM9	Tubulin beta-2A chain	49,907
P03995	Glial fibrillary acidic protein	49,900
P68372	Tubulin beta-4B chain	49,831
P99024	Tubulin beta-5 chain	49,671
Q9R1T4	Septin-6	49,62
Q9D6F9	Tubulin beta-4A chain	49,586
B2M1R6	Heterogeneous nuclear ribonucleoprotein K	48,562
P46096	Synaptotagmin-1	47,418
P17183	Gamma-enolase	47,297
P17182	Alpha-enolase	47,141
P16330	2',3'-cyclic-nucleotide 3'-phosphodiesterase	47,123
H3BKT5	Adenosylhomocysteinase	45,055
P09411	Phosphoglycerate kinase 1	44,550
Q04447	Creatine kinase B-type	42,713
E9Q1F2	Actin, cytoplasmic 1	32,564
P26645	Myristoylated alanine-rich C-kinase substrate	29,661
F6WWS1	Synaptopodin-2 (Fragment)	24,470
P06837	Neuromodulin	23,632
Q3TUE8	4-aminobutyrate aminotransferase, mitochondrial	22,727
E9Q3D6	Heat shock protein HSP 90-beta (Fragment)	22,482
Q91XV3	Brain acid soluble protein 1	22,087
D3Z2F2	60 kDa heat shock protein, mitochondrial (Fragment)	21,501
F7ALS6	Aspartate aminotransferase, cytoplasmic (Fragment)	20,378
A0A0A6YX05	Sodium/potassium-transporting ATPase subunit beta-1 (Fragment)	15,253
G3UXT7	RNA-binding protein FUS (Fragment)	14,009
D3YVN7	Elongation factor Tu	-

Appendix V: Mascot search results for the tryptic peptide R.SGYSSPGSPGTPGS.R

Mascot Search Results

Peptide View

MS/MS Fragmentation of **SGYSSPGSPGTPGSR**
Found in **P10637-3** in **Uniprot_Mouse**, Isoform Tau-B of Microtubule-associated protein tau OS=Mus musculus GN=Mapt

Match to Query 882: 1392.636694 from(697.325623,2+) intensity(7475.0000) rtinseconds(1118.0) index(373)
Title: Cmpd 8, +MS2(697.3256), 27.8eV, 18.6 min #1090 (id=56294995365073466) (id=56294995365078224)
Local Instrument: ESI-QUAD-TOF
Data file 56294995342141725.mgf

Click mouse within plot area to zoom in by factor of two about that point
Or, Plot from 200 to 1150 Da Full range
Label all possible matches ○ Label matches used for scoring ◉
Show Y-axis ☐

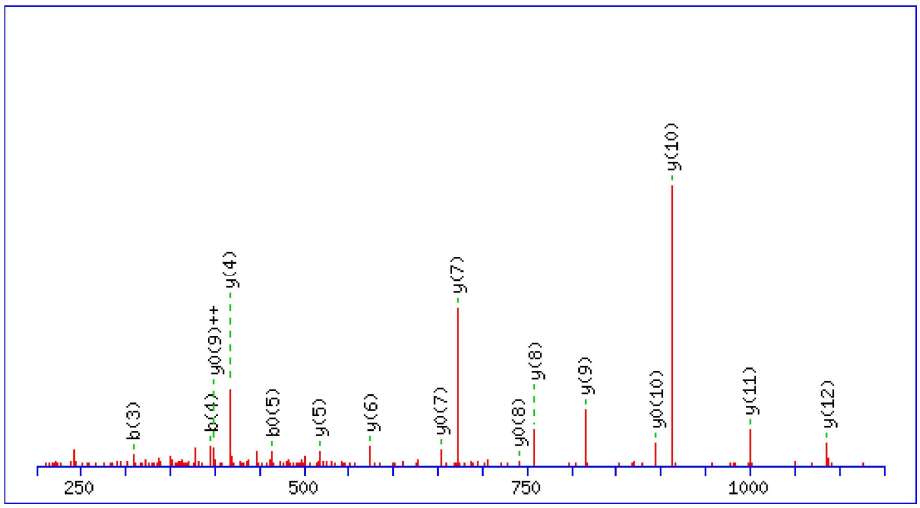

Monoisotopic mass of neutral peptide Mr(calc): 1392.6270
Fixed modifications: Carbamidomethyl (C) (apply to specified residues or termini only)
Ions Score: 83 **Expect:** 9.7e-007
Matches : 17/138 fragment ions using 19 most intense peaks (help)

#	b	b^{++}	b^{0}	b^{0++}	Seq.	y	y^{++}	y*	y^{*++}	y^{0}	y^{0++}	#
1	88.0393	44.5233	70.0287	35.5180	S							15
2	145.0608	73.0340	127.0502	64.0287	G	1306.6022	653.8047	1289.5757	645.2915	1288.5917	644.7995	14
3	**308.1241**	154.5657	290.1135	145.5604	Y	1249.5808	625.2940	1232.5542	616.7807	1231.5702	616.2887	13
4	**395.1561**	198.0817	377.1456	189.0764	S	***1086.5174***	543.7624	1069.4909	535.2491	1068.5069	534.7571	12
5	482.1882	241.5977	464.1776	232.5924	S	***999.4854***	500.2463	982.4588	491.7331	981.4748	491.2411	11
6	579.2409	290.1241	561.2304	281.1188	P	***912.4534***	456.7303	895.4268	448.2170	894.4428	447.7250	10
7	636.2624	318.6348	618.2518	309.6295	G	***815.4006***	408.2039	798.3741	399.6907	797.3900	399.1987	9
8	723.2944	362.1508	705.2838	353.1456	S	***758.3791***	379.6932	741.3526	371.1799	740.3686	370.6879	8
9	820.3472	410.6772	802.3366	401.6719	P	***671.3471***	336.1772	654.3206	327.6639	653.3365	327.1719	7
10	877.3686	439.1880	859.3581	430.1827	G	***574.2944***	287.6508	557.2678	279.1375	556.2838	278.6455	6
11	978.4163	489.7118	960.4058	480.7065	T	***517.2729***	259.1401	500.2463	250.6268	499.2623	250.1348	5
12	1075.4691	538.2382	1057.4585	529.2329	P	***416.2252***	208.6162	399.1987	200.1030	398.2146	199.6110	4
13	1132.4905	566.7489	1114.4800	557.7436	G	319.1724	160.0899	302.1459	151.5766	301.1619	151.0846	3
14	1219.5226	610.2649	1201.5120	601.2596	S	262.1510	131.5791	245.1244	123.0659	244.1404	122.5738	2
15					R	175.1190	88.0631	158.0924	79.5498			1

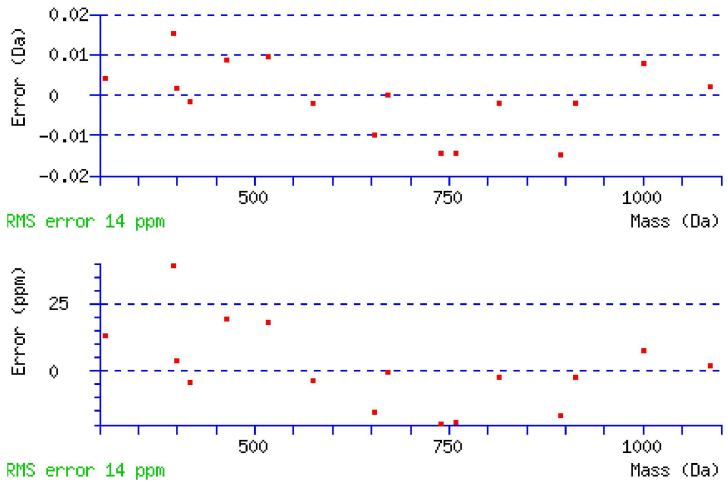

NCBI **BLAST** search of SGYSSPGSPGTPGSR
(Parameters: blastp, nr protein database, expect=20000, no filter, PAM30)
Other BLAST web gateways

All matches to this query

Score	Mr(calc)	Delta	Sequence
83.3	1392.6270	0.0097	SGYSSPGSPGTPGSR
1.6	1391.6446	0.9921	VEPGLGADNSVVR
0.2	1392.6344	0.0023	VFNDSTNIMHAK
0.0	1392.6221	0.0146	KSVSHNMTAPNK

Mascot: http://www.matrixscience.com/

Mascot Search Results

Peptide View

MS/MS Fragmentation of **SGYSSPGSPGTPGSR**
Found in **P10637-3** in **Uniprot_Mouse**, Isoform Tau-B of Microtubule-associated protein tau OS=Mus musculus GN=Mapt

Match to Query 935: 1472.605932 from(737.310242,2+) intensity(16205.0000) rtinseconds(1225.8) index(383)
Title: Cmpd 18, +MS2(737.3103), 28.9eV, 20.4 min #1195 (id=56294995365073476) (id=56294995365078234)
Local Instrument: ESI-QUAD-TOF
Data file 56294995342141725.mgf

Click mouse within plot area to zoom in by factor of two about that point
Or, Plot from 150 to 1200 Da Full range
Label all possible matches ○ Label matches used for scoring ◉
Show Y-axis ☐

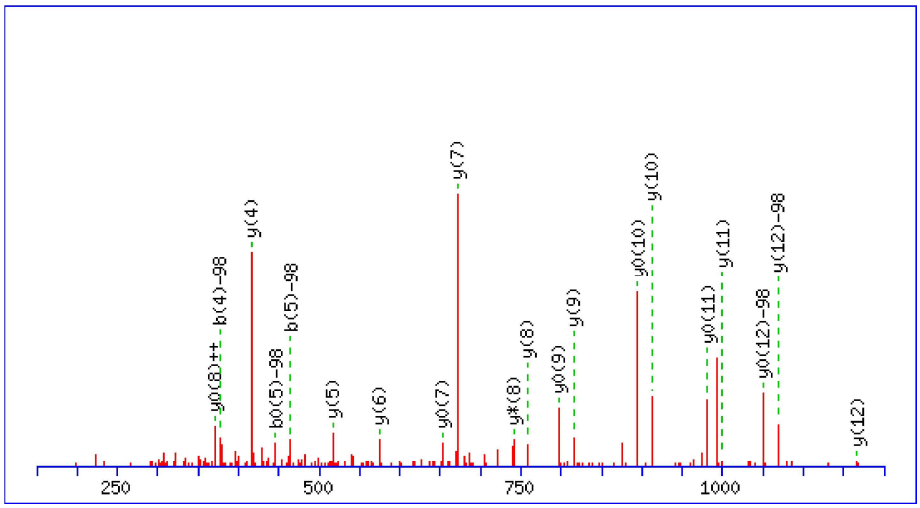

Monoisotopic mass of neutral peptide Mr(calc): 1472.5933
Fixed modifications: Carbamidomethyl (C) (apply to specified residues or termini only)
Variable modifications:
S4 : Phospho (ST), with neutral losses 97.9769(shown in table), 0.0000
Ions Score: 66 **Expect:** 3.8e-005
Matches : 20/200 fragment ions using 30 most intense peaks (help)

#	b	b^{++}	b^{0}	b^{0++}	Seq.	y	y^{++}	y*	y^{*++}	y^{0}	y^{0++}	#
1	88.0393	44.5233	70.0287	35.5180	S							15
2	145.0608	73.0340	127.0502	64.0287	G	1288.5917	644.7995	1271.5651	636.2862	1270.5811	635.7942	14
3	308.1241	154.5657	290.1135	145.5604	Y	1231.5702	616.2887	1214.5436	607.7755	1213.5596	607.2835	13
4	377.1456	189.0764	359.1350	180.0711	S	*1068.5069*	534.7571	1051.4803	526.2438	1050.4963	525.7518	12
5	464.1776	232.5924	446.1670	223.5871	S	*999.4854*	500.2463	982.4589	491.7331	981.4748	491.2411	11
6	561.2304	281.1188	543.2198	272.1135	P	*912.4534*	456.7303	895.4268	448.2170	894.4428	447.7250	10
7	618.2518	309.6295	600.2413	300.6243	G	*815.4006*	408.2039	798.3741	399.6907	797.3900	399.1987	9
8	705.2838	353.1456	687.2733	344.1403	S	*758.3791*	379.6932	741.3526	371.1799	740.3686	370.6879	8
9	802.3366	401.6719	784.3260	392.6667	P	*671.3471*	336.1772	654.3206	327.6639	653.3366	327.1719	7
10	859.3581	430.1827	841.3475	421.1774	G	*574.2944*	287.6508	557.2678	279.1375	556.2838	278.6455	6
11	960.4058	480.7065	942.3952	471.7012	T	*517.2729*	259.1401	500.2463	250.6268	499.2623	250.1348	5
12	1057.4585	529.2329	1039.4480	520.2276	P	*416.2252*	208.6162	399.1987	200.1030	398.2146	199.6110	4
13	1114.4800	557.7436	1096.4694	548.7383	G	319.1724	160.0899	302.1459	151.5766	301.1619	151.0846	3
14	1201.5120	601.2596	1183.5014	592.2544	S	262.1510	131.5791	245.1244	123.0659	244.1404	122.5738	2
15					R	175.1190	88.0631	158.0924	79.5498			1

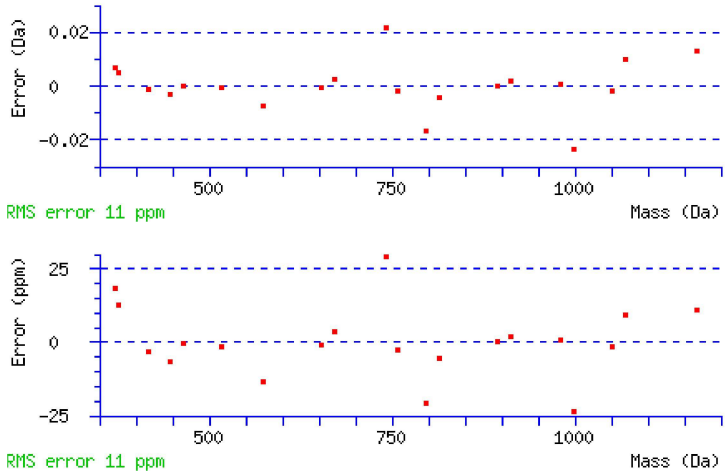

NCBI **BLAST** search of SGYSSPGSPGTPGSR
(Parameters: blastp, nr protein database, expect=20000, no filter, PAM30)
Other BLAST web gateways

All matches to this query

Score	Mr(calc)	Delta	Sequence	Site Analysis
66.3	1472.5933	0.0126	SGYSSPGSPGTPGSR	Phospho S4 59.52%
64.2	1472.5933	0.0126	SGYSSPGSPGTPGSR	Phospho S5 36.28%
53.3	1472.5933	0.0126	SGYSSPGSPGTPGSR	Phospho S1 2.96%
49.5	1472.5933	0.0126	SGYSSPGSPGTPGSR	Phospho S8 1.23%
30.4	1472.5933	0.0126	SGYSSPGSPGTPGSR	Phospho T11 0.02%
22.4	1472.5933	0.0126	SGYSSPGSPGTPGSR	Phospho S14 0.00%

Mascot: http://www.matrixscience.com/

Mascot Search Results

Peptide View

MS/MS Fragmentation of **SGYSSPGSPGTPGSR**
Found in **P10637-3** in **Uniprot_Mouse**, Isoform Tau-B of Microtubule-associated protein tau OS=Mus musculus GN=Mapt

Match to Query 933: 1472.605566 from(737.310059,2+) intensity(11251.0000) rtinseconds(1218.8) index(14)
Title: Cmpd 15, +MS2(737.3100), 28.9eV, 20.3 min #1196 (id=56294995365073106) (id=56294995365077865)
Local Instrument: ESI-QUAD-TOF
Data file 56294995342141725.mgf

Click mouse within plot area to zoom in by factor of two about that point
Or, Plot from 150 to 1200 Da Full range
Label all possible matches ○ Label matches used for scoring ◉
Show Y-axis ☐

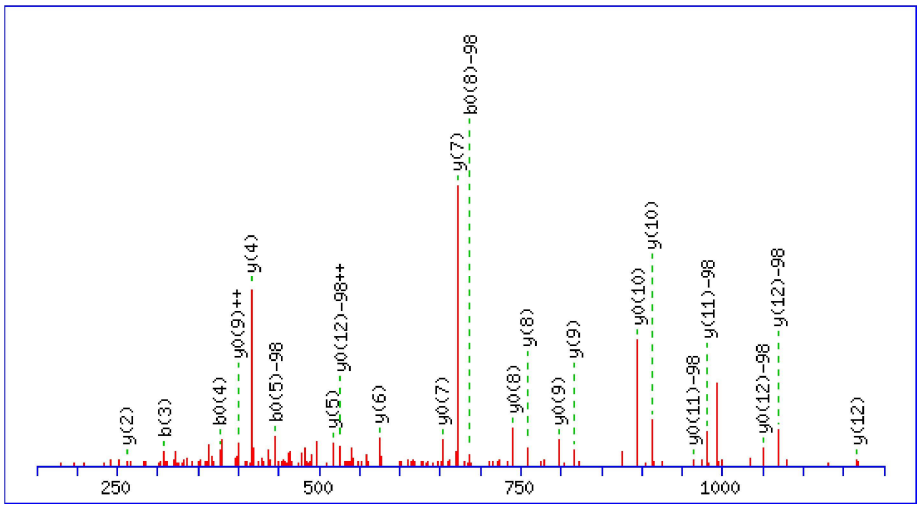

Monoisotopic mass of neutral peptide Mr(calc): 1472.5933
Fixed modifications: Carbamidomethyl (C) (apply to specified residues or termini only)
Variable modifications:
S5 : Phospho (ST), with neutral losses 97.9769(shown in table), 0.0000
Ions Score: 70 **Expect:** 1.5e-005
Matches : 24/202 fragment ions using 39 most intense peaks (help)

#	b	b^{++}	b^{0}	b^{0++}	Seq.	y	y^{++}	y*	y^{*++}	y^{0}	y^{0++}	#
1	88.0393	44.5233	70.0287	35.5180	S							15
2	145.0608	73.0340	127.0502	64.0287	G	1288.5917	644.7995	1271.5651	636.2862	1270.5811	635.7942	14
3	**308.1241**	154.5657	290.1135	145.5604	Y	1231.5702	616.2887	1214.5436	607.7755	1213.5596	607.2835	13
4	395.1561	198.0817	377.1456	189.0764	S	***1068.5069***	534.7571	1051.4803	526.2438	1050.4963	525.7518	12
5	464.1776	232.5924	446.1670	223.5871	S	***981.4748***	491.2411	964.4483	482.7278	963.4643	482.2358	11
6	561.2304	281.1188	543.2198	272.1135	P	***912.4534***	456.7303	895.4268	448.2170	894.4428	447.7250	10
7	618.2518	309.6295	600.2413	300.6243	G	***815.4006***	408.2039	798.3741	399.6907	797.3900	399.1987	9
8	705.2838	353.1456	687.2733	344.1403	S	***758.3791***	379.6932	741.3526	371.1799	740.3686	370.6879	8
9	802.3366	401.6719	784.3260	392.6667	P	***671.3471***	336.1772	654.3206	327.6639	653.3366	327.1719	7
10	859.3581	430.1827	841.3475	421.1774	G	***574.2944***	287.6508	557.2678	279.1375	556.2838	278.6455	6
11	960.4058	480.7065	942.3952	471.7012	T	***517.2729***	259.1401	500.2463	250.6268	499.2623	250.1348	5
12	1057.4585	529.2329	1039.4480	520.2276	P	***416.2252***	208.6162	399.1987	200.1030	398.2146	199.6110	4
13	1114.4800	557.7436	1096.4694	548.7383	G	319.1724	160.0899	302.1459	151.5766	301.1619	151.0846	3
14	1201.5120	601.2596	1183.5014	592.2544	S	***262.1510***	131.5791	245.1244	123.0659	244.1404	122.5738	2
15					R	175.1190	88.0631	158.0924	79.5498			1

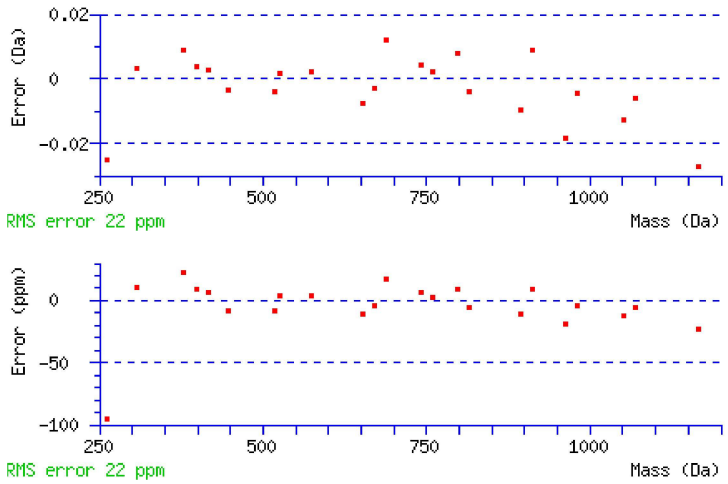

NCBI **BLAST** search of SGYSSPGSPGTPGSR
(Parameters: blastp, nr protein database, expect=20000, no filter, PAM30)
Other BLAST web gateways

All matches to this query

Score	Mr(calc)	Delta	Sequence	Site Analysis
70.3	1472.5933	0.0123	SGYSSPGSPGTPGSR	Phospho S5 68.49%
66.4	1472.5933	0.0123	SGYSSPGSPGTPGSR	Phospho S8 27.52%
57.8	1472.5933	0.0123	SGYSSPGSPGTPGSR	Phospho S4 3.81%
43.3	1472.5933	0.0123	SGYSSPGSPGTPGSR	Phospho S1 0.14%
38.4	1472.5933	0.0123	SGYSSPGSPGTPGSR	Phospho T11 0.04%
20.3	1472.5933	0.0123	SGYSSPGSPGTPGSR	Phospho S14 0.00%
0.3	1471.5828	1.0228	SSLAGDGTPQSESR	

Mascot: http://www.matrixscience.com/

Mascot Search Results

Peptide View

MS/MS Fragmentation of **SGYSSPGSPGTPGSR**
Found in **P10637-3** in **Uniprot_Mouse**, Isoform Tau-B of Microtubule-associated protein tau OS=Mus musculus GN=Mapt

Match to Query 931: 1472.605444 from(737.309998,2+) intensity(9712.0000) rtinseconds(1219.8) index(380)
Title: Cmpd 15, +MS2(737.3100), 28.9eV, 20.3 min #1189 (id=56294995365073473) (id=56294995365078231)
Local Instrument: ESI-QUAD-TOF
Data file 56294995342141725.mgf

Click mouse within plot area to zoom in by factor of two about that point
Or, Plot from 200 to 1200 Da Full range
Label all possible matches ○ Label matches used for scoring ◉
Show Y-axis ☐

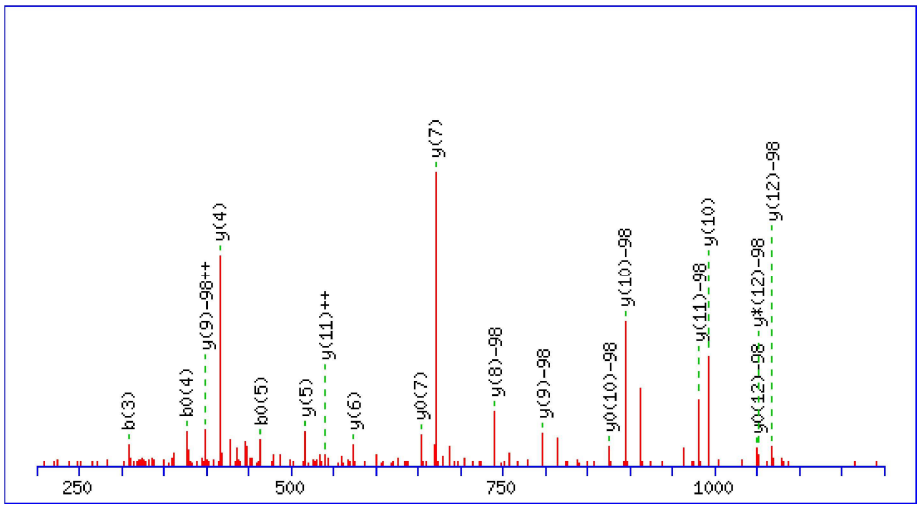

Monoisotopic mass of neutral peptide Mr(calc): 1472.5933
Fixed modifications: Carbamidomethyl (C) (apply to specified residues or termini only)
Variable modifications:
S8 : Phospho (ST), with neutral losses 97.9769(shown in table), 0.0000
Ions Score: 63 **Expect:** 7.9e-005
Matches : 20/208 fragment ions using 29 most intense peaks (help)

#	b	b^{++}	b^{0}	b^{0++}	Seq.	y	y^{++}	y*	y^{*++}	y^{0}	y^{0++}	#
1	88.0393	44.5233	70.0287	35.5180	S							15
2	145.0608	73.0340	127.0502	64.0287	G	1288.5917	644.7995	1271.5651	636.2862	1270.5811	635.7942	14
3	**308.1241**	154.5657	290.1135	145.5604	Y	1231.5702	616.2887	1214.5436	607.7755	1213.5596	607.2835	13
4	395.1561	198.0817	377.1456	189.0764	S	***1068.5069***	534.7571	1051.4803	526.2438	1050.4963	525.7518	12
5	482.1882	241.5977	464.1776	232.5924	S	***981.4748***	491.2411	964.4483	482.7278	963.4643	482.2358	11
6	579.2409	290.1241	561.2304	281.1188	P	***894.4428***	447.7250	877.4163	439.2118	876.4322	438.7198	10
7	636.2624	318.6348	618.2518	309.6295	G	***797.3900***	399.1987	780.3635	390.6854	779.3795	390.1934	9
8	705.2838	353.1456	687.2733	344.1403	S	***740.3686***	370.6879	723.3420	362.1747	722.3580	361.6826	8
9	802.3366	401.6719	784.3260	392.6667	P	***671.3471***	336.1772	654.3206	327.6639	653.3366	327.1719	7
10	859.3581	430.1827	841.3475	421.1774	G	***574.2944***	287.6508	557.2678	279.1375	556.2838	278.6455	6
11	960.4058	480.7065	942.3952	471.7012	T	***517.2729***	259.1401	500.2463	250.6268	499.2623	250.1348	5
12	1057.4585	529.2329	1039.4480	520.2276	P	***416.2252***	208.6162	399.1987	200.1030	398.2146	199.6110	4
13	1114.4800	557.7436	1096.4694	548.7383	G	319.1724	160.0899	302.1459	151.5766	301.1619	151.0846	3
14	1201.5120	601.2596	1183.5014	592.2544	S	262.1510	131.5791	245.1244	123.0659	244.1404	122.5738	2
15					R	175.1190	88.0631	158.0924	79.5498			1

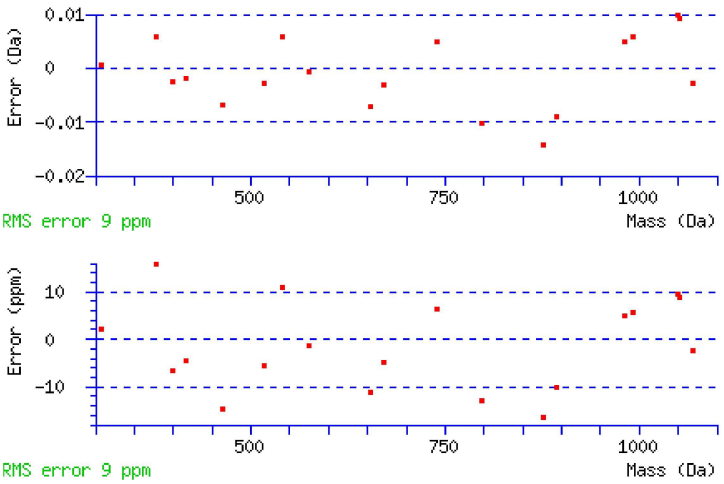

NCBI **BLAST** search of SGYSSPGSPGTPGSR
(Parameters: blastp, nr protein database, expect=20000, no filter, PAM30)
Other BLAST web gateways

All matches to this query

Score	Mr(calc)	Delta	Sequence	Site Analysis
63.2	1472.5933	0.0121	SGYSSPGSPGTPGSR	Phospho S8 66.57%
59.3	1472.5933	0.0121	SGYSSPGSPGTPGSR	Phospho S5 27.24%
52.5	1472.5933	0.0121	SGYSSPGSPGTPGSR	Phospho S4 5.74%
39.7	1472.5933	0.0121	SGYSSPGSPGTPGSR	Phospho S1 0.30%
36.0	1472.5933	0.0121	SGYSSPGSPGTPGSR	Phospho T11 0.13%
24.8	1472.5933	0.0121	SGYSSPGSPGTPGSR	Phospho S14 0.01%
0.0	1471.5828	1.0227	SSLAGDGTPQSESR	

Mascot: http://www.matrixscience.com/

Mascot Search Results

Peptide View

MS/MS Fragmentation of **SGYSSPGSPGTPGSR**
Found in **P10637-3** in **Uniprot_Mouse**, Isoform Tau-B of Microtubule-associated protein tau OS=Mus musculus GN=Mapt

Match to Query 953: 1552.564428 from(777.289490,2+) intensity(2506.0000) rtinseconds(1393.6) index(387)
Title: Cmpd 22, +MS2(777.2895), 39.0eV, 23.2 min #1358 (id=56294995365073480) (id=56294995365078238)
Local Instrument: ESI-QUAD-TOF
Data file 56294995342141725.mgf

Click mouse within plot area to zoom in by factor of two about that point
Or, Plot from 200 to 1100 Da Full range
Label all possible matches ○ Label matches used for scoring ◉
Show Y-axis ☐

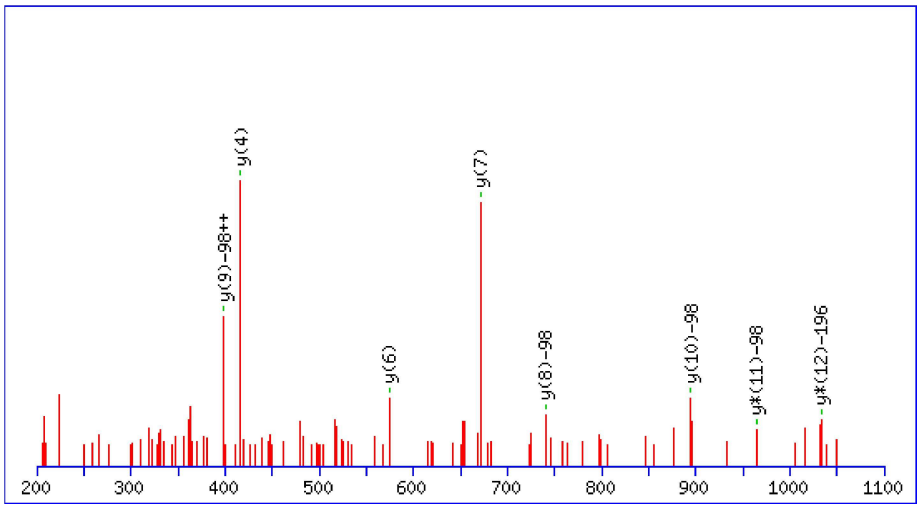

Monoisotopic mass of neutral peptide Mr(calc): 1552.5596
Fixed modifications: Carbamidomethyl (C) (apply to specified residues or termini only)
Variable modifications:
S4 : Phospho (ST), with neutral losses 97.9769(shown in table), 0.0000
S8 : Phospho (ST), with neutral losses 97.9769(shown in table), 0.0000
Ions Score: 39 **Expect:** 0.011
Matches : 9/224 fragment ions using 9 most intense peaks (help)

#	b	b^{++}	b^0	b^{0++}	Seq.	y	y^{++}	y*	y^{*++}	y^0	y^{0++}	#
1	88.0393	44.5233	70.0287	35.5180	S							15
2	145.0608	73.0340	127.0502	64.0287	G	1270.5811	635.7942	1253.5545	627.2809	1252.5705	626.7889	14
3	308.1241	154.5657	290.1135	145.5604	Y	1213.5596	607.2835	1196.5331	598.7702	1195.5491	598.2782	13
4	377.1456	189.0764	359.1350	180.0711	S	1050.4963	525.7518	1033.4697	517.2385	1032.4857	516.7465	12
5	464.1776	232.5924	446.1670	223.5871	S	981.4748	491.2411	964.4483	482.7278	963.4643	482.2358	11
6	561.2304	281.1188	543.2198	272.1135	P	***894.4428***	447.7250	877.4163	439.2118	876.4322	438.7198	10
7	618.2518	309.6295	600.2413	300.6243	G	797.3900	399.1987	780.3635	390.6854	779.3795	390.1934	9
8	687.2733	344.1403	669.2627	335.1350	S	***740.3686***	370.6879	723.3420	362.1747	722.3580	361.6826	8
9	784.3260	392.6667	766.3155	383.6614	P	***671.3471***	336.1772	654.3206	327.6639	653.3365	327.1719	7
10	841.3475	421.1774	823.3369	412.1721	G	***574.2944***	287.6508	557.2678	279.1375	556.2838	278.6455	6
11	942.3952	471.7012	924.3846	462.6959	T	517.2729	259.1401	500.2463	250.6268	499.2623	250.1348	5
12	1039.4480	520.2276	1021.4374	511.2223	P	***416.2252***	208.6162	399.1987	200.1030	398.2146	199.6110	4
13	1096.4694	548.7383	1078.4588	539.7331	G	319.1724	160.0899	302.1459	151.5766	301.1619	151.0846	3
14	1183.5014	592.2544	1165.4909	583.2491	S	262.1510	131.5791	245.1244	123.0659	244.1404	122.5738	2
15					R	175.1190	88.0631	158.0924	79.5498			1

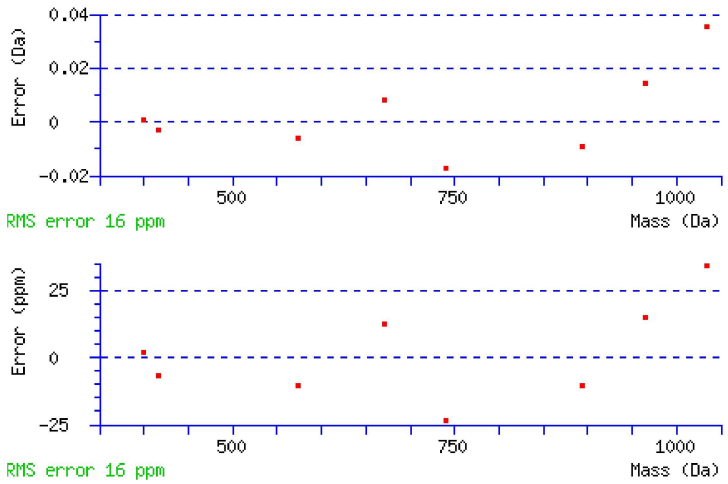

NCBI **BLAST** search of SGYSSPGSPGTPGSR
(Parameters: blastp, nr protein database, expect=20000, no filter, PAM30)
Other BLAST web gateways

All matches to this query

Score	Mr(calc)	Delta	Sequence	Site Analysis
39.0	1552.5596	0.0048	SGYSSPGSPGTPGSR	Phospho S4, S8 46.78%
36.9	1552.5596	0.0048	SGYSSPGSPGTPGSR	Phospho S5, S8 28.91%
34.9	1552.5596	0.0048	SGYSSPGSPGTPGSR	Phospho S1, S8 18.28%
25.4	1552.5596	0.0048	SGYSSPGSPGTPGSR	Phospho S4, T11 2.06%
24.1	1552.5596	0.0048	SGYSSPGSPGTPGSR	Phospho S5, T11 1.53%
18.7	1552.5596	0.0048	SGYSSPGSPGTPGSR	Phospho S4, S5 0.44%
17.5	1552.5596	0.0048	SGYSSPGSPGTPGSR	Phospho S4, S14 0.34%
16.3	1552.5596	0.0048	SGYSSPGSPGTPGSR	Phospho S1, T11 0.25%
16.1	1552.5596	0.0048	SGYSSPGSPGTPGSR	Phospho S5, S14 0.24%
16.0	1552.5596	0.0048	SGYSSPGSPGTPGSR	Phospho S1, S5 0.23%

Mascot: http://www.matrixscience.com/

Mascot Search Results

Peptide View

MS/MS Fragmentation of **SGYSSPGSPGTPGSR**
Found in **P10637-3** in **Uniprot_Mouse**, Isoform Tau-B of Microtubule-associated protein tau OS=Mus musculus GN=Mapt

Match to Query 952: 1552.562718 from(777.288635,2+) intensity(3375.0000) rtinseconds(1403.0) index(391)
Title: Cmpd 26, +MS2(777.2887), 39.0eV, 23.4 min #1367 (id=56294995365073484) (id=56294995365078242)
Local Instrument: ESI-QUAD-TOF
Data file 56294995342141725.mgf

Click mouse within plot area to zoom in by factor of two about that point
Or, Plot from 200 to 1100 Da Full range
Label all possible matches ○ Label matches used for scoring ◉
Show Y-axis ☐

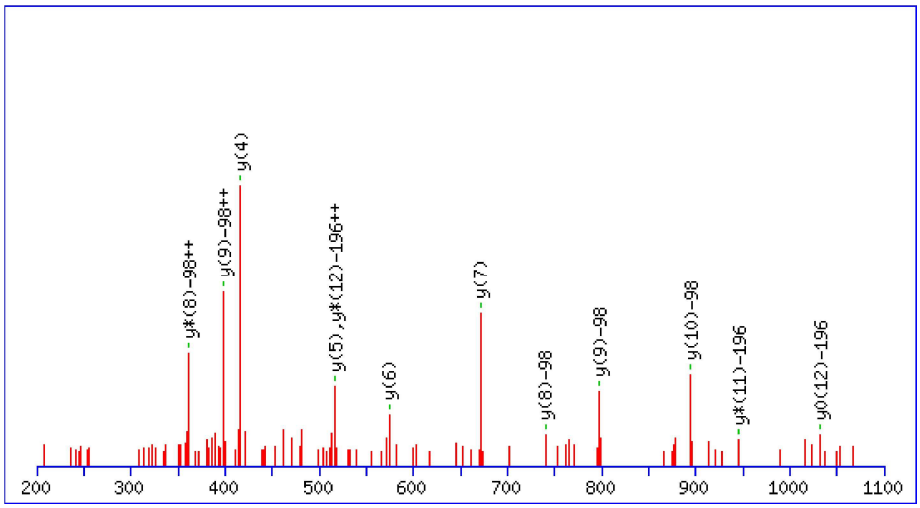

Monoisotopic mass of neutral peptide Mr(calc): 1552.5596
Fixed modifications: Carbamidomethyl (C) (apply to specified residues or termini only)
Variable modifications:
S5 : Phospho (ST), with neutral losses 97.9769(shown in table), 0.0000
S8 : Phospho (ST), with neutral losses 97.9769(shown in table), 0.0000
Ions Score: 46 **Expect:** 0.0022
Matches : 13/220 fragment ions using 18 most intense peaks (help)

#	b	b^{++}	b^{0}	b^{0++}	Seq.	y	y^{++}	y*	y^{*++}	y^{0}	y^{0++}	#
1	88.0393	44.5233	70.0287	35.5180	S							15
2	145.0608	73.0340	127.0502	64.0287	G	1270.5811	635.7942	1253.5545	627.2809	1252.5705	626.7889	14
3	308.1241	154.5657	290.1135	145.5604	Y	1213.5596	607.2835	1196.5331	598.7702	1195.5491	598.2782	13
4	395.1561	198.0817	377.1456	189.0764	S	1050.4963	525.7518	1033.4697	517.2385	1032.4857	516.7465	12
5	464.1776	232.5924	446.1670	223.5871	S	963.4643	482.2358	946.4377	473.7225	945.4537	473.2305	11
6	561.2304	281.1188	543.2198	272.1135	P	***894.4428***	447.7250	877.4163	439.2118	876.4322	438.7198	10
7	618.2518	309.6295	600.2413	300.6243	G	***797.3900***	399.1987	780.3635	390.6854	779.3795	390.1934	9
8	687.2733	344.1403	669.2627	335.1350	S	***740.3686***	370.6879	723.3420	362.1747	722.3580	361.6826	8
9	784.3260	392.6667	766.3155	383.6614	P	***671.3471***	336.1772	654.3206	327.6639	653.3365	327.1719	7
10	841.3475	421.1774	823.3369	412.1721	G	***574.2944***	287.6508	557.2678	279.1375	556.2838	278.6455	6
11	942.3952	471.7012	924.3846	462.6959	T	***517.2729***	259.1401	500.2463	250.6268	499.2623	250.1348	5
12	1039.4480	520.2276	1021.4374	511.2223	P	***416.2252***	208.6162	399.1987	200.1030	398.2146	199.6110	4
13	1096.4694	548.7383	1078.4588	539.7331	G	319.1724	160.0899	302.1459	151.5766	301.1619	151.0846	3
14	1183.5014	592.2544	1165.4909	583.2491	S	262.1510	131.5791	245.1244	123.0659	244.1404	122.5738	2
15					R	175.1190	88.0631	158.0924	79.5498			1

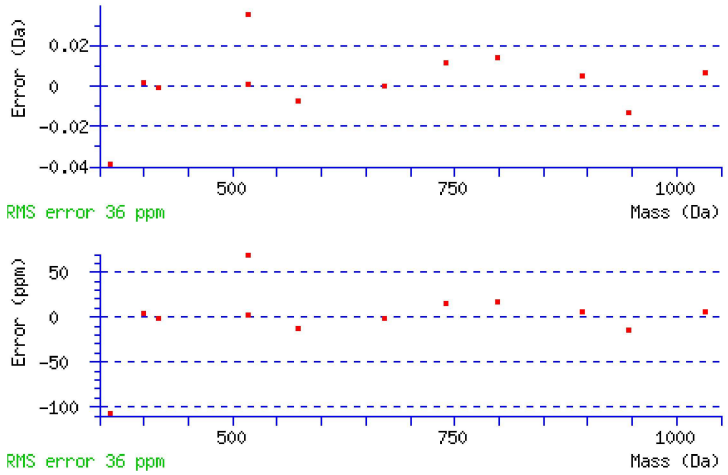

NCBI **BLAST** search of SGYSSPGSPGTPGSR
(Parameters: blastp, nr protein database, expect=20000, no filter, PAM30)
Other BLAST web gateways

All matches to this query

Score	Mr(calc)	Delta	Sequence	Site Analysis
45.6	1552.5596	0.0031	SGYSSPGSPGTPGSR	Phospho S5, S8 54.29%
43.0	1552.5596	0.0031	SGYSSPGSPGTPGSR	Phospho S4, S8 29.50%
40.3	1552.5596	0.0031	SGYSSPGSPGTPGSR	Phospho S1, S8 15.91%
16.6	1552.5596	0.0031	SGYSSPGSPGTPGSR	Phospho S4, S5 0.07%
15.9	1552.5596	0.0031	SGYSSPGSPGTPGSR	Phospho S5, T11 0.06%
14.3	1552.5596	0.0031	SGYSSPGSPGTPGSR	Phospho S1, S5 0.04%
14.3	1552.5596	0.0031	SGYSSPGSPGTPGSR	Phospho S1, S4 0.04%
13.7	1552.5596	0.0031	SGYSSPGSPGTPGSR	Phospho S4, T11 0.04%
10.6	1552.5596	0.0031	SGYSSPGSPGTPGSR	Phospho S1, T11 0.02%
7.2	1552.5596	0.0031	SGYSSPGSPGTPGSR	Phospho S5, S14 0.01%

Mascot: http://www.matrixscience.com/